DISSERTATION

MODELING LANDSCAPE DYNAMICS AND ENVIRONMENTAL ASSOCIATION FOR

SPRUCE MORTALITY

Submitted by

Warong Suksavate

Department Forest and Rangeland Stewardship

In partial fulfillment of the requirements

For the Degree of Doctor of Philosophy

Colorado State University

Fort Collins, Colorado

Summer 2016

Doctoral Committee:

    Advisor: Yu Wei

    John Lundquist
    Seth Ex
    Boris Kondratieff

ABSTRACT

MODELING LANDSCAPE DYNAMICS AND ENVIRONMENTAL ASSOCIATION FOR

SPRUCE MORTALITY

This study addresses important issues related to mortality of spruce species (*Picea* sp.) associate with outbreaks of spruce beetle (*Dendroctonus rufipennis* Kirby) by 1) modeling large scale landscape dynamics of spruce mortality associated with long-term climate in Colorado and Alaska; 2) modeling environmental association between spruce mortality and small scale environmental covariates including climatic factors. In the first chapter, we review the ecology and etiology of spruce mortality in Colorado.

In the second chapter, we evaluate landscape dynamics of spruce mortality at the regional scale of Colorado and Alaska. We used climate transition matrices (CTMs) as a method to assess the influence of climate on spruce forest extent and mortality. We quantify the probabilities of observing spruce forest, spruce mortality, and the mismatches between probabilities for the presence of host and mortality as indicated by differential effects. All values were calculated to populate elements of CTMs. The polynomial functions of ordinary regressive model and spatial autoregressive model were implemented to represent the association between climate zones and the responses. The results show us that there are influences of long-term precipitation and temperature on both probabilities. Presence of spruce forest in Colorado is associated with high precipitation at moderately low temperatures while probability of spruce mortality has a similar association. High probability of observing spruce forest in Alaska is associated with low to moderate precipitation while the probabilities of observing spruce mortality are positively associated with high precipitation at warmer temperatures. From the differential effects, there are mismatches of responses between host and mortality implying the advantageous of host associate with moderate temperatures and high precipitation in Colorado while healthy forest is found in the moderately low temperature and moderate precipitation in Alaska.

In the third chapter, we describe associations between stand scale environmental conditions and spruce mortality. We modeled the association using zero-and-one inflated beta regression model based on hierarchical Bayesian framework. Two-stage Bernoulli logistic models were applied to indicate the occurrence of the extreme values represent presence and absence of mortality; continuous proportional responses were then addressed by beta regressive model. Multivariate Gaussian latent process was included in the function to express the exponential spatial errors term. The results indicate that spatial distribution of the occurrence and intensity of spruce mortality were both associated with the local stand covariates of temperature zone, precipitation zone, class of stand structure level, relative dominance class, and size class. The colder temperature zones have highly negative effects on both the probability of mortality occurrence and the probability of full mortality occurrence, while the warmer temperature zone is positively associated with the presence of full mortality. The results also indicate that stand characteristics are important factors associated with mortality. Mortality occurrence is positively associated with single-story stands with medium to large size classes. The higher-complexity stand structures have highly positive associations with the probability of entire stand mortality, while medium to high dominance classes have negative effects on full mortality. The largest size class and the highest dominance class have negative associations with the proportion of partial mortality.

ACKNOWLEDGEMENTS

TABLE OF CONTENTS

LIST OF TABLES

LIST OF FIGURES

CHAPTER 1

INTRODUCTION

The spruce bark beetle (*Dendroctonus rufipennis* Kirby) is a common species of beetle (Coleoptera: Curculionidae: Scolytinae) native to temperate coniferous forest in North America (Massey and Wygant, 1954). The spruce bark beetle is an oligophagous herbivore that colonizes, develops broods, and emerges for dispersal from a host tree that usually dies in the process. The death of the infested host is caused blockage of the flow of nutrients (Hart et al., 2013). Spruce beetles infest all species of conifers in genus *Picea* (Spruce). In Canada and Alaska, white spruce [*P. glauca* (Moench) Voss], Sitka spruce [*P. sitchensis* (Bong.) Carr] and Lutz's spruce (*P. x lutzii* Little) are major host species, whereas the black spruce (*P. mariana*) is not usually infested (Holsten and Werner, 1990; Schmid and Frye, 1977). In the Rocky Mountains, Engelmann spruce (*P. engelmannii* Parry ex. Engelmann) is the main host species, whereas blue spruce (*P. pungens* Engelmann) is rarely a host (Holsten and Werner, 1990). In some conditions, Lodgepole pine (*Pinus contorta* Douglas) in mixed spruce stands can be an accidental host in an outbreak.

Epidemics of spruce bark beetles have ecological and socioeconomic impacts in both natural and managed forest ecosystems. The bark beetle is a major disturbance in North American forests, affecting a larger area than wildland fire (Veblen et al., 1991). Stand structure is modified by outbreak, especially in old-aged and high basal area stands, leaving suppressed and intermediate trees, reducing composition of spruce tree in the stand, releasing understory, increasing composition of light-tolerant plants, or even transforming the whole stand to non-host species (Schmid and Frye, 1977; Veblen et al., 1991). Other effects of outbreak relate to streamflow due to loss of vegetation cover. Outbreak causes streamflow to increase (Bethlahmy, 1975), as well as nitrogen compound in the streamflow (Griffin et al., 2011). The effects of an outbreak are similar to the changes that occur after removing large vegetation from an area,

but with standing dead trees (Schmid and Frye, 1977). Nutrient cycling, succession, forest structure, solar reflectance, soil dynamics, hydrology, fire, biodiversity, and forested landscape heterogeneity are also affected by outbreaks (Griffin et al., 2011; Kaiser et al., 2013; Kurz et al., 2008). Outbreak builds up dead standing trees across the landscape, resulting in alteration of fire behavior from widespread fuel accumulation increase, and changing stand structure leads to more potential for wildland fire intensity, severity, and occurrence (DeRose and Long, 2009; Jenkins et al., 2012; Schmid and Frye, 1977).

Characteristics and life cycle

Holsten et al. (1999) provided a detailed morphological description of the spruce beetle The oligophagous adults are typical of the genus and are characterized by a cylindrical shape with reddish-brown or black elytra, while the apodous larvae are creamy in color and slight C-shaped and stout. T. Female beetles bore through host bark and construct an egg gallery in the phloem with a slightly grooved pattern (Massey and Wygant, 1954). Knight (1969) proposed that egg quantity laid by female is associated with the stage of infestation for endemic populations. Deposition of eggs usually occurs inside feeding galleries less than a week after successful attack, and the incubation period is a few weeks (1963). Larvae feed by boring outward from the main egg gallery and feed as group until the third stage of instar. After that, each larva constructs an individual feeding gallery before the pupation period. Pupation takes place at the end of individual galleries and lasts about two weeks. Clusters of needles die and discolor to yellowish-green and fall approximately a year after the successful attack (Massey and Wygant, 1954).

The spruce beetle life cycle is identified as bivoltine, a two-year life cycle, but under some conditions the life cycle can be univoltine (one year) or multivoltine (more than two years) (Massey and Wygant, 1954). However, the spruce beetle life cycle rarely exceeds two years. McCambridge and Knight (1972) documented that geographical location, weather, especially low temperatures can delay brood development. Adult emergence occurs from May to October in a period of three to four consecutive days. Beetles usually emerge when maximum shade temperature exceeds an approximate threshold of 16°C (Dyer, 1973). In the southern Rocky Mountains, the first emergence occurs between June and July

(McCambridge and Knight, 1972). In British Columbia, the emerging flight begins in late May (Dyer, 1973). In Alaska, spruce beetles usually begin to emerge between May and June (Beckwith et al., 1977).

Maroja et al. (2007) studied how the historic glaciation period affects the differentiation of spruce beetle phylogenetic groups in North America. Past isolation separated the spruce beetle population into three allopatric population groups. The first two groups inhabit Alaska and Canada, infesting several *Picea* hosts. Another group inhabits the Rocky Mountains and specializes in infesting the Engelmann spruce host. This reflects how geographical location, especially in Alaska and Colorado, climate, host selection, and other factors can impact spruce beetle populations. Spruce beetle populations in southern Rocky Mountain compose of distinct subgroup from subpopulations reside in subalpine forest of Colorado, Montana, and Washington, while the potential hybrid population is found in British Columbia (Jenkins et al., 2014).

Ecology of spruce bark beetle

Bark beetle outbreak intensity is determined by the size of devastated population in a large-scale area. Population dynamics of spruce beetle are influenced by density-dependent and density-independent factors (Raffa et al., 2008). Density-independent factors or exogenous factors are the population unrelated factors including the occurrence of both random and nonrandom events, such as weather-related events and seasonal patterns. Density-dependent factors, or endogenous factors, act as positive or negative feedbacks of population dynamics those may occur instantly (first-order feedback) and the temporal lag that affects after generation time (second-order feedback); such as predation, competition, etc. (Kärvemo, 2010).

Seeking an available and suitable host tree is crucial for the survival of a bark beetle population. In endemic populations, the behavioral state where insect population is low and cannot cause high-intensity and widespread host mortality, the endemic population of spruce beetle typically inhabits shaded aspects of fallen host (Hebertson and Jenkins, 2007; Wallin and Raffa, 2004). After emergence, flight orientation of most bark beetle species depends on semiochemicals, the chemicals used to associate with other individuals, consisting of aggregation and anti-aggregation pheromones. For the spruce beetle, both

visual cues and chemical sensory are used by females to seek a suitable host for brood development (Berryman, 1982; Hard, 1985; Wallin and Raffa, 2000). Short-range olfaction or gustation during flight are also used (Byers, 1996). The utilization of pheromones is critical to overcoming host defense mechanisms. Dispersal and reproductive processes of spruce beetle relies on behavioral dynamics mediated by pheromonal substances in aggregating the attacking population until density of attacking emerged populations are sufficient to overcome the defenses of host tree (Hard, 1989).

Anti-aggregation pheromones serve to control spruce population density by reducing intraspecific competition from a highly aggregated population (Hard, 1989). Lewis and Lindgren (2002) observed that spruce beetles avoided attacking trees already infested with a high degree of bark beetle population. Wallin and Raffa (2004) found that female beetles from epidemic populations, where population density is high, prefer media with chemical substances similar to that of healthier trees. These findings can express that spruce beetles have an anti-overpopulation mechanism: during outbreak when population rapidly increases, spruce beetles switch to attack a healthy, highly resistant host due to increasing intraspecific competition.

Leptographium engelmannii Davidson is a species of blue stain fungus most commonly associated with the spruce beetle and Engelmann spruce (Hinds and Buffam, 1971; Six and Bentz, 2003). In Alaska, *L. abietinum* is associated with epidemic populations of the spruce bark beetle (Aukema et al., 2005). Damage from both the blue stain fungus and bark beetle can weaken host defenses and accelerate host death (Paine et al., 1997). Many species of bark beetle help in dispersion of fungi by carrying fungal spores in specialized adapted mouth structures, called mycangia. Even though spruce beetles lack mycangia, they can carry fungal spores in both elytra and uncovered cuticular pits on the head, called prosternum (Solheim, 1994).

The association with fungi also relates to weakening the host tree and brood development. Blue stain fungi carried to host xylem tissues by the spruce beetle can also weaken spruce defense mechanisms by interrupting water transportation (Werner et al., 2006; Werner and Illman, 1994). The content of ergosterol, a type of plant secondary metabolite important for brood development, is also significantly

4

higher in phloem infected by blue stain fungi compared with uninfected phloem (Bentz and Six, 2006), implying that brood development not only acquires necessary compounds from phloem tissues, but also from association with host fungal diseases. Cardoza et al. (2008) observed that weight gain of a brood feeding on *L. abietinum*–infected substances was higher than those feeding on uninfected substances. However, some fungi can have negative effects on spruce beetle gallery construction and oviposition, causing a high brood mortality rate.

The most important natural predators of the spruce bark beetle are woodpeckers. Knight (1958) stated that the northern three-toed woodpecker (*Picoides tridactylus* Baird), hairy woodpecker [*Picoides villosus* (Anthony)], and downy woodpecker [*Picoides pubescens* (Hartlaub)] consume spruce bark beetles primarily during outbreak. In the outbreak population, woodpeckers play a significant role in controlling spruce beetle brood by causing between 19 and 98 percent mortality of total population, depending on the spruce beetle population density (Fayt et al., 2005).

Schmid and Frye (1977) summarized that insect predators and parasites are known to kill high percentages of spruce beetle populations. Insect natural enemies consist of several species of *clerid* beetle, dipteran predators, and hymenopteran parasites. *Thanasimus undatulus* Say (Coleoptera: Cleridae) adults are active between July and August and are aggregated to living spruce trees by frontalin kairomone from the bark beetle (Dyer, 1975). *Enoclerus sphegeus* Fabricius (Coleoptera: Cleridae). (Coleoptera: Cleridae) adults prey on adult spruce beetles during the period of emergence. There are also natural enemies in other orders. *Coeloides dendroctoni* (Cushman) (Hymenoptera: Braconidae) is an important parasite with a 9- to 12-month life cycle (Schmid and Frye, 1977). *Cecidostiba burkei* Crawford (Hymenoptera: Pteromalidae) is parasitic to beetle larvae (Massey and Wygant, 1954). Other common predaceous species include *Enoclerus lecontei* Wolcott (Coleoptera: Cleridae), *Thanasimus undatulus* Say (Coleoptera: Cleridae), and *Medetera aldrichii* Wheeler (Diptera: Dolichopodidae). Although natural enemies may locally control spruce beetle populations in endemic populations, the epidemic state of bark beetle population can erupt regardless of the present of these natural enemies. These agents also have never been related to the collapse of epidemics (Berryman, 1982; Schmid and Frye, 1977).

Since insects are poikilothermic, temperature is one of the most important density-independent factors for survival and brood development due to the effect of body temperature on enzymic activities. Warmer climate has the potential to increase the performance of insects (Bale et al., 2002; Harrington et al., 2001). Ambient temperatures have large effects on success of population at multiple points during outbreak (Raffa et al., 2008). A critical temperature threshold is crucial to bark beetle survival over the winter months. A study in the Rocky Mountains found that subcortical temperatures of –26°C will kill adult beetles, while –34°C is lethal for larval stages (Massey and Wygant, 1954). In Alaska, the critical temperature threshold is slightly higher (Miller and Werner, 1987) at –30°C for mortality of larvae. Extremely cold periods could kill a large bark beetle population at a landscape scale (Frye et al., 1974). For example, the extremely low temperatures in the mid-20th century are cited as a major factor in ending the outbreak in White River National Forest (Wygant, 1956). However, high precipitation like snow in the winter can contribute to high overwinter survival. The insulation from the below snow line can help bark beetles survive the cold because they are not subjected to extremely low ambient temperatures (McCambridge and Knight, 1972). Even in subfreezing temperatures above the threshold temperature, bark beetles can survive due to the accumulation of intracellular cryoprotectant compounds, such as glycerol, which cause cells to have a subzero supercooling point (Miller and Werner, 1987). On the other hand, an overheating temperature, exceeding 54.5°C, could also kill the bark beetle (Mitchell and Schmid, 1973).

Research based on laboratory experiments shows that spruce beetle population growth favors warm temperatures because larval development rate and survival are increased (Bentz et al., 2010; Chapman et al., 2012; Hansen et al., 2001). Warm periods during the summer (Knight, 1961) or warm temperatures in a specific microclimate (Dyer, 1969) can shorten the life cycle from two years to one year. Warm temperatures inhibit larval diapauses, contributing to a faster development rate (Dyer, 1970). On the contrary, low temperatures during the brood development period can induce a longer life cycle (Knight, 1961; McCambridge and Knight, 1972). A shortened life cycle earlier in the spring and fall could allow beetles to increase the number of generations completed in the developing season (Bale et al.,

2002) and may reduce the likelihood of exposure to adverse conditions and predation (Hansen and Bentz, 2003). The accumulation of populations could induce the greater likelihood of epidemics. The time of exposure to temperature affects the voltinism of the spruce bark beetle. The voltinism model indicates that the best criterion for estimating brood univoltine is the number of cumulative temperature-hours spent above 17°C between 40 and 90 days after peak flight (Hansen et al., 2001). On the other hand, accelerated development at inappropriate times could cause increased beetle mortality due to entering winter in a developmental stage susceptible to freezing temperatures (e.g., pupae) (Bentz et al., 2010; Bentz and Mullins, 1999; Miller and Werner, 1987; Trần et al., 2007). Strong deviation of temperature from the ordinary may also cause the loss of synchrony in development and dispersion, which could be detrimental to a beetle population (Bentz et al., 2010; Logan and Bentz, 1999).

Spruce bark beetle feeds only on *Picea* hosts. Host suitability and host susceptibility is important, as well as the availability of host. Host suitability is the quality of the host as indicated by relative fecundity, rate of larval development, and brood survival. Host susceptibility is a measure of the host's ability to withstand a bark beetle attack. Usually, bark beetle outbreaks are incited by events that weaken host defenses, such as drought and pathogens (Christiansen et al., 1987). In an endemic state where bark beetle population is too low to overcome host defenses, bark beetle population stays low and sparse across the landscape, even when suitable host species, host age, and climatic conditions are present (Raffa et al., 2005). Endemic populations of bark beetle primarily colonize host material, residuals, and rarely weakened hosts with low defenses (Paine et al., 1997; Wallin and Raffa, 2004). Spruce bark beetles prefer attacking defense-lacking hosts and only attack healthy trees after a susceptible host has been depleted, which usually occurs during outbreak. Large and old trees are preferred by spruce beetles. These characteristics presumably imply for higher suitability for brood development due to higher nutritional support (DeRose and Long, 2012a; Schmid and Frye, 1977; Wallin and Raffa, 2004). However, in an epidemic population where the bark beetle can more easily overcome healthy trees, most available hosts are attacked during outbreak, regardless of vigor (DeRose and Long, 2012a, 2012b; Dymerski et al., 2001).

7

Oleoresin is an important component of conifer defense against bark beetles. Hosts with low oleoresin flow rates are susceptible to beetle attack (Hard, 1985). The flow of resin can create a physical barrier, in addition to the formation of necrotic tissues. These defense mechanisms deprive beetles of nutrient-rich living tissues and induce secondary metabolites, which are toxic to the beetles and their broods and inhibit associated fungal growth (Christiansen et al., 1987).

Susceptibility of Landscape and Spruce Bark Beetle Outbreak

Compared to other species of bark beetle, the spruce beetle is the most widely scaled destructive forest insect in North America—it can kill almost available hosts within the stand (DeRose and Long, 2007). In the past several decades, coniferous forests have experienced mortality of billions of trees because of the spruce beetle (Bentz et al., 2009; Berg et al., 2006). Hart et al. (2013) utilized historical documents and tree-ring records to recount the history of spruce beetle outbreaks in northwestern Colorado to construct a timeline of broad-scale outbreak, with the most recent outbreaks occurred between 2004 and 2010. They found out that duration between outbreaks has median of 75 years with at least 17 years between outbreaks. In another study, spruce beetle populations were shown to have periodic outbreaks in 30- to 50-year intervals (Holsten and Werner, 1990).

Disturbance is a key factor related to all known major bark beetle outbreaks (Wygant and Lejeune, 1967). Knight (1961) stated that the occurrence of spruce bark beetle outbreak is related to windthrow and timber harvesting. Windthrow typically causes a uniform predisposition of fallen logs and uprooting that the spruce beetle can use as breeding material to build up populations (Hebertson and Jenkins, 2007; Schmid and Amman, 1992; Veblen et al., 1991). Other disturbances, such as timber harvesting, landslides, fire, and avalanches, can also create host materials for spruce beetles and are associated with most historic outbreaks (Berg et al., 2006; Hebertson and Jenkins, 2008; Wallin and Raffa, 2004). Root disease is also a major disturbance associated with bark beetle outbreak. Most of the root disease–infected subalpine stands in Colorado have been infested by bark beetles and borers (James and Goheen, 1981). In south-central Utah, spruce bark beetle outbreak has been associated with *Armillaria* [*Armillaria ostoyae* (Romagnesi) Herink] root disease (McDonald, 1998). In contrast,

disturbance is not always associated with bark beetle outbreak. Kulakowski and Veblen (2003) found that historic blowdown event in Colorado did not result in increased spruce beetle–induced host mortality. This implies that, despite the disturbance, the other conditions such as susceptibility of host, stand structure, and population dynamics of bark beetle must all be met along with the increased breeding materials from the disturbances. However, disturbance sometimes reduces the likelihood of epidemics by reducing host availability from changing stand composition (Berg et al., 2006).

A number of studies have examined the association between bark beetle infestation and climate across space and time (Berg et al., 2006; Campbell et al., 2007; Chavardès et al., 2012; Hart et al., 2013; Hebertson and Jenkins, 2008; Sherriff et al., 2011). Colorado subalpine forests have experienced periodic mortality coincident with a warmer and drier climate since the late 20th century (Bigler et al., 2007; Smith et al., 2015). Recent study has suggested that drought induced by Atlantic Multidecadal Oscillation (AMO), Pacific Decadal Oscillation (PDO), and global warming affects forest health, decreasing host tree defenses and being highly associated with the occurrence of spruce beetle outbreak in Colorado (Chavardès et al., 2012; Hansen et al., 2001; Hart et al., 2013). AMO is one of the most important factors in predicting drought and bark beetle outbreak in Colorado (Berg et al., 2006; McCabe et al., 2004). In Alaska, spruce beetle outbreak is more negatively associated with PDO, related to increasing warmth and more precipitation in the winter and El Niño Southern Oscillations (ENSO), united with drought during late summer leading to water deficit (Sherriff et al., 2011). Historically, tree mortality from bark beetles in the southwest is associated with drought events (Kleinman et al., 2012). Climate change also has the potential to disturb forest regimes and affect forest ecosystem functioning, which increases susceptibility across the landscape (Ayres and Lombardero, 2000; Dale et al., 2000).

Host defense against beetles is also significantly associated with local climate (Hard, 1985). The spruce beetle outbreak in Alaska that initiated in the 1990's has been demonstrated to be associated with high summer temperatures at the local scale (Berg et al., 2006). Recent decades of spruce beetle outbreaks in the Rocky Mountains are associated with warm and dry yearly climate (Hebertson and Jenkins, 2008). Spruce beetle outbreaks in the 1990s of Utah were also associated with high maximum summer

temperatures, high minimum winter temperatures, and prolonged drought (DeRose and Long, 2012b). The changing of local climate due to climate change can affect the spatial distribution of susceptible hosts at the local scale and can shift into a new area insect that have never experienced outbreak (Logan and Bentz, 1999; Parmesan et al., 1999; Rouault et al., 2006; Sambaraju et al., 2012; Williams and Liebhold, 2002). The shifting of habitat range into a new geographic region causes the bark beetle to encounter new ecological complexes, and it is beyond our knowledge how the interactions will be settled in new habitat (Gaylord, 2014). In addition, beetles may encounter new hosts. Since climate models (Seager et al., 2007) forecast more frequent drought in North America, the possibility is implied that outbreak can be shifted to a new area. A recent study in Canada showed that hosts in regions that have never been climatically suitable to bark beetles may be less adapted to the bark beetle and may be more susceptible to outbreak (Cudmore et al., 2010).

Changing distribution of climatic conditions across a landscape spatially affects both beetle population dynamics and host susceptibility (Bentz et al., 2010). The directional changing of climate can favor growth for bark beetle populations that usually reside from low-level endemic to epidemic, in which large populations have more likelihood to successfully attack a healthy, living tree (Christiansen et al., 1987). Widespread drought stress of a host can increase the susceptibility of the forest at the landscape scale; furthermore, increasing temperatures could also increase the level of water stress from a high evaporation rate (Williams et al., 2013). Drought weakens the defense mechanisms of an individual host by reducing its carbon balance, which is a source for maintenance and raw materials for defense mechanisms such as resinous flows (Chavardès et al., 2012). Several studies have expressed that high temperature and water deficit are the most important factors impacting climate-related plant mortality due to physiological damage (Anderegg et al., 2012; Breshears et al., 2005; McDowell, 2011; Williams et al., 2013) and stress-induced pathogens (Hicke et al., 2012; Raffa et al., 2008).

The plant stress hypothesis (Larsson, 1989) is a popular hypothesis depicting the relationship between plant defenses depending on environmental factors, especially water, and the success of insect herbivores. Water stress contributes to reducing photosynthesis and leads to lower carbon assimilation,

10

which weakens the defense mechanism from lower resin production (Gaylord et al., 2007; McDowell et al., 2008). Stressed plants also attract more bark beetles from chemical emissions (Kelsey et al., 2014; Mattson and Haack, 1987). Experiments have shown that water stress on a host has a positive effect on the performance of wood borer and phloem feeder insects (Huberty and Denno, 2004). The success of a bark beetle attack can be determined by modeling the population threshold for success with the level of host vigor; the population can exceed the threshold by both increasing the beetle population and depleting host defenses (Berryman, 1982; Mattson and Haack, 1987).

The age and structure of stand is another significant factor contributing to bark beetle outbreak. Structure, composition, past management, and other stand characteristics, combined with climate variability, influence the success of spruce beetle population and also affect outbreak intensity, spread, and duration (Bentz et al., 2010; Chapman et al., 2012; DeRose and Long, 2012b, 2007; Fettig et al., 2008; Raffa et al., 2008; Reynolds and Holsten, 1994). DeRose et al. (2013) showed that proportion of spruce in stand and total basal area are the most influential factors impacting spruce beetle outbreak. Susceptibility of natural stands can be determined using average diameter, basal area, species composition, and physiographic location (Schmid and Frye, 1977). A study in Alaska showed large-diameter old spruce to be the most susceptible to outbreak (Doak, 2004). Increases in stand densities from aggressive fire suppression can lead to high competition among hosts for limited water resources (Breece et al., 2008; Kolb et al., 1998), while prescribed fire application for general management does not show evidence of increasing outbreak likelihood (Tabacaru et al., 2016). Diversity of forest ecosystem, connectivity of host, and heterogeneity of forested landscape also influence the development of spruce beetle outbreaks. Although predation and parasitism are important for regulating an endemic population, they have only a small effect on bark beetle outbreak at the landscape scale (Berryman, 1982).

The heterogeneity of ecological configurations in time and space is the causation of spatial variability of forest mortality across the landscape. They have the direct influence on both population and behavioral dynamics of causal agents and their associated organisms but the effect of landscape structure on spatial extent of spruce mortality is loosely understood (Lundquist and Reich, 2014). Landscape

heterogeneity directly affects dispersal of bark beetles by altering life cycle, changing the probabilities of confrontation of natural enemies, competition and symbiotic organisms (Hughes et al., 2001). The different features of the spatio-temporal dynamics also indirectly affect dispersion of bark beetle by influencing the geographical and meteorological factors. The important constituents that made the site suitable are affected by the heterogeneity and connectivity of ecological features those could be altered through time or by feedbacks of the events. Due to the limited mobility of bark beetle in dispersal, heterogeneity of dynamics of host availability resulting in the unsuitable area in-between which can interfere the spread of outbreak between infested stands and susceptible stands (DeRose and Long, 2012a; Fettig et al., 2008; Kausrud et al., 2012). Highly associated environmental factors those effectively increases the connectivity between suitable patches could facilitate the spread of outbreak across the landscape (Aukema et al., 2008). However, using other studies (Berg et al., 2006; Reynolds and Holsten, 1994), DeRose and Long (2012a) suggested from autocorrelation tests that spruce beetle outbreak does not originate from a single epicenter, but rather is initiated from a synchrony of multiple locations those have certain characteristics to initiate outbreak (Kausrud et al., 2012).

The eruption at stand-level depend on threshold that was defined as a causal agent's population capacity contribute to landscape-level of outbreak's eruptions. This threshold depends on the suitability and availability of host trees those affected by susceptibility of host due to environmental stress, depletion of host, availability of suitable hosts in the spatially proximate patches, and synchronization of causal agent's populations (Raffa et al., 2008). These factors are influences by pattern of landscape dynamics across space and time. Environmental factors and processes that alter landscape heterogeneity of suitable host such as natural or anthropogenic disturbances, and temperature or drought events those favor the growth of bark beetle's population and affect susceptibility of host may spatially synchronize and involve in the eruptive of bark beetle populations in the regional scale (Aukema et al., 2006).

Modeling the Influences of Climate on the Spatial Extent of Forest Insects

Pattern and distribution of interaction between organisms and environment at the landscape level have been long interesting to researchers (Pielou, 1977; Turner, 1989). Developing a method to model

climate change effect on the distribution and intensity of bark beetle outbreaks in the landscape context is a major goal for forest entomologists and land managers. In the regime of climate shift, we need more understanding, and modeling can provide us information on how the processes interact at various spatiotemporal scales (Lundquist and Reich, 2014). Outbreak in space and time is hard to determine because bark beetles are not uniformly distributed across the landscape. Outbreak is usually determined by population dynamics directly affected by environmental conditions, especially climate, that play an important role in determining spatial extent dynamics and insect population abundance (Bale et al., 2002; Dukes et al., 2009). A climate-driven mechanistic model is usually created using environmental covariates that directly affect population development and survival (Hansen et al., 2001). Probabilistic methods have also been applied in modeling the influences of climate and other environmental factors on forest insects, called ecological niche modeling or bioclimatic enveloped modeling (Araújo and Peterson, 2012). Understanding the effects of climate on the spatial extent of outbreaks through combined effects with stand structure and other characteristics is crucial for predicting future outbreak (Hart et al., 2015).

The mechanistic model was used to develop a model accounting for influences of environmental factors on forest insect and disease processes from the bottom-up, from the individual to landscape levels. Geiszler et al. (1980) modeled the dynamics of mountain pine beetle aggregation using a mathematical model. The concept of transitional threshold between epidemic and endemic behavior of forest insect population was modeled based on resource accumulation and depletion (Økland and Bjørnstad, 2006) and the influences of climate (Crozier et al., 2006). A simulation model was developed to analyze the effects of climate on daily bark beetle activity in the large spatial extent using daily temperature data (Joensson and Bärring, 2011). Cellular automata have also been used to model spatial extent dynamics at the landscape scale. Bone et al. (2006) developed a geographic information system (GIS)–based cellular automata model by incorporating the non-discrete fuzzy theory to predict the dynamics of forest susceptibility with mountain pine beetle population dynamics. The population dynamics model of insect pests was applied for insect mortality incorporating management approaches (Wang et al., 2010). Hart and Veblen (2015) used a time series of high- and medium-resolution remote sensing imagery to model

tree-level mortality from spruce beetle outbreak. The equation-based model for dispersal of mountain pine beetle was developed using pheromones aggregate mechanism and other population-based variables (Logan and Bentz, 1999). Perez and Dragicevic (2010) implemented agent-based model to predict mortality and behaviors of bark beetle populations at the individual tree and landscape levels.

Probabilistic model or statistical model was used to represent effects of environmental covariates on the presence of forest insect epidemic across space and time from the top-down. Merril et al. (2008) used logistic regression to model the probability of occurrence of insect pest based on elevation gradient. Although many models offer important insights into forest insect outbreaks, they need consideration of the spatial structure involved in the dynamics of forested landscape. Berg et al. (2006) included spatial autocorrelation in a logistic regression to model probability of spruce beetle outbreak, assuming temperature as the crucial factor in life cycle development. From a set of temporal climate data, the annual presence of historic spruce beetle outbreak was predicted using dichotomous classification regression tree (CART) analysis (Hebertson and Jenkins, 2008). Lundquist et al. (2012) defined the spatial distribution of amber-marked birch leaf miner in Anchorage, Alaska, by modeling small-scale spatial variability using kriging. Although these models offer important insights into forest insect outbreaks, they need consideration of the spatial structure involved in the dynamics of forested landscape.

Recently, many fields in ecology have increasingly used the occupancy model for questioning ecosystem changes and the emergence of vulnerabilities to address theoretical and practical issues (Clark, 2005; Keith et al., 2008). Approaches have been developed to deal with the association of known covariates (Meier et al., 2010; Zimmermann and Kienast, 1999) and with unknown latent processes (Royle et al., 2007) related to the concept of ecological niche (MacArthur et al., 1966). Generalized linear models (GLM) are developed to represent association between species distribution and environmental factors (Guisan and Thuiller, 2005). Skewness from dispersed and non-normal responses can violate the assumption of model severely bias the model estimates (Shono, 2008). Zero-inflated models are types of mixture models developed to represent the association of zero and non-zero responses. Zero/nonzero data usually been treated with appropriate link function (Chelgren et al., 2011).

Bayesian approach is the method developed for a hierarchical structure of mixed models (Gelman and Hill, 2006). To implement the Bayesian methods, multilevel parameters of model were simulated using the Markov chain Monte Carlo (MCMC) method (Hooten and Hobbs, 2015). A multilevel model can incorporate generalized linear mixed model (GLMM) with link function to address excessive zero with spatio-temporal structure (Chelgren et al., 2011; Zuur et al., 2009). Spatial dependence could be defined by the geostatistical point-process using the multivariate Gaussian process for spatial errors (Banerjee et al., 2008; Diggle, 1983) that the error responses at every sample location are associated to each other.

Climate Transition Matrices (CTMs) with spatially-explicit climatic data were used to describe relationships between causal agents, host and climate. Spatial data is summarized in a table where the rows represent temperature zones and the columns represent precipitation zones. Climate zones provides an opportunity to examine the influence on the landscape dynamics of host mortality from long term climate characteristics. Reich et al (2010; Robin M. Reich et al., 2008) developed climate zones to define the specific strata in a natural resources monitoring program in Jalisco, Mexico. Afterward, climate zones were implemented to model stand structure (Reich et al., 2011), and characterize the composition of soil textures (Pongpattananurak et al., 2012). The climate zones can be used to predict the spatial characteristics and extent of mortality of host from forest insects (Reich et al., 2016, 2014, 2013, 2008). Reich et al (2016) used CTMs to characterize environmental mismatches those contributing to subalpine-fir decline in Colorado. The usage of climate zones provides perspective on the effect of climate entities on insect outbreak distribution, as well as opportunities to study the relationship between climate and insect population (Guisan and Zimmermann, 2000).

Research Questions

Not much research has been focused on combining small-scale sampling and large-scale data to model the extent of spruce bark beetles at the landscape scale. In this research, we combine aerial survey detection and stand-scale plot sampling to explore the relationship between environmental covariates and spruce forest extent and spruce mortality due to the spruce bark beetle. To better understand the response

of spruce beetle outbreaks to climatic factors and other local stand characteristics, we ask two specific research questions:

1. How does long-term climate affect the presence of mortality from spruce bark beetle outbreak? What is the proportion of observed spruce mortality to the presence of spruce forest? What do the results imply about the environmental advantage of climate adaptation for host and spruce bark beetle?

2. How can we develop a multistage hierarchical Bayesian model from stand characteristic sampling? How does model create a description on the influences of small scale environmental factors for predicting spruce mortality extent and severity of the outbreak?

LITERATURE CITED

Anderegg, W.R.L., Berry, J.A., Field, C.B., 2012. Linking definitions, mechanisms, and modeling of drought-induced tree death. Trends Plant Sci. 17, 693–700.

Araújo, M.B., Peterson, A.T., 2012. Uses and misuses of bioclimatic envelope modeling. Ecology 93, 1527–1539.

Aukema, B.H., Carroll, A.L., Zheng, Y., Zhu, J., Raffa, K.F., Dan Moore, R., Stahl, K., Taylor, S.W., 2008. Movement of outbreak populations of mountain pine beetle: influences of spatiotemporal patterns and climate. Ecography 31, 348–358.

Aukema, B.H., Carroll, A.L., Zhu, J., Raffa, K.F., Sickley, T.A., Taylor, S.W., 2006. Landscape level analysis of mountain pine beetle in British Columbia, Canada: Spatiotemporal development and spatial synchrony within the present outbreak. Ecography 29, 427–441.

Aukema, B.H., Werner, R.A., Haberkern, K.E., Illman, B.L., Clayton, M.K., Raffa, K.F., 2005. Quantifying sources of variation in the frequency of fungi associated with spruce beetles: Implications for hypothesis testing and sampling methodology in bark beetle–symbiont relationships. For. Ecol. Manag. 217, 187–202.

Ayres, M.P., Lombardero, M.J., 2000. Assessing the consequences of global change for forest disturbance from herbivores and pathogens. Sci. Total Environ. 262, 263–286.

Bale, J.S., Masters, G.J., Hodkinson, I.D., Awmack, C., Bezemer, T.M., Brown, V.K., Butterfield, J., Buse, A., Coulson, J.C., Farrar, J., Good, J.E.G., Harrington, R., Hartley, S., Jones, T.H., Lindroth, R.L., Press, M.C., Symrnioudis, I., Watt, A.D., Whittaker, J.B., 2002. Herbivory in global climate change research: direct effects of rising temperature on insect herbivores. Glob. Change Biol. 8, 1–16.

Banerjee, S., Gelfand, A.E., Finley, A.O., Sang, H., 2008. Gaussian predictive process models for large spatial data sets. J. R. Stat. Soc. Ser. B Stat. Methodol. 70, 825–848.

Beckwith, R.C., Wolff, J.O., Zasada, J.C., Or.), P.N.F. and R.E.S. (Portland, Service, U.S.F., 1977. Bark beetle response to clearcut and shelterwood systems in interior Alaska after whole tree logging. Dept. of Agriculture, Forest Service, Pacific Northwest Forest and Range Experiment Station. 8 p.

Bentz, B.J., Mullins, D.E., 1999. Ecology of mountain pine beetle (Coleoptera: Scolytidae) Cold hardening in the intermountain west. Environ. Entomol. 28, 577–587.

Bentz, B.J., Régnière, J., Fettig, C.J., Hansen, E.M., Hayes, J.L., Hicke, J.A., Kelsey, R.G., Negrón, J.F., Seybold, S.J., 2010. Climate change and bark beetles of the western United States and Canada: Direct and indirect effects. BioScience 60, 602–613.

Bentz, B.J., Six, D.L., 2006. Ergosterol content of fungi associated with *Dendroctonus ponderosae* and *Dendroctonus rufipennis* (Coleoptera: Curculionidae, Scolytinae). Ann. Entomol. Soc. Am. 99, 189–194.

Bentz, B., Logan, J., MacMahon, J., Allen, C.D., Ayres, M., Berg, E., Carroll, A., Hansen, M., Hicke, J., Joyce, L., Macfarlane, W., Munson, S., Negron, J., Paine, T., Powell, J., Raffa, K., Regniere, J., Reid, M., Romme, B., Seybold, S., Six, D., Tomback, D., Vandygriff, J., Veblen, T., White, M., Witcosky, J., Wood, D., 2009. Bark beetle outbreaks in western North America: Causes and consequences. Bark Beetle Symposium, 42p.

Berg, E.E., David Henry, J., Fastie, C.L., De Volder, A.D., Matsuoka, S.M., 2006. Spruce beetle outbreaks on the Kenai Peninsula, Alaska, and Kluane National Park and Reserve, Yukon Territory: Relationship to summer temperatures and regional differences in disturbance regimes. For. Ecol. Manag., 227, 219–232.

Berryman, A.A., 1982. Population dynamics of bark beetles. Bark Beetles North Am. Conifers., 264–314.

Bethlahmy, N., 1975. A Colorado episode: beetle epidemic, ghost forests, more streamflow. Northwest Sci. 49, 95–105.

Bigler, C., Gavin, D.G., Gunning, C., Veblen, T.T., 2007. Drought induces lagged tree mortality in a subalpine forest in the Rocky Mountains. Oikos 116, 1983–1994.

Bone, C., Dragicevic, S., Roberts, A., 2006. A fuzzy-constrained cellular automata model of forest insect infestations. Ecol. Model. 192, 107–125.

Breece, C.R., Kolb, T.E., Dickson, B.G., McMillin, J.D., Clancy, K.M., 2008. Prescribed fire effects on bark beetle activity and tree mortality in southwestern ponderosa pine forests. For. Ecol. Manag. 255, 119–128.

Breshears, D.D., Cobb, N.S., Rich, P.M., Price, K.P., Allen, C.D., Balice, R.G., Romme, W.H., Kastens, J.H., Floyd, M.L., Belnap, J., Anderson, J.J., Myers, O.B., Meyer, C.W., 2005. Regional vegetation die-off in response to global-change-type drought. Proc. Natl. Acad. Sci. U. S. A. 102, 15144–15148.

Campbell, E.M., Alfaro, R.I., Hawkes, B., 2007. Spatial distribution of mountain pine beetle outbreaks in relation to climate and stand characteristics: A Dendroecological Analysis. J. Integr. Plant Biol. 49, 168–178.

Cardoza, Y.J., Moser, J.C., Klepzig, K.D., Raffa, K.F., 2008. Multipartite symbioses among fungi, mites, nematodes, and the spruce beetle, *Dendroctonus rufipennis*. Environ. Entomol. 37, 956–963.

Chapman, T.B., Veblen, T.T., Schoennagel, T., 2012. Spatiotemporal patterns of mountain pine beetle activity in the southern Rocky Mountains. Ecology 93, 2175–2185.

Chavardès, R.D., Daniels, L.D., Waeber, P.O., Innes, J.L., Nitschke, C.R., 2012. Did the 1976–77 switch in the Pacific Decadal Oscillation make white spruce in the southwest Yukon more susceptible to spruce bark beetle?. For. Chron. 88, 513–518.

Chelgren, N.D., Adams, M.J., Bailey, L.L., Bury, R.B., 2011. Using multilevel spatial models to understand salamander site occupancy patterns after wildfire. Ecology 92, 408–421.

Christiansen, E., Waring, R.H., Berryman, A.A., 1987. Resistance of conifers to bark beetle attack: Searching for general relationships. For. Ecol. Manag. 22, 89–106.

Clark, J.S., 2005. Why environmental scientists are becoming Bayesians. Ecol. Lett. 8, 2–14.

Crozier, L., Dwyer, G., Fagan, A.E.W.F., DeAngelis, E.D.L., 2006. Combining population-dynamic and ecophysiological models to predict climate-induced insect range shifts. Am. Nat. 167, 853–866.

Cudmore, T.J., Björklund, N., Carroll, A.L., Staffan Lindgren, B., 2010. Climate change and range expansion of an aggressive bark beetle: evidence of higher beetle reproduction in naïve host tree populations. J. Appl. Ecol. 47, 1036–1043.

19

Dale, V.H., Joyce, L.A., McNulty, S., Neilson, R.P., 2000. The interplay between climate change, forests, and disturbances. Sci. Total Environ. 262, 201–204.

DeRose, R.J., Bentz, B.J., Long, J.N., Shaw, J.D., 2013. Effect of increasing temperatures on the distribution of spruce beetle in Engelmann spruce forests of the Interior West, USA. For. Ecol. Manag. 308, 198–206.

DeRose, R.J., Long, J.N., 2012a. Factors influencing the spatial and temporal dynamics of Engelmann spruce mortality during a spruce beetle outbreak on the Markagunt Plateau, Utah. For. Sci. 58, 1–14.

DeRose, R.J., Long, J.N., 2012b. Drought-driven disturbance history characterizes a southern Rocky Mountain subalpine forest. Can. J. For. Res. 42, 1649–1660.

DeRose, R.J., Long, J.N., 2009. Wildfire and spruce beetle outbreak: simulation of interacting disturbances in the central Rocky Mountains. Ecoscience 16, 28–38.

DeRose, R.J., Long, J.N., 2007. Disturbance, structure, and composition: spruce beetle and Engelmann spruce forests on the Markagunt Plateau, Utah. For. Ecol. Manag. 244, 16–23.

Diggle, P.J., 1983. Statistical analysis of spatial point patterns. Hodder Education Publishers, 148 p.

Doak, P., 2004. The impact of tree and stand characteristics on spruce beetle (Coleoptera: Scolytidae) induced mortality of white spruce in the Copper River Basin, Alaska. Can. J. For. Res. 34, 810–816.

Dukes, J.S., Pontius, J., Orwig, D., Garnas, J.R., Rodgers, V.L., Brazee, N., Cooke, B., Theoharides, K.A., Stange, E.E., Harrington, R., Ehrenfeld, J., Gurevitch, J., Lerdau, M., Stinson, K., Wick, R., Ayres, M., 2009. Responses of insect pests, pathogens, and invasive plant species to climate change in the forests of northeastern North America: What can we predict? NE Forests 2100: A synthesis of climate change impacts on forests of the northeastern US and eastern Canada. Can. J. For. Res. 39, 231–248.

Dyer, E.D.A., 1975. Frontalin attractant in stands infested by the spruce beetle, *Dendroctonus rufipennis* (Coleoptera: Scolytidae). Can. Entomol. 107, 979–988.

Dyer, E.D.A., 1973. Spruce beetle aggregated by the synthetic pheromone frontalin. Can. J. For. Res. 3, 486–494.

Dyer, E.D.A., 1970. Larval diapause in *Dendroctonus obesus* (Mannerheim) (Coleoptera: Scolytidae). J. Entomol. Soc. Br. Columbia 67, 18–21.

Dyer, E.D.A., 1969. Influence of temperature inversion on development of spruce beetle *Dendroctonus obesus* (Mannerheim) (Coleoptera: Scolytidae). J. Entomol. Soc. Br. Columbia 66, 41–45.

Dymerski, A.D., Anhold, J.A., Munson, A.S., 2001. Spruce beetle (*Dendroctonus rufipennis*) outbreak in Engelmann spruce (*Picea engelmannii*) in central Utah, 1986-1998. West. North Am. Nat. 19–24.

Fayt, P., Machmer, M.M., Steeger, C., 2005. Regulation of spruce bark beetles by woodpeckers—a literature review. For. Ecol. Manag. 206, 1–14.

Fettig, C.J., Borys, R.R., McKelvey, S.R., Dabney, C.P., 2008. Blacks mountain experimental forest: bark beetle responses to differences in forest structure and the application of prescribed fire in interior ponderosa pine. Special forum on ecological studies in interior Ponderosa pine — First findings from Blacks Mountain interdisciplinary research. Can. J. For. Res. 38, 924–935.

Frye, R.H., Flake, H.W., Germain, C.J., 1974. Spruce beetle winter mortality resulting from record low temperatures in Arizona. Environ. Entomol. 3, 752–754.

Gaylord, M.L., 2014. Working Paper 31: Climate change impacts on bark beetle outbreaks and the impact of outbreaks on subsequent fires. 7 p.

Gaylord, M.L., Kolb, T.E., Wallin, K.F., Wagner, M.R., 2007. Seasonal dynamics of tree growth, physiology, and resin defenses in a northern Arizona ponderosa pine forest. Can. J. For. Res. 37, 1173–1183.

Geiszler, D.R., Gallucci, V.F., Gara, R.I., 1980. Modeling the dynamics of mountain pine beetle aggregation in a lodgepole pine stand. Oecologia 46, 244–253.

Gelman, A., Hill, J., 2006. Data analysis using regression and multilevel/hierarchical models. Cambridge University Press, 648 p.

Griffin, J.M., Turner, M.G., Simard, M., 2011. Nitrogen cycling following mountain pine beetle disturbance in lodgepole pine forests of Greater Yellowstone. For. Ecol. Manag. 261, 1077–1089.

Guisan, A., Thuiller, W., 2005. Predicting species distribution: offering more than simple habitat models. Ecol. Lett. 8, 993–1009.

Guisan, A., Zimmermann, N.E., 2000. Predictive habitat distribution models in ecology. Ecol. Model. 135, 147–186.

Hansen, E.M., Bentz, B.J., 2003. Comparison of reproductive capacity among univoltine, semivoltine, and re-emerged parent spruce beetles (Coleoptera: Scolytidae). Can. Entomol. 135, 697–712.

Hansen, E.M., Bentz, B.J., Turner, D.L., 2001. Temperature-based model for predicting univoltine brood proportions in spruce beetle (Coleoptera: Scolytidae). Can. Entomol. 133, 827–841.

Hard, J.S., 1989. Sequence of trees attacked by spruce beetles in a mature even-aged spruce stand in South-Central Alaska. Northwest Sci. 63, 5-12.

Hard, J.S., 1985. Spruce beetles attack slowly growing spruce. For. Sci. 31, 839–850.

Harrington, R., Fleming, R.A., Woiwod, I.P., 2001. Climate change impacts on insect management and conservation in temperate regions: can they be predicted? Agric. For. Entomol. 3, 233–240.

Hart, S.J., Veblen, T.T., 2015. Detection of spruce beetle-induced tree mortality using high- and medium-resolution remotely sensed imagery. Remote Sens. Environ. 168, 134–145.

Hart, S.J., Veblen, T.T., Eisenhart, K.S., Jarvis, D., Kulakowski, D., 2013. Drought induces spruce beetle (*Dendroctonus rufipennis*) outbreaks across northwestern Colorado. Ecology 95, 930–939.

Hart, S.J., Veblen, T.T., Mietkiewicz, N., Kulakowski, D., 2015. Negative feedbacks on bark beetle outbreaks: widespread and severe spruce beetle infestation restricts subsequent infestation. PLoS ONE 10, 16 p.

Hebertson, E.G., Jenkins, M.J., 2008. Climate Factors Associated with historic spruce beetle (Coleoptera: Curculionidae) outbreaks in Utah and Colorado. Environ. Entomol. 37, 281–292.

Hebertson, E.G., Jenkins, M.J., 2007. The influence of fallen tree timing on spruce beetle brood production. West. North Am. Nat. 67, 452–460.

Hicke, J.A., Johnson, M.C., Hayes, J.L., Preisler, H.K., 2012. Effects of bark beetle-caused tree mortality on wildfire. For. Ecol. Manag. 271, 81–90.

Hinds, T.E., Buffam, P.E., 1971. Blue stain in Engelmann spruce trap trees treated with cacodylic acid. US For. Serv Res Note RM. 4 p.

Holsten, E.H., Thier, R.W., Munson, A.S., Gibson, K.E., 1999. The spruce beetle. Forest Insect & Disease Leaflet 127. US Dep. Agric. Serv. Wash. DC.

Holsten, E.H., Werner, R.A., 1990. Comparison of white, Sitka, and Lutz spruce as hosts of the spruce beetle in Alaska. Can. J. For. Res. 20, 292–297.

Hooten, M.B., Hobbs, N.T., 2015. A guide to Bayesian model selection for ecologists. Ecol. Monogr. 85, 3–28.

Huberty, A.F., Denno, R.F., 2004. Plant water stress and its consequences for herbivorous insects: a new synthesis. Ecology 85, 1383–1398.

Hughes, J., Drever, R., Parks, C., 2001. Salvaging solutions: Science-based management of BC's pine beetle outbreak. David Suzuki Foundation, 39 p.

James, R.L., Goheen, D.J., 1981. Conifer mortality associated with root disease and insects in Colorado. Plant Dis. 65, 506–507.

Jenkins, M.J., Hebertson, E.G., Munson, A.S., 2014. Spruce beetle biology, ecology and management in the Rocky Mountains: An addendum to spruce beetle in the Rockies. Forests 5, 21–71.

Jenkins, M.J., Page, W.G., Hebertson, E.G., Alexander, M.E., 2012. Fuels and fire behavior dynamics in bark beetle-attacked forests in Western North America and implications for fire management. For. Ecol. Manag. 275, 23–34.

Joensson, A., Bärring, L., 2011. Future climate impact on spruce bark beetle life cycle in relation to uncertainties in regional climate model data ensembles. Tellus A 63, 158–173.

Kaiser, K.E., McGlynn, B.L., Emanuel, R.E., 2013. Ecohydrology of an outbreak: mountain pine beetle impacts trees in drier landscape positions first. Ecohydrology 6, 444–454.

Kärvemo, S., 2010. Population dynamics of tree-killing bark beetles-a comparison of the European spruce bark beetle and the North American mountain pine beetle. Introductory Research Essay, No. 10. Introd. Res. Essay SLU Dep. Ecol. Upps, 23 p.

Kausrud, K., Økland, B., Skarpaas, O., Grégoire, J.C., Erbilgin, N., Stenseth, N.C., 2012. Population dynamics in changing environments: the case of an eruptive forest pest species. Biol. Rev. 87, 34–51.

Keith, D.A., Akçakaya, H.R., Thuiller, W., Midgley, G.F., Pearson, R.G., Phillips, S.J., Regan, H.M., Araújo, M.B., Rebelo, T.G., 2008. Predicting extinction risks under climate change: coupling stochastic population models with dynamic bioclimatic habitat models. Biol. Lett. 4, 560–563.

Kelsey, R.G., Gallego, D., Sánchez-García, F.J., Pajares, J.A., 2014. Ethanol accumulation during severe drought may signal tree vulnerability to detection and attack by bark beetles. Can. J. For. Res. 44, 554–561.

Kleinman, S.J., DeGomez, T.E., Snider, G.B., Williams, K.E., 2012. Large-scale Pinyon Ips (*Ips confusus*) outbreak in southwestern United States tied with elevation and land cover. J. For. 110, 194–200.

Knight, F., 1958. The effects of woodpeckers on populations of the Engelmann spruce beetle. J. Econ. Entomol. 51, 603–607.

Knight, F.B., 1969. Egg production by the Engelmann spruce beetle, *Dendroctonus obesus*, in relation to status of infestation. Ann. Entomol. Soc. Am. 62, 448–448.

Knight, F.B., 1961. Variations in the life history of the Engelmann spruce beetle. Ann. Entomol. Soc. Am. 54, 209–214.

Kolb, T.E., Holmberg, K.M., Wagner, M.R., Stone, J.E., 1998. Regulation of ponderosa pine foliar physiology and insect resistance mechanisms by basal area treatments. Tree Physiol. 18, 375–381.

Kulakowski, D., Veblen, T.T., 2003. Subalpine forest development following a blowdown in the Mount Zirkel Wilderness, Colorado. J. Veg. Sci. 14, 653–660.

Kurz, W.A., Dymond, C.C., Stinson, G., Rampley, G.J., Neilson, E.T., Carroll, A.L., Ebata, T., Safranyik, L., 2008. Mountain pine beetle and forest carbon feedback to climate change. Nature 452, 987–990.

Larsson, S., 1989. Stressful times for the plant stress: Insect performance hypothesis. Oikos 56, 277–283.

Lewis, K.J., Lindgren, B.S., 2002. Relationship between spruce beetle and *tomentosus* root disease: two natural disturbance agents of spruce. Can. J. For. Res. 32, 31–37.

Logan, J.A., Bentz, B.J., 1999. Model analysis of mountain pine beetle (Coleoptera: Scolytidae) seasonality. Environ. Entomol. 28, 924–934.

Lundquist, J.E., Reich, R.M., 2014. Landscape dynamics of mountain pine beetles. For. Sci. 60, 464–475.

Lundquist, J.E., Reich, R.M., Tuffly, M., 2012. Spatial dynamics of the invasive defoliator Amber-marked Birch leafminer Across the Anchorage Landscape. J. Econ. Entomol. 105, 1659–1667.

MacArthur, R., Recher, H., Cody, M., 1966. On the relation between habitat selection and species diversity. Am. Nat. 100, 319–332.

Maroja, L.S., Bogdanowicz, S.M., Wallin, K.F., Raffa, K.F., Harrison, R.G., 2007. Phylogeography of spruce beetles (*Dendroctonus rufipennis* Kirby) (Curculionidae: Scolytinae) in North America. Mol. Ecol. 16, 2560–2573.

Massey, C., Wygant, N., 1954. Biology and control of the Engelmann spruce beetle in Colorado. Bark beetles fuels fire Bibliogr, 37 p.

Mattson, W.J., Haack, R.A., 1987. The role of drought in outbreaks of plant-eating insects. BioScience 110–118.

McCabe, G.J., Palecki, M.A., Betancourt, J.L., 2004. Pacific and Atlantic Ocean influences on multidecadal drought frequency in the United States. Proc. Natl. Acad. Sci. 101, 4136–4141.

McCambridge, W.F., Knight, F.B., 1972. Factors affecting spruce beetles during a small outbreak. Ecology 830–839.

McDonald, G.I., 1998. Preliminary report on the ecology of *Armillaria* in Utah and the inland west, in: Proceedings of the 46th Annual Western International Forest Disease Work Conference, Compiled by L. Trummer. USDA Forest Service, Region. pp. 85–92.

McDowell, N.G., 2011. Mechanisms linking drought, hydraulics, carbon metabolism, and vegetation mortality. Plant Physiol. 155, 1051–1059.

McDowell, N., Pockman, W.T., Allen, C.D., Breshears, D.D., Cobb, N., Kolb, T., Plaut, J., Sperry, J., West, A., Williams, D.G., Yepez, E.A., 2008. Mechanisms of plant survival and mortality during drought: why do some plants survive while others succumb to drought? New Phytol. 178, 719–739.

Meier, E.S., Kienast, F., Pearman, P.B., Svenning, J.-C., Thuiller, W., Araújo, M.B., Guisan, A., Zimmermann, N.E., 2010. Biotic and abiotic variables show little redundancy in explaining tree species distributions. Ecography 33, 1038–1048.

Merrill, R.M., Gutiérrez, D., Lewis, O.T., Gutiérrez, J., Díez, S.B., Wilson, R.J., 2008. Combined effects of climate and biotic interactions on the elevational range of a phytophagous insect. J. Anim. Ecol. 77, 145–155.

Miller, L.K., Werner, R.A., 1987. Cold-hardiness of adult and larval spruce beetles *Dendroctonus rufipennis* (Kirby) in interior Alaska. Can. J. Zool. 65, 2927–2930.

Mitchell, J.C., Schmid, J.M., 1973. Spruce beetle Coleoptera-Scolytidae-mortality from solar heat in cull logs of Engelmann spruce. J. Econ. Entomol. 66, 401–403.

Økland, B., Bjørnstad, O.N., 2006. A resource-depletion model of forest insect outbreaks. Ecology 87, 283–290.

Paine, T.D., Raffa, K.F., Harrington, T.C., 1997. Interactions among Scolytid bark beetles, their associated fungi, and live host conifers. Annu. Rev. Entomol. 42, 179–206.

Parmesan, C., Ryrholm, N., Stefanescu, C., Hill, J.K., Thomas, C.D., Descimon, H., Huntley, B., Kaila, L., Kullberg, J., Tammaru, T., Tennent, W.J., Thomas, J.A., Warren, M., 1999. Poleward shifts in geographical ranges of butterfly species associated with regional warming. Nature 399, 579–583.

Perez, L., Dragicevic, S., 2010. Modeling mountain pine beetle infestation with an agent-based approach at two spatial scales. Environ. Model. Softw. 25, 223–236.

Pielou, E.C., 1977. The latitudinal spans of seaweed species and their patterns of overlap. J. Biogeogr. 4 299–311.

Pongpattananurak, N., Reich, R.M., Khosla, R., Aguirre-Bravo, C., 2012. Modeling the spatial distribution of soil texture in the State of Jalisco, Mexico. Soil Sci. Soc. Am. J. 76, 199.

Raffa, K.F., Aukema, B.H., Bentz, B.J., Carroll, A.L., Hicke, J.A., Turner, M.G., Romme, W.H., 2008. Cross-scale drivers of natural disturbances prone to anthropogenic amplification: The dynamics of bark beetle eruptions. BioScience 58, 501–517.

Raffa, K.F., Aukema, B.H., Erbilgin, N., Klepzig, K.D., Wallin, K.F., 2005. Interactions among conifer Terpenoids and bark beetles across multiple levels of scale: An attempt to understand links between population patterns and physiological processes, in: Romeo, J.T. (Ed.), Recent Advances in Phytochemistry, Chemical Ecology and Phytochemistry of Forest Ecosystems. Elsevier, 79–118.

Reich, R.M., Aguirre-Bravo, C., Bravo, V.A., 2008. New approach for modeling climatic data with applications in modeling tree species distributions in the states of Jalisco and Colima, Mexico. J. Arid Environ. 72, 1343–1357.

Reich, R.M., Aguirre-Bravo, C., Bravo, V.A., Briseño, M.M., 2011. Empirical evaluation of confidence and prediction intervals for spatial models of forest structure in Jalisco, Mexico. J. For. Res. 22, 159–166.

Reich, R.M., Aguirre-Bravo, C., Briseño, M.A.M., 2008. An innovative approach to inventory and monitoring of natural resources in the Mexican State of Jalisco. Environ. Monit. Assess. 146, 383–396.

Reich, R.M., Bonham, C.D., Aguirre-Bravo, C., Chazaro-Basañeza, M., 2010. Patterns of tree species richness in Jalisco, Mexico: relation to topography, climate and forest structure. Plant Ecol. 210, 67–84.

Reich, R.M., Lundquist, J.E., Acciavatti, R.E., 2014. Influence of climatic conditions and elevation on the spatial distribution and abundance of *Trypodendron* ambrosia beetles (Coleoptera: Curculionidae: Scolytinae) in Alaska. For. Sci. 60, 308–316.

Reich, R.M., Lundquist, J.E., Bravo, V.A., 2013. Characterizing spatial distributions of insect pests across Alaskan forested landscape: A case study using aspen leaf miner (*Phyllocnistis populiella* Chambers). J. Sustain. For. 32, 527–548.

Reich, R.M., Lundquist, J.E., Hughes, K., 2016. Host-environment mismatches associated with subalpine fir decline in Colorado. J. For. Res, 13 p.

Reynolds, K.M., Holsten, E.H., 1994. Relative importance of risk factors for spruce beetle outbreaks. Can. J. For. Res. 24, 2089–2095.

Rouault, G., Candau, J.-N., Lieutier, F., Nageleisen, L.-M., Martin, J.-C., Warzée, N., 2006. Effects of drought and heat on forest insect populations in relation to the 2003 drought in Western Europe. Ann. For. Sci. 63, 12 p.

Royle, J.A., Kéry, M., Gautier, R., Schmid, H., 2007. Hierarchical spatial models of abundance and occurrence from imperfect survey data. Ecol. Monogr. 77, 465–481.

Sambaraju, K.R., Carroll, A.L., Zhu, J., Stahl, K., Moore, R.D., Aukema, B.H., 2012. Climate change could alter the distribution of mountain pine beetle outbreaks in western Canada. Ecography 35, 211–223.

Schmid, J., Amman, G., 1992. *Dendroctonus* beetles and old-growth forests in the Rockies. For. Southwest Rock Mt. Reg. Proc. Workshop, 51–59.

Schmid, J., Frye, R., 1977. Spruce beetle in the Rockies. Bark Beetles Fuels Fire Bibliogr.

Seager, R., Ting, M., Held, I., Kushnir, Y., Lu, J., Vecchi, G., Huang, H.-P., Harnik, N., Leetmaa, A., Lau, N.-C., Li, C., Velez, J., Naik, N., 2007. Model projections of an imminent transition to a more arid climate in Southwestern North America. Science 316, 1181–1184.

Sherriff, R.L., Berg, E.E., Miller, A.E., 2011. Climate variability and spruce beetle (*Dendroctonus rufipennis*) outbreaks in south-central and southwest Alaska. Ecology 92, 1459–1470.

Shono, H., 2008. Confidence interval estimation of CPUE year trend in delta-type two-step model. Fish. Sci. 74, 712–717.

Six, D.L., Bentz, B.J., 2003. Fungi associated with the North American spruce beetle, *Dendroctonus rufipennis*. Can. J. For. Res. 33, 1815–1820.

Smith, J.M., Paritsis, J., Veblen, T.T., Chapman, T.B., 2015. Permanent forest plots show accelerating tree mortality in subalpine forests of the Colorado Front Range from 1982 to 2013. For. Ecol. Manag. 341, 8–17.

Solheim, H., 1994. A comparison of blue-stain fungi associated with the North American spruce beetle *Dendroctonus rufipennis* and the Eurasian spruce bark beetle *Ips typographus*, in: Forest Pathology Research in the Nordic Countries. Proceedings from the SNS Meeting in Forest Pathology, Norway, 9–12.

Tabacaru, C.A., Park, J., Erbilgin, N., 2016. Prescribed fire does not promote outbreaks of a primary bark beetle at low-density populations. J. Appl. Ecol. 53, 222–232.

Trần, J.K., Ylioja, T., Billings, R.F., Régnière, J., Ayres, M.P., 2007. Impact of minimum winter temperatures on the population dynamics of *dendroctonus frontalis*. Ecol. Appl. 17, 882–899.

Turner, M.G., 1989. Landscape ecology: The effect of pattern on process. Annu. Rev. Ecol. Syst. 20, 171–197.

Veblen, T.T., Hadley, K.S., Reid, M.S., 1991. Disturbance and stand development of a Colorado subalpine forest. J. Biogeogr 18, 707–716.

Wallin, K.F., Raffa, K.F., 2004. Feedback between individual host selection behavior and population dynamics in an eruptive herbivore. Ecol. Monogr. 74, 101–116.

Wallin, K.F., Raffa, K.F., 2000. Influences of external chemical cues and internal physiological parameters on the multiple steps of post-landing host selection behavior of *Ips pini* (Coleoptera: Scolytidae). Environ. Entomol. 29, 442–453.

Wang, L., Chen, L., Nieto, J.J., 2010. The dynamics of an epidemic model for pest control with impulsive effect. Nonlinear Anal. Real World Appl. 11, 1374–1386.

Werner, R.A., Holsten, E.H., Matsuoka, S.M., Burnside, R.E., 2006. Spruce beetles and forest ecosystems in south-central Alaska: A review of 30 years of research. For. Ecol. Manag. 227, 195–206.

Werner, R.A., Illman, B.L., 1994. Response of Lutz, Sitka, and white spruce to attack by *Dendroctonus rufipennis* (Coleoptera: Scolytidae) and Blue Stain Fungi. Environ. Entomol. 23, 472–478.

Williams, A.P., Allen, C.D., Macalady, A.K., Griffin, D., Woodhouse, C.A., Meko, D.M., Swetnam, T.W., Rauscher, S.A., Seager, R., Grissino-Mayer, H.D., others, 2013. Temperature as a potent driver of regional forest drought stress and tree mortality. Nat. Clim. Change 3, 292–297.

Williams, D.W., Liebhold, A.M., 2002. Climate change and the outbreak ranges of two North American bark beetles. Agric. For. Entomol. 4, 87–99.

Wood, S.L., 1963. A revision of the bark beetle genus *Dendroctonus Erichson* (Coleoptera: Scolytidae). Gt. Basin Nat. 23, 1–117.

Wygant, N.D., 1956. Engelmann spruce beetle control in Colorado, in: Proceedings of the 10th International Congress of Entomology, 181–184.

Wygant, N.D., Lejeune, R.R., 1967. Engelmann Spruce Beetle *Dendroctonus obesus* (Mann.)(*D. engelmannii* Hopk.). Important For. Insects Dis. Mutual Concern Can. U. S. Mex. Can, 248 p.

Zimmermann, N.E., Kienast, F., 1999. Predictive mapping of alpine grasslands in Switzerland: Species versus community approach. J. Veg. Sci. 10, 469–482.

Zuur, A.F., Ieno, E.N., Walker, N.J., Saveliev, A.A., Smith, G.M., 2009. Mixed effects modelling for nested data, in: Mixed effects models and extensions in Ecology with R, Statistics for Biology and Health. Springer New York, 101–142.

CHAPTER 2

ESTIMATING SPRUCE FOREST AND SPRUCE MORTALITY PROBABILITY AND

QUANTIFYING CLIMATIC MISMATCH BETWEEN HOST AND MORTALITY IN

COLORADO AND ALASKA

Introduction

The spruce bark beetle (*Dendroctonus rufipennis* Kirby, Family: Curculionidae) is one of the most destructive forest insects, causing large-scale forest mortality in North America (Bentz et al., 2009; Berg et al., 2006). Spruce beetle outbreak exists from the spruce forest of Alaska to the high-elevation subalpine forest of the Rocky Mountains (Jenkins et al., 2014; Schmid and Frye, 1977; Werner et al., 2006). The spruce beetle infests nearly all species of the genus *Picea.* In Alaska this includes white spruce [*P. glauca* (Moench) Voss], Sitka spruce [*P. sitchensis* (Bong.) Carr], and Lutz's spruce (*P. x lutzii* Little) (Holsten and Werner, 1990; Schmid and Frye, 1977). Engelmann spruce (*P. engelmannii* Parry ex Engelm.) is the only host species in the Rockies for the spruce bark beetle.

Hart et al. (2013) expressed that prolonged climatic factors causing physiological stress are associated with most historic spruce beetle outbreaks. Climate patterns across the landscape affect both precipitation and temperature at the local and temporal scale. Even though precipitation and temperature are not direct causes of forest mortality, plant physiological stress might occur from the contribution of these suboptimal exogenous factors. Suboptimal climatic factors can act as predisposing factors that provide a higher likelihood of short-term inciting factors, such as drought, and that allow opportunistic contributing factors such as insects and diseases to overcome host plant defenses (Bentz et al., 2010; Hart et al., 2013). However, the influences of the mortality-inducing factors and their interactions are not well understood in the spatial context.

31

It is difficult to specify the complex interactions between the roles of biotic causal agents and exogenous environmental factors in spruce mortality due to bark beetle outbreak because these factors and the occurrence of mortality have a high variability at the spatial and temporal scales. At the landscape scale, the distribution of outbreaks is spatially designated to specific climate zones, which specify suboptimal marginal population zone where there is a mismatch of suitable conditions between host and causal agent, implying host population is not adaptive to the condition favoring the causal agent population. The presence of spruce mortality depends on interaction between climate factors, including precipitation and temperature, where the host and the causal agents both encounter climate conditions favoring the occurrence of mortality. A suboptimal climatic condition for a marginal host population could have detrimental effects of either physiological stress on the host or promotion of growth and development of causal agent population. A suitable climatic condition might increase the populations of spruce beetles and associated organisms. The large population of causal agents then becomes overwhelming to defensive mechanisms of host.

In this study, we assign spatially explicit data to each climate zone using Climate Transition Matrices (CTMs) to describe the relationship between the occurrences of host and mortality and climatic factors. CTMs are visualized using a two-way table, where columns represent precipitation zones and rows represent temperature zones. A particular climate zone is defined by a specific pair of temperature and precipitation. Each element of the table represents the probability of observing host, host mortality, and the quantified mismatches between host and mortality, differential effects, in a given climate zone. The benefits of using climate zones are (1) the opportunity to examine the roles of each climate factor on outbreak dynamics across the landscape (Aquirre-Bravo and Reich, 2006; Reich et al., 2014) and (2) the ability to reduce the temporal variability and model error by using exact measurement predictions for climate covariates. The idea of climate zones has been used in many previous researches. Reich et al. (2010) defined climate zones for a natural resources monitoring program in Jalisco, Mexico. The program has been used to model composition of soil textures (Pongpattananurak et al., 2012), to model the influence of climate on the richness of tree species (Reich et al., 2008), to model forest stand structure

32

(Reich et al., 2011), to model the abundance of damage agent by forest type (Masoud, 2012), and to determine the influence of climate on forest insects in Alaska (Reich et al., 2013). Reich et al (2016) applied climate transition matrices (CTM) to represent the environmental mismatch between host and subalpine fir decline.

In this study, I create separate CTMs to represent the combination of two climatic factors and use them to identify the influence of climate on the presence of spruce forest and spruce mortality in Colorado and Alaska. We hypothesize that spruce mortality will be more commonly observed in a more severe climate zone or in a climate zone that is extremely different from the optimum by asking three questions from the critical method proposed by Reich and colleagues (2016) to describe interaction between climate and outbreaks:

1. How do varying climatic conditions influence the distribution of spruce forest in the forested landscape of the Colorado and Alaska?

2. How do varying climatic conditions influence the distribution of spruce mortality in the forested landscape of the Colorado and Alaska?

3. How can climatic conditions influence the climatic mismatches represented by differential effects between spruce forests and the causal agents of spruce mortality across the landscape of the Colorado and Alaska?

Methods

Establishing spruce forest and spruce mortality extent

Data from the raster layer of the vegetation cover were obtained from the Colorado Division of Wildlife as part of the Gap Analysis Program (http://ndis1.nrel.colostate.edu/cogap/cogaphome.html) to analyze the spruce forest (*P. engelmanni*) in Colorado, while data from the raster layer of major vegetation types were obtained from the Department of Natural Resources of Alaska to analyze spruce forest in Alaska, including *P. mariana, P. glauca,* and *P. sitchensis*. The raster layers containing spruce species were selected and converted into a binary raster representing the presence and absence of spruce forest. Data from Colorado were converted into raster data with 30 meters of spatial resolution; the

smallest feature that can be accurately delineated is one acre (Herold, 2011), which is also the minimum

mapping unit for aerial forest health surveys (Johnson and Ross, 2008). Alaska data were resampled into

raster data with 1,000 meters of spatial resolution for the convenience of computing a large study area.

Raster data on spruce forest presence were clipped in polygons to cover the area of Colorado, excluding

the area where forest is absent (e.g., the Great Plains in eastern Colorado) to reduce data redundancy. The

whole extent of mainland Alaska and nearby islands was studied for the presence of spruce forest because

spruce species are commonly distributed across the Alaskan landscape.

Feature layers of Colorado aerial pest survey maps, produced by Region 2 Forest Health

Protection from 1994 to 2013, were obtained from the United States Forest Service to identify forest

insects and diseases in Colorado. Layers of Alaska aerial pest survey maps, produced by Region 10 Forest

Health Protection of the United States Forest Service from 1989 to 2010, were obtained to identify the

presence of forest insects and diseases from the aerial survey flight line in Alaska. Feature data for spruce

mortality due to spruce beetle outbreaks were extracted from the data of each polygon. Spruce mortality

usually appears as a single species patch, mixed subalpine species patch, or scattered across the

landscape. The polygon pattern of spruce mortality is related to the method in aerial surveys, in which

observed forest mortality events are grouped into polygons by the observers (Johnson and Ross, 2008).

Individual feature layers for each year were joined to obtain an estimated total accumulated area

of spruce mortality, and, using ArcGIS 10, the layer was converted to raster data with a 30-meter spatial

resolution for Colorado and 1,000 meters for Alaska (ESRI, 2011). The "majority" rule was used in

converting polygons to raster data: each cell was assigned the value of the polygon occupying the

majority in the cell area. Some of the minor polygons were ignored in assigning cell value; Wade et al.

(2003) observed no significant differences and no substantial information loss from landscape metrics

using this conversion method.

Establishing climate zones

Thirty-six unique climate zones (Figure 1) and six temperature zones including six precipitation

zones were defined for Colorado area using 30-meter spatial resolution raster data from the predicted

climate model. The climate model was composed using average monthly temperature (°C) and

precipitation (mm) data of the past 50 years from previous study (Aquirre-Bravo and Reich, 2006).

Climate data for Alaska were obtained from average monthly climate data produced by the United States

Geological Survey Alaska Science Center with a resolution of 1,000 meters. Monthly average

temperature and precipitation were partitioned into 25 unique zones (Figure 2) and five temperature zones

with five precipitation zones, as in the study completed by Reich et al. (2014). To define the climate

zones, a histogram equalization approach was used to partition the average monthly climate data by

uniform distribution across the study area (Acharya and Ray, 2005). There is a strong linear relationship

between defined climate zone and original average monthly climate data (Acharya and Ray, 2005; Reich

et al., 2014). Zonal statistics were used to summarize climate data for each climate zone in Colorado

(Table 1) and Alaska (Table 2). To prepare climate zone raster data for the calculation of conditional

probability given spruce forest presence, the raster layers of climate zones in Colorado were clipped to the

extent that spruce forest is present to create the layers of climate zones within the area with spruce

present. Statewide climate zone layers of Alaska were clipped by aerial survey flight transect zone and

layer of spruce forest presence in flight transect.

Calculating spruce forest and spruce mortality probability

      To estimate the probability of observing spruce forest in each climate zone, the binary raster layer

represents the presence (1) or absence (0) of spruce forest intersecting with climate zones. Probability was

calculated by averaging the binary layer in each climate zone using zonal statistics (ESRI, 2011). The

probability of observing spruce forest in a given climate zone, $P(S|C_i)$, can be calculated as the ratio of

the area (or number of cells) of spruce forest presence in a classified climate zone, $A(S_{c_i})$, and total area

in that climate zone, $A(C_i)$ (Equation 1). Each CTM element was populated by this information, with

rows representing temperature zones and columns representing precipitation zones (Reich et al., 2014).

$$P(S|C_i) = \frac{A(S_{c_i})}{A(C_i)} \tag{1}$$

The probability of observing spruce mortality in a given climate zone, $P(D|C_i)$, was calculated in the same way as the probability of observing spruce forest in a given climate zone, $P(S|C_i)$. The binary layer of spruce mortality presence-absence was intersected with climate zones. Probability was calculated by averaging of presence and absence of spruce mortality in each climate zone using zonal statistics. The probability of observing spruce mortality in a given climate zone, $P(D|C_i)$, can be calculated as the ratio of the area (or number of cells) of spruce mortality in a classified climate zone, $A(D_{c_i})$, and total area in that climate zone, $A(C_i)$ (Equation 2). For layers of Alaska, which the mortality data is conditional on flight lines, the probabilities of mortality were calculated within the total area, $A(C_i)$, given by the area that is covered by flight lines. The conditional probability of observing spruce mortality given spruce forest presence for each climate zone, $P(D|S, C_i)$, was also calculated as the ratio of the intersected area of spruce mortality in a given climate zone, $A(D_{c_i})$, and total area of spruce forest in that climate zone, $A(S|C_i)$ (Equation 3). Each CTM element was populated from the estimated information, with rows representing temperature zones and columns representing precipitation zones.

$$P(D|C_i) = \frac{A(D_{c_i})}{A(C_i)} \tag{2}$$

$$P(D|S, C_i) = \frac{A(D_{c_i})}{A(S|C_i)} \tag{3}$$

To quantify the influence of climate factors on the distribution of spruce forest and spruce mortality, linear second-degree polynomial and third-degree polynomial regression models were developed to estimate the natural logarithm of rescaled probabilities on the CTMs as a function of the integers representing temperature zones, T, and precipitation zones, P. The natural logarithm transformation was used to stabilize the variability in probabilities.

Differential effects of climate on spruce mortality probability

The influence of climatic factors on the probability of observing active spruce mortality from spruce bark beetle outbreaks can be assessed by an index measuring the differential effects of climate between the probability of spruce forest and spruce mortality. Firstly, we created a null hypothesis to

define this index by assuming that the mortality in the defined area (or number of cells) is proportional to the host availability in the defined area and is independent from climatic conditions. We presume that host distribution may be influenced by the climatic conditions, while the distribution of causal agent might be influenced by availability of host within climate zones, climatic conditions, or the combination of both. We can quantify this relationship in terms of probabilities and conditional probability by comparing the probability of spruce forest given climate zone, $P(S|C_i)$, with the conditional probability of spruce mortality conditional on host presence in a given climate zone, $P(D|S, C_i)$ (Equation 4).

$$P(D|S, C_i) = \alpha P(S|C_i) \tag{4}$$

where α is a constant, thought of as the intrinsic rate of increase for the difference in proportion of probability. In this study, we normalized the scale of probability values on both sides by dividing the individual probabilities in an element of a given CTM by the maximum probability of the CTM. In this case, we divide $P(D|S, C_i)$ by $P_{max}(D|S, C_i)$ and divide $\alpha P(S|C_i)$ by $\alpha P_{max}(S|C_i)$ (Equation 5). Because the scale of probabilities was normalized, α was also canceled out, providing the rescaled probabilities, $P_r(D|S, C_i)$ and $P_r(S|C_i)$, on both sides of equation to be on the same scale. Then we made a simple expression for evaluating the effects of climate on the probability of spruce mortality from this equation (Equation 6).

$$\frac{P(D|S, C_i)}{P_{max}(D|S, C_i)} = \frac{\alpha P(S|C_i)}{\alpha P_{max}(S|C_i)} \tag{5}$$

$$P_r(D|S, C_i) = P_r(S|C_i) \tag{6}$$

Under the null hypothesis that probability of observing host mortality is proportional to host availability, the rescaled probabilities on both sides of the equation are equal. If the probabilities are not equal, we can consider the null hypothesis to be false. The new variable, Δ_i, for each climate zone, i, was added to the equation to represent the deviation from the null hypothesis. Δ_i was calculated from the difference between $P_r(D|S, C_i)$ and $P_r(S|C_i)$ (see Equations 7 and 8).

$$P_r(D|S, C_i) + \Delta_i = P_r(S|C_i) \tag{7}$$

$$\Delta_i = P_r(S|C_i) - P_r(D|S, C_i) \tag{8}$$

The differential effects that climate has on the probability of spruce mortality, Δ_i ranges in value

from –1 to 1. If $\Delta_i = 0$, spruce mortality probability is assumed null. Positive values of Δ_i indicate that

spruce mortality probability is lower than expected, implying that the host has a competitive advantage

over the spruce bark beetle in adapting to climate. Negative values of Δ_i indicate that the mortality

probability is higher than expected, implying that the spruce beetle and its complex mutualism have a

competitive advantage over the spruce host in climatic adaptation.

Secondly, the regression models were developed to assess the influences of climatic factors on

the distribution of host and mortality across different climate zones in Colorado and Alaska. The models

were developed to regress on each CTM element for the rescaled probability of observing spruce forest,

$P_r(S|C_i)$, the rescaled probability of observing spruce mortality conditional on observing spruce forest,

$P_r(D|S, C_i)$, and the differential effect, Δ_i. The climate raster layers were then used to calculate the

estimated probabilities and differential effects to obtain area estimates associated with seven score levels

representing the competitive climatic adaptation between spruce host and spruce beetle:

1. High advantage for spruce host: $\Delta_i > 0.7$

2. Medium advantage for spruce host: $0.4 < \Delta_i < 0.7$

3. Low advantage for spruce host: $0.15 < \Delta_i < 0.4$

4. No advantage for either (null hypothesis): $-0.15 < \Delta_i < 0.15$

5. Low advantage for spruce beetle: $-0.4 < \Delta_i < -0.15$

6. Medium advantage for spruce beetle: $-0.7 < \Delta_i < -0.4$

7. High advantage for spruce beetle: $\Delta_i < -0.7$

Regression model and model selection

To account for the influence of climate on the variability in probability of observing spruce forest and

spruce mortality, the ordinary least squares (OLS) approach was applied to create the regression function.

A spatial autoregressive (SAR) model was also used to account for spatial structure among the

probabilities within the CTMs. The spatial autocorrelation within CTMs does not account for spatial association between locations in the landscape, but it does account for similarity among climate zones. The OLS model used to estimate the parameters of the model can be formulated as the following (Reich and Davis, 2008):

$$Y = X\beta + \varepsilon \tag{9}$$

$$\varepsilon \sim Normal(0, \sigma^2) \tag{10}$$

where Y is a column vector of the natural logarithm of the probability of observing spruce forest and spruce mortality; X is a design matrix representing covariates of climate data, temperature zones ($T = 1, 2, 3, 4, 5, 6$ and $T = 1, 2, 3, 4, 5$ for Colorado and Alaska, respectively), and precipitation zones ($P = 1, 2, 3, 4, 5, 6$ and $P = 1, 2, 3, 4, 5$ for Colorado and Alaska, respectively); β is a vector of regression coefficients; and ε is a vector of regression errors arising from independent and identically normal distributions with zero mean and σ^2 variance. The SAR model used to account for similarity among climate zones can be formulated as the following (Reich and Davis, 2008; Upton and Fingleton, 1985):

$$Y = X\beta + \varepsilon \tag{11}$$

$$\varepsilon = \lambda W \epsilon + \eta \tag{12}$$

$$\eta \sim Normal(0, \sigma^2) \tag{13}$$

where Y is the vector of dependent variables for the rescaled probability of observing spruce forest, spruce mortality, and differential effects; X is a design matrix of climate covariates; β is a vector of the regression coefficients; ε is an overall error term in regressing Y on X; ϵ is a spatially correlated error portion of the error term; η is a spatially independent error portion of the error arising from normal distribution with zero mean and σ^2 variance; W is a binary spatial weights matrix used to define the spatial joins of the 6×6 and 5×5 CTMs for Colorado and Alaska, respectively [spatial join was defined by the first-degree neighbors of chess moves for a rook (up, down, left, right)]; and λ, a value between –1 and 1, is a measure of the degree of spatial autocorrelation. A backward stepwise Akaike Information

Criterion (AIC) model selection algorithm was used to select the climate variables (temperature and precipitation zones), the higher degree of climate variables (through third-degree polynomial), and the interaction among climate variables to include in the final models. A likelihood ratio test was applied to test the null hypothesis that the SAR model is an improvement over the OLS model (Reich and Davis, 2008) (Equation 14).

$$\text{Likelihood ratio} = \frac{l(\lambda, \ \hat{\beta}_{MLE}, \hat{\sigma}^2_{MLE})}{l(0, \ \hat{\beta}_{MLE}, \hat{\sigma}^2_{MLE})} \tag{14}$$

where $l(0, \ \hat{\beta}_{MLE}, \hat{\sigma}^2_{MLE})$ is the maximum natural log likelihood for the OLS model and $l(\lambda, \ \hat{\beta}_{MLE}, \hat{\sigma}^2_{MLE})$ is the maximum natural log likelihood for the SAR model. Moran's I (Equation 15) was used to test the spatial autocorrelation between the regression's residuals, which has the null hypothesis that regression errors are spatially independent ($H_0: \lambda = 0$). P-values of the spatially independent hypothesis testing were calculated under the randomization assumption, given that each permutation has an equal probability to occur (Reich and Davis, 2008; Upton and Fingleton, 1985). The calculation of continuous Moran's I is as follows:

$$I = \frac{n}{2A} \frac{\sum_{i=1}^{n} \sum_{j=1}^{n} \delta_{ij}(Z_i - \bar{Z})(Z_j - \bar{Z})}{\sum_{i=1}^{n}(Z_i - \bar{Z})^2} \tag{15}$$

where Z_i and Z_j are continuous data, residuals in our study, of location i and neighboring location j of the total n locations; δ_{ij} is the indicator that i and j are joined to the spatially weighted matrix (W); and A is the total number of neighbors joined in the data.

A new set of CTMs was created from the predicted rescaled probability of observing spruce forest, $P(S|C_i)$, spruce mortality, $P(D|C_i)$, and differential effects of spruce mortality, Δ_i, in a given climate zone by the fitted regression model. The CTMs based on the predicted values of the regression models were used to develop raster layers representing the distribution of expected probabilities across the landscape. All regression models were developed by the spatial library of R (R Core Team, 2014).

Results

Influences of climatic factors on the distribution of spruce forest

Spruce species are a major component of the alpine forested landscape in Colorado (Figure 3) and throughout Alaska (Figure 4). The CTMs of rescaled probabilities of observing spruce forest were calculated using the area (number of cells) of observed spruce forest in a given climate zone for Colorado (Table 3) and Alaska (Table 7). In Colorado, spruce forest is present in 32 of 36 climate zones, excluding the driest, coldest climate and the wettest, warmest climate. In Alaska, spruce forest is present in 24 of 25 climate zones, excluding the driest, warmest climate.

The third-degree polynomial function of OLS regression and SAR were applied as a full model to account for the variability in rescaled probability of observing spruce forest in a given climate zone, $P_r(S|C_i)$, for Colorado (Table 11). The OLS model accounted for 92% of the variability in rescaled probability of observing spruce forest in a given climate zone. Because the residuals from the OLS model were spatially correlated (Moran's I = –0.47, p-value = <0.001), the SAR model did significantly improve over the OLS model (likelihood ratio = 13, p-value = < 0.001) and accounted for 99% of the variability in rescaled probability of observing spruce forest, with 95% correlation between predicted and observed probabilities. The probability of observing spruce forest in Colorado was highest in the region with a climate characterized by moderate temperature (T = 2, 3, and 4) and high precipitation (P = 5 and 6). The lowest probability of observing spruce forest was in the zone characterized by either extremely low or high temperature (T = 1, 5, and 6) and low precipitation (P = 1 and 2) (Table 3). Geographically, the probability of observing spruce forest was highest in the central Rocky Mountain region (Figure 3).

The third-degree polynomial function of OLS regression and SAR were applied as a full model to account for the variability in rescaled probability of observing spruce forest in a given climate zone, $P_r(S|C_i)$, for Alaska (Table 15). The OLS model accounted for 97.43% of the variability in rescaled probability of observing spruce forest in a given climate zone. Because the residuals from the OLS model were spatially correlated (Moran's I = –0.4881, p-value = 0.003), the SAR model did significantly

41

improve over the OLS model (likelihood ratio = 15.51, p-value = < 0.001) and accounted for 99.8% of the variability in rescaled probability of observing spruce forest, with 99.03% correlation between predicted and observed probabilities. The probability of observing spruce forest in Alaska was highest in the region with a climate characterized by moderate temperature (T = 2, 3, and 4) and moderate precipitation (P = 2 and 3). The lowest probability of observing spruce forest was in the zone characterized by extremely low temperature (T = 1) and high precipitation (P = 5) (Table 7). The probability of observing spruce forest in Alaska was shown in Figure 4.

Influences of climatic factors on the distribution of spruce mortality

The CTMs of rescaled probabilities of observing spruce mortality were calculated using the area (number of cells) of observed spruce mortality in a given climate zone for Colorado and Alaska. The pattern of observed spruce mortality is similar to the pattern of observed spruce forest in a climate zone. In Colorado, spruce forest is present in 25 of 36 climate zones (Table 4). In Alaska, spruce forest is present in 16 of 25 climate zones (Table 8).

The third-degree polynomial function of OLS regression and SAR were applied as a full model to account for variability in rescaled probability of observing spruce mortality in a given climate zone, $P_r(D|C_i)$, for Colorado (Table 12). The OLS model accounted for 74.7% of variability in rescaled probability of observing spruce mortality in a given climate zone. Because residuals from the OLS model have some degree of spatial autocorrelation (Moran's I = –0.254, p-value = 0.091), the SAR model did significantly improve over the OLS model (likelihood ratio = 5.24, p-value = 0.022) and accounted for 94.7% of the variability in rescaled probability of observing spruce mortality, with 80.8% correlation between predicted and observed probabilities. The probability of observing spruce mortality in Colorado was highest in the region with a climate characterized by moderate to low temperature (T = 2 and 3) and high precipitation (P = 6). The lowest probability of observing spruce mortality was in the zone characterized by either extremely low or high temperature (T = 1, 5, and 6) and low precipitation (P = 1) (Table 4). Geographically, the probability of observing spruce forest was highest in the central mountain region of Colorado.

The third-degree polynomial function of OLS regression and SAR were applied as a full model to account for the variability in rescaled probability of observing spruce mortality in a given climate zone, $P_r(D|C_i)$, for Alaska (Table 16). The OLS model accounted for 79.98% of the variability in rescaled probability of observing spruce mortality in a given climate zone. Because residuals from the OLS model have some degree of spatial autocorrelation (Moran's I = –0.309, p-value = 0.085), the SAR model did significantly improve over the OLS model (likelihood ratio = 5.491, p-value = 0.019) and accounted for 96.94% of the variability in rescaled probability of observing spruce mortality, with 86.25% correlation between predicted and observed probabilities. The probability of observing spruce mortality in Alaska was highest in the region with a climate characterized by high temperatures (T = 4 and 5) and high precipitation (P = 4 and 5), excluding the wettest and warmest climate zone (T = 5 and P = 5). The lowest probability of observing spruce mortality was in the zones characterized by extremely low temperature (T = 1 and 2), regardless of precipitation, and those with the highest temperature and low precipitation (T = 5 and P = 2) (Table 8). Geographically, the probability of observing spruce mortality was highest in the coastal region and lowest in the northern region of Alaska (Figure 4).

Influences of climatic factors on the distribution of spruce mortality conditional on spruce forest presence

To measure the impact of spruce mortality, conditional probabilities of spruce mortality on the presence of spruce forest were applied to account for climatic influences in Colorado (Table 5) and Alaska (Table 9). The conditional probabilities were calculated in the climate zones with available spruce forest, 32 out of 36 climate zones for Colorado, with most absences at the CTM's bottom left, and 24 out of 25 climate zones in Alaska, with most absences in the coldest climate zone regardless of precipitation.

The third-degree polynomial function of OLS regression and SAR were applied as a full model to account for the variability in rescaled conditional probability of observing spruce mortality given the presence of spruce forest in a given climate zone, $P_r(D|S, C_i)$, for Colorado (Table 13). The OLS model accounted for 69.18% of the variability in rescaled conditional probability of observing spruce mortality given the presence of spruce forest in a given climate zone. Because residuals from the OLS model are

spatially independent (Moran's I = 0.023, p-value = 0.677), the SAR model did not significantly improve over the OLS model (likelihood ratio = 0.035, p-value = 0.851) and accounted for 79.02% of the variability in rescaled conditional probability of observing spruce mortality given the presence of spruce forest, with 68.94% correlation between predicted and observed probabilities. The conditional probability of observing spruce mortality given spruce forest presence in Colorado was highest in the region with a climate characterized by low temperature (T = 1, 2 and 3) and high precipitation (P = 4, 5, and 6). The lowest conditional probability of observing spruce mortality given spruce forest presence was in the zone characterized by either extremely low or high temperature (T = 5 and 6) and low precipitation (P = 1); the highest temperature zone showed low probabilities regardless of precipitation. There was evidence of climate shift between conditional and unconditional probabilities of observing spruce mortality. The probabilities increased most in the low temperature zones with moderate precipitation (Table 5).

The third-degree polynomial function of OLS regression and SAR were applied as a full model to account for the variability in rescaled conditional probability of observing spruce mortality given the presence of spruce forest in a given climate zone, $P_r(D|S, C_i)$, for Alaska (Table 17). The OLS model accounted for 84.92% of the variability in rescaled conditional probability of observing spruce mortality given the presence of spruce forest in a given climate zone. Despite the fact that residuals from the OLS model are spatially independent (Moran's I = –0.248, p-value = 0.190), the SAR model did significantly improve over the OLS model (likelihood ratio = 3.943, p-value = 0.047) and accounted for 97.6% of the variability in rescaled conditional probability of observing spruce mortality given the presence of spruce forest, with 88.69% correlation between predicted and observed probabilities. The conditional probability of observing spruce mortality given spruce forest presence in Alaska was highest in the region with a climate characterized by moderate to high temperature (T = 4) and high precipitation (P = 5). The lowest conditional probability of observing spruce mortality given spruce forest presence was in the zone characterized by low temperature (T = 1 and 2), regardless of precipitation (Table 9). There was no evidence of significant climate shift between conditional and unconditional probabilities of observing spruce mortality.

Differential effects of climatic factors on spruce mortality

The differential effects of climate on spruce mortality given the availability of spruce forest were calculated by subtracting the rescaled probability of observing spruce forest by the rescaled conditional probability of observing spruce mortality given spruce forest presence (Table 6 and Table 10). Differential effects were estimated using the regression models with climate covariates. Positive values indicate a differential increase that the probability of mortality is below the host availability, while negative values indicate a differential increase that the probability of mortality is above the host availability. Values near zero ($-0.15 < \Delta_i < 0.15$) indicate that the mortality proportionally increases with host availability (null hypothesis). For Colorado, the climate zones that satisfy the negative differential effects (probability of mortality is higher than expected) cover the majority of the CTM. The climate zones satisfying positive values (probability of mortality is lower than expected) are those with moderate temperature (T = 3 and 4) and high precipitation (P = 5 and 6). For Alaska, the climate zones that satisfy the negative differential effects (probability of mortality is higher than expected) are in the CTM's bottom right regions that represent climate zones with high temperature (T = 4 and 5) and moderate to high precipitation (P = 3, 4, and 5). To spatially represent the results, the differential effect layers were intersected with the binary layer associated with the presence of spruce forest to obtain area estimates associated with differential effect classes, which were developed to characterize the influential levels of climate on the probability of spruce mortality for Colorado (Table 19) and Alaska (Table 20).

The third-degree polynomial function of OLS regression and SAR were applied as a full model to account for the variability in differential effects on spruce mortality in a given climate zone, Δ_i, for Colorado (Table 14). The OLS model accounted for 78.7% of the variability in differential effects on spruce mortality in a given climate zone. Because residuals from the OLS model are spatially independent (Moran's I = –0.104, p-value = 0.596), the SAR model did not significantly improve over the OLS model (likelihood ratio = 0.840, p-value = 0.359) and accounted for 85.42% of the variability in differential effects on spruce mortality, with 79.64% correlation between predicted and observed probabilities. From the areal representation (Table 19), 3.44% of spruce forest has higher differential effects of host

45

availability to host mortality ($\Delta_i > 0.15$) (green area in Figure 5), while 78.91% of spruce forest has differential effects of host mortality proportionally increasing with host availability (null hypothesis) ($-0.15 < \Delta_i < 0.15$) (blue areas in Figure 5). 17.66% of spruce forest has differential effects of host mortality being lower than expected ($\Delta_i < -0.15$) (red areas in Figure 5). Geographically, spruce forest with a high positive differential in probability of mortality occurs in the outer region of Colorado, while spruce forest with a high negative differential in probability of mortality occurs in the central region of the Colorado mountains.

The third-degree polynomial function of OLS regression and SAR were applied as a full model to account for the variability in differential effects on spruce mortality in a given climate zone, Δ_i, for Alaska (Table 18). The OLS model accounted for 87.02% of the variability in differential effects on spruce mortality in a given climate zone. Despite the fact that residuals from the OLS model are spatially independent (Moran's I = –0.273, p-value = 0.163), the SAR model did significantly improve over the OLS model (likelihood ratio = 4.059, p-value = 0.044) and accounted for 96.56% of the variability in differential effects on spruce mortality, with 90.13% correlation between predicted and observed probabilities. From the areal representation (Table 20), approximately 61.05% of spruce forest has a higher differential effect of host mortality ($\Delta_i > 0.15$) (green areas in Figure 6). 27.30% of spruce forest has the differential effect that host mortality proportionally increases with host availability (null hypothesis) ($-0.15 < \Delta_i < 0.15$) (blue areas in Figure 6). 13.59% of spruce forest has the differential effect of host availability to host mortality being lower than expected ($\Delta_i < -0.15$) (red areas in Figure 6). Geographically, spruce forest with a high positive differential in probability of mortality occurs in the inland region of Alaska, while spruce forest with a high negative differential in probability of mortality mostly occurs in the southern coastal region of Alaska, especially on the Kenai Peninsula.

Discussion

Climate is the crucial factor in determining the distribution of forest insects and diseases and the availability of susceptible hosts across the landscape (Allen et al., 2010; Breshears et al., 2005). However, lack of information on the interactions between climatic factors and host's susceptibility and dynamics

causal agents associated with spruce mortality lead to difficulty in defining these complex and spatially variant processes. The influences of temperature and precipitation on landscape dynamics of spruce mortality are not well understood. We need to explore the effects of changing climate on the expansion of spruce forest mortality to a new area without a history of infestation. This study indicates that spruce stands become more susceptible to mortality due to spruce beetles when the spruce forest encounters suboptimal climatic conditions over the long term. Suboptimal climate could affect the forest by being a predisposing factor causing long-term suppression of growth and vigor or by inducing a condition favoring growth and development of insects and diseases. Because climate factors are spatially distributed across the forested landscape, the climate characteristics within a site can be used to indicate the heterogeneity of the stand condition across the landscape (Lundquist, 2005). In a time of climate change, the shift of environmental conditions from optimal to marginal could be possible. Because climate will tend to be warmer and drier in the near future (Seager et al., 2007), more optimal sites in the current landscape may shift to marginal, possibly causing more spruce forest to become more susceptible to insects and diseases.

In this study, we applied a critical method proposed by Reich and colleagues (2016) to describe interactions between climatic effects and spruce mortality using fifty years of climate data to represent long-term effects of abiotic factors on both presences of host and mortality. We adopted the approaches of using CTMs with regression model as the inference for interactions between climate and spruce mortality and implementing third degree polynomial regression function instead of the second degree polynomial to capture the non-linearity of the association. We hypothesized that spruce mortality is associated with climate zones where host trees confront physiological stress of marginal conditions. Additionally, marginal condition also does not support the growth and survival of host's population which implying environmental mismatch between host and causal agent. We use CTMs and regression model to test the hypothesis that there are either positive or negative effect from long-term conditions of temperature and precipitation on the probability of observing spruce forest and spruce mortality across the landscape. The results suggest that climatic environments are at part etiology of spruce mortality. However, other exempt

environmental factors could affect landscape dynamics of hosts and their causal agents (Allen et al., 2010; Breshears et al., 2005; Hanson and Weltzin, 2000).

Based on the calculation of probability in CTMs (Table 3 to Table 10) and from the results of regression models, the presence of spruce forest in Colorado is mostly located in high precipitation zones throughout cold to moderate temperature zones while probability of spruce mortality follows a similar trend, as does the probability of spruce host presence. Especially, the probability of mortality positively correlates with higher precipitation zones in colder temperatures (Zone 3 and below). However, probability of mortality is negatively associate with higher precipitation in the warmer temperature zones (Figure 7). The latter case indicates that there is evidence of increased mortality when precipitation is lower in warmer climate zones, according to historic spruce mortality in Colorado associated with a drought period (Chavardès et al., 2012; Hart et al., 2013). In contrast, observing spruce forest in Alaska has the highest probability in the low to moderate precipitation zones and decreases as precipitation increases, except in the warmest temperature zone where the unimodal peak of probabilities is between the moderate to high precipitation zones (Figure 10 and Figure 13). While the probabilities of spruce mortality in Alaska are low across many climate zones, there is an increasing trend as the precipitation increases in the two warmest temperature zones (Figure 10 and Figure 13). According to a previous study in Alaska, spruce beetle outbreaks are positively associated with increasing precipitation in the winter and is negatively associated with more precipitation in warmer periods (Sherriff et al., 2011). The results are quite similar to previous study of the same approach on subalpine fir decline (Reich et al., 2016), which results indicate that host is found mostly in cold to moderate temperatures and high precipitation climatic zones while relatively warm and dry climate are associated with the suboptimal zones. Nevertheless, subalpine fir decline only subject to dry climate, the probability of spruce mortality has a positive association with higher precipitation in some levels of temperature zones. These interactions with climate were referred as the mismatch of environment/host which marginal population inhabit these sites confront with the various kinds of biotic and abiotic stress that lead to more probability of mortality.

48

The adopted methods also aim at characterizing the differential effects between climate and spruce mortality associated with outbreaks of spruce beetles. The results indicate that the presence of spruce forest inhabit in sites with optimal climatic conditions favor persistence of local population while populations those are mismatched with the favorable climatic conditions are vulnerable to stress and being prone to mortality. Differential effects of forested landscape for Colorado and Alaska were shown that there're less area of host's disadvantage compare to the total area of host's presence (Table 19 and Table 20). The differential effects of outbreaks of spruce beetle occurred in the limited area where the suboptimal conditions prevail. These results could delineate the future distribution of spruce forest and outbreaks. Results show that healthy forest is found mostly in climatic zones with moderate temperatures and high precipitation in Colorado which comparable to previous study on the differential effects of subalpine fir decline in Colorado while the probability of greatest negative differential effects is observed in sites with low temperature and high precipitation. While healthy forest is found in the moderately low temperature and moderate precipitation in Alaska, whereas, the probability of observing negative differential effects is greatest in zone with extremely high and low precipitation.

The applications of statistical modeling approaches on spatial data could help us determine the importance of climatic factors on the spatial extent and distribution of forest mortality. From our study, we model the presence of host and mortality through OLS regression and SAR models. The models were used to describe the association between climatic characteristics and the observation of forest insects and diseases (Figure 8, to Figure 12). The models were also used to extrapolate the association between host and mortality in the unobserved climatic covariates and area. This kind of model, called the climate enveloped model, was used to define the climatic niche of species (Farber and Kadmon, 2003; Pearson and Dawson, 2003). The climate enveloped model was employed to predict the spatial response of species to the fundamental climatic conditions. It delineates the spatial extent of the probabilities of observing host and mortality based on climatic characteristics across the landscape. However, the climate enveloped model only represents the response due to large-scale effects of climatic conditions. In other words, the model describes the fundamental niche of the host and its mortality and cannot account for species

49

distribution within climate zones due to small-scale environmental factors such as mutualism, competition, predator-prey, communities structure, anthropogenic effects, etc., which account for the realized niche (Araújo and Peterson, 2012; Austin and Smith, 1990; Reich et al., 2010).

From our model, the climatic covariates represent the long-term conditions of temperature and precipitation for each site. The model can be used to show the response of organisms to the spatiotemporal trajectories of ecological and climatic conditions (Blois et al., 2013; Pickett, 1989). The assumption of our study is that the species respond to specific climatic factors that are constant over time, but the extent of the species can change by a shift in distribution of climatic factors through time and space. Therefore, future species distribution can be determined by the current distribution and its association with climate. In this study, we are interested in the probabilities for host and mortality that were created based on the reaction to the climatic covariates in each of the spatial units. The spatial units with extreme or suboptimal conditions could favor the emergence of outbreaks causing host mortality. The CTMs developed from the data and the model prediction are able to quantify and predict changes due to climate shift however the application of CTMs also have the limits. Due to long temporal scale CTMs cover, it is difficult to use this method to predict the future outbreaks at a specific location with specific time. CTMs only yield regionally large-scale climatic effects on host and mortality which can provide us risk map. Moreover, the implementing of aerial survey detection in modeling could result in high sampling errors from both false positive and false negative. Integration of sampling errors into the models could help us deal with this kind of bias. This could be done by further sampling on local scale to check the accuracy of aerial surveys and implementing likelihood or Bayesian approach to deal with the model with multi-structure of errors.

Despite the fact that temperature and precipitation patterns used in our study are long-term static, under the changing-climate scenario, the distribution of marginal sites [where the probability of mortality is high relative to the probability of host presence ($\Delta_i < 0$)] would be changed by the altered landscape pattern of climate (Seastedt et al., 2008). However, it is difficult to completely quantify the marginal sites of any species due to the complexity of the interaction. The responses of host and mortality are not only

involved with the pattern of large-scale factors like climate, but also with other small-scale environmental factors and how these variables and interactions have changed over space and time. On the other hand, the outbreaks of insects and diseases can change large-scale spatial distribution of host species, and mortality depletes the available resources for forest pests. These also contribute to the change in spatial response of the occurrence of outbreaks over the temporal scale.

The extreme climate compared to the typical climatic niche might contribute to the absence of the establishment of forest tree species, and it can also cause mortality of existing forest communities (Anderegg et al., 2012; Wargo, 1985). The marginal population of the spruce residing in suboptimal climatic conditions could have more risk of encountering physiological stress by living in variable environmental conditions and disturbances and by living under the risk of contributing factors. Suboptimal temperature and precipitation can cause a reduction in growth rate to below the maximum level underlying the phenotype (Ayres, 1984). This detrimental effect is directly and indirectly involved with the physiological processes of trees, resulting in changing function and performance (Huberty and Denno, 2004). Suboptimal temperature affects growth by interrupting enzymic activities involved in photosynthesis and respiration. The interference of plant function involves lower carbon assimilation (Gaylord et al., 2007), which reduces the carbon source of host trees. Because carbon-based compounds are the building blocks of the organism and are crucial for physiological maintenance, the scarcity of carbon due to climate stress could deplete vigor and lessen defense mechanisms of the host tree, causing it to be more susceptible to insects and diseases (Gaylord et al., 2007; McDowell et al., 2008). Moreover, high temperature increases the rate of evapotranspiration due to high water vapor deficit, causing loss of water from the host tree (Williams et al., 2013). On the other hand, drought stress caused by low precipitation levels also causes stress on plants because they lose water through transpiration that exceeds the amount required by the root system. This leads to disruption of the acquisition of carbon by closing the stomata (Anderegg et al., 2012).

Moreover, climate also affect life histories and population dynamics of forest pathogens and insects, resulting in detrimental effects to the host tree (Bale et al., 2002; Huberty and Denno, 2004). In

51

studies of insect pests, the plant stress and climate release hypotheses were developed to describe the relationship among plants, insects, and climate (Huberty and Denno, 2004; Larsson, 1989). The plant stress hypothesis focuses on the increasing susceptibility of a host and increased suitable resources for pest populations caused by extreme abiotic conditions. For example, coniferous trees under drought stress produce less oleoresin, which is the mechanical defense deterring wood-boring and phloem-feeding insects (Hard, 1985). This also leads to increased emission of insects attracted to volatile conditions from stressed plants (Kelsey et al., 2014; Mattson and Haack, 1987). The climate release hypothesis focuses not only on the changed susceptibility of the host, but also on the concept being joined with the effects on pest populations and behaviors favoring the availability of resources (Larsson, 1989; Mattson and Haack, 1987).

Table 1. Summary statistics for the average annual temperature and precipitation associated with the temperature (T) and precipitation (P) zones identified Colorado.

Zone	Min.	Mean	Max.	CV%
	Average precipitation (mm)			
P1	4.8	27.0	30.4	9.9
P2	30.4	33.9	36.7	5.2
P3	36.7	39.5	42.7	4.3
P4	42.7	46.0	50.7	4.8
P5	50.7	55.5	60.6	5.2
P6	60.6	65.6	83.7	5.2
	Average temperature ($^{\circ}$C)			
T1	–5.7	–1.7	–0.3	55.1
T2	–0.3	1.3	2.4	54.7
T3	2.4	3.5	4.4	16.6
T4	4.4	5.3	6.3	10.0
T5	6.3	7.4	8.4	8.0
T6	8.4	9.4	13.9	8.3

Table 2. Summary statistics for the average annual temperature and precipitation associated with the temperature (T) and precipitation (P) zones identified in Alaska.

Zone	Min.	Mean	Max.	CV%
Average precipitation (mm)				
P1	4.6	14.8	20.6	27.8
P2	20.7	25.0	29.1	9.0
P3	29.2	33.0	37.5	7.1
P4	37.6	46.2	62.0	14.1
P5	62.1	116.0	275.5	36.0
Average temperature (^{o}C)				
T1	–34.3	–12.0	–10.2	15.9
T2	–10.1	–8.6	–7.4	9.3
T3	–7.3	–6.2	–5.1	10.7
T4	–5.0	–3.6	–2.1	23.4
T5	–2.0	1.0	9.0	243.8

Table 3. Rescaled probability of observing spruce forest in a given climate zone, $P(S|C_i)$, in Colorado. Probabilities are rescaled so the maximum probability is equal to one (maximum probability = 0.8274).

Temperature Zone	Precipitation Zone					
	1	2	3	4	5	6
1		0.0000	0.0310	0.4223	0.3612	0.2679
2	0.0042	0.0287	0.1148	0.3978	0.6736	0.8089
3	0.0018	0.0124	0.0849	0.2979	0.8273	1.0000
4	0.0001	0.0037	0.0227	0.1505	0.4322	0.8671
5	0.0000	0.0001	0.0022	0.0073	0.0087	0.0000
6	0.0000	0.0000	0.0002	0.0006	0.0016	

Table 4. Rescaled probability of observing spruce mortality in a given climate zone, $P(D|C_i)$, in Colorado. Probabilities are rescaled so the maximum probability is equal to one (maximum probability = 0.1939).

Temperature Zone	Precipitation Zone					
	1	2	3	4	5	6
1		0.0000	0.0000	0.6647	0.4787	0.3963
2	0.0011	0.0104	0.0478	0.2591	0.6581	1.0000
3	0.0003	0.0052	0.0372	0.1748	0.6750	0.9382
4	0.0000	0.0023	0.0132	0.1046	0.2964	0.5606
5	0.0000	0.0001	0.0015	0.0066	0.0063	0.0000
6	0.0000	0.0000	0.0000	0.0004	0.0000	

Table 5. Rescaled probability of observing spruce mortality conditional on spruce forest presence in a given climate zone, $P(D|S, C_i)$, in Colorado. Probabilities are rescaled so the maximum probability is equal to one (maximum probability = 0.2428).

Temperature Zone	Precipitation Zone					
	1	2	3	4	5	6
1			0.0000	1.0000	0.8795	0.9092
2	0.0821	0.1040	0.1970	0.4388	0.7265	0.9833
3	0.0022	0.0974	0.1703	0.3217	0.6458	0.8053
4	0.0000	0.0600	0.1523	0.3189	0.4127	0.3121
5	0.0000	0.0000	0.1181	0.2233	0.0503	
6	0.0000	0.0000	0.0000	0.0000	0.0000	

Table 6. Differential between probability of observing spruce forest and rescaled probability of observing spruce mortality conditional on observing spruce forest in a given climate zone, Δ_i, in Colorado.

Temperature	Precipitation Zone					
Zone	1	2	3	4	5	6
1			0.0310	–0.5777	–0.5184	–0.6413
2	–0.0778	–0.0753	–0.0822	–0.0410	–0.0528	–0.1744
3	–0.0004	–0.0850	–0.0854	–0.0239	0.1815	0.1947
4	0.0001	–0.0563	–0.1296	–0.1685	0.0195	0.5550
5	0.0000	0.0001	–0.1159	–0.2159	–0.0417	
6	0.0000	0.0000	0.0002	0.0006	0.0016	

Table 7. Rescaled probability of observing spruce forest in a given climate zone, $P(S|C_i)$, in Alaska.

Probabilities are rescaled so the maximum probability is equal to one (maximum probability = 0.3736).

Temperature Zone	Precipitation Zone				
	1	2	3	4	5
1	0.2680	0.3483	0.0980	0.0270	0.0010
2	0.5454	0.6858	0.8076	0.1714	0.0207
3	0.6102	0.9539	1.0000	0.4578	0.1106
4	0.3973	0.7914	0.9453	0.6334	0.2546
5		0.1673	0.2742	0.5145	0.0468

Table 8. Rescaled probability of observing spruce mortality in a given climate zone, $P(D|C_i)$, in Alaska. Probabilities are rescaled so the maximum probability is equal to one (maximum probability = 0.1253).

Temperature Zone	Precipitation Zone				
	1	2	3	4	5
1	0.0000	0.0000	0.0000	0.0000	0.0000
2	0.0005	0.0012	0.0000	0.0000	0.0074
3	0.0102	0.0072	0.0495	0.0134	0.0549
4	0.0266	0.1160	0.1124	0.0743	1.0000
5		0.0000	0.4686	0.7257	0.1709

Table 9. Rescaled probability of observing spruce mortality conditional on spruce forest presence in a given climate zone, $P(D|S, C_i)$, in Alaska. Probabilities are rescaled so the maximum probability is equal to one (maximum probability = 0.3115).

Temperature Zone	Precipitation Zone				
	1	2	3	4	5
1	0.0000	0.0000	0.0000	0.0000	0.0000
2	0.0004	0.0012	0.0000	0.0000	0.0000
3	0.0036	0.0025	0.0242	0.0035	0.0716
4	0.0059	0.0803	0.0518	0.0480	1.0000
5		0.0000	0.4016	0.5276	0.7332

Table 10. Differential between probability of observing spruce forest and rescaled probability of observing spruce mortality conditional on observing spruce forest in a given climate zone, Δ_i, in Alaska.

Temperature	Precipitation Zone				
Zone	1	2	3	4	5
1	0.2680	0.3483	0.0980	0.0270	0.0010
2	0.5450	0.6845	0.8076	0.1714	0.0207
3	0.6067	0.9514	0.9758	0.4543	0.0391
4	0.3913	0.7112	0.8935	0.5854	–0.7454
5		0.1673	–0.1274	–0.0132	–0.6864

Table 11. Comparison between OLS model and SAR model for the natural logarithm of the rescaled probability of observing spruce forest in a given climate zone, Pr(S|Ci), in the Colorado as a polynomial function of the temperature and precipitation zones.

Variable	OLS Model		SAR Model	
	Coefficient	Standard Error	Coefficient	Standard Error
Intercept	−13.401	3.4672	−14.125	1.743
T	5.234	1.6122	6.048	0.823
P	2.548	1.4072	2.232	0.687
T^2	−1.486	0.2637	−1.653	0.135
P^2	−0.082	0.2470	0.015	0.124
TP				
T^3				
P^3				
T^2P	0.212	0.0582	0.248	0.030
TP^2	−0.125	0.0623	−0.161	0.033
λ			−0.655	(0.0001)
R^2	0.92		0.99	
FIT			0.95	
AICC	147		134	
Likelihood Ratio			13	(4e–04)
Moran's I for Residuals	−0.47	(0.00047)	−0.0065	(0.85)

OLS full model:$\ln(P_r) = \beta_0 + \beta_1 T + \beta_2 P + \beta_3 T^2 + \beta_4 P^2 + \beta_5 TP + \beta_6 T^3 + \beta_7 P^3 + \beta_8 T^2 P + \beta_9 TP^2 + U$, where $U \sim N(0, \sigma^2)$;

SAR full model:$\ln(P_r) = \beta_0 + \beta_1 T + \beta_2 P + \beta_3 T^2 + \beta_4 P^2 + \beta_5 TP + \beta_6 T^3 + \beta_7 P^3 + \beta_8 T^2 P + \beta_9 TP^2 + \varepsilon$, where $\varepsilon = \lambda W \epsilon + \eta$ and $\eta \sim N(0, \sigma^2)$;

P_r = rescaled probability; T = temperature zone; P = precipitation zone; W = binary spatial weights matrix based on the rook's move on CTM; $-1 < \lambda < 1$, spatial correlation of the residuals; ε = spatially correlated errors, $U \sim N(0,1)$ is spatially independent errors. The final model is selected by stepwise regression based on AICC.

FIT is correlation between the observed and predicted values squared (more reliable than R-squared in evaluation of SAR model).

Likelihood ratio tests the hypothesis that the SAR model is an improvement over the OLS model. The p-value associated with the test statistic is given in parentheses.

Table 12. Comparison between OLS model and SAR model for the natural logarithm of the rescaled probability of observing spruce mortality in a given climate zone, Pr(D│Ci), in the Colorado as a polynomial function of the temperature and precipitation zones

Variable	OLS Model		SAR Model	
	Coefficient	Standard Error	Coefficient	Standard Error
Intercept	–21.730	12.460	–15.841	7.476
T	7.051	4.112	5.055	2.455
P	–1.522	6.487	–3.543	3.934
T^2	–1.729	0.382	–1.605	0.224
P^2	0.704	0.876	0.900	0.536
TP	2.588	1.683	3.071	1.044
T^3				
P^3				
T^2P				
TP^2	–0.422	0.242	–0.466	0.152
λ			–0.560	(0.0021)
R^2	0.747		0.947	
FIT			0.808	
AICC	202		197	
Likelihood Ratio			5.24	(0.0221)
Moran's I for Residuals	–0.254	(0.0907)	–0.113	(0.536)

OLS full model:$\ln(P_r) = \beta_0 + \beta_1 T + \beta_2 P + \beta_3 T^2 + \beta_4 P^2 + \beta_5 TP + \beta_6 T^3 + \beta_7 P^3 + \beta_8 T^2 P + \beta_9 TP^2 + U$, where $U \sim N(0, \sigma^2)$;

SAR full model:$\ln(P_r) = \beta_0 + \beta_1 T + \beta_2 P + \beta_3 T^2 + \beta_4 P^2 + \beta_5 TP + \beta_6 T^3 + \beta_7 P^3 + \beta_8 T^2 P + \beta_9 TP^2 + \varepsilon$, where $\varepsilon = \lambda W \epsilon + \eta$ and $\eta \sim N(0, \sigma^2)$;

P_r = rescaled probability; T = temperature zone; P = precipitation zone; W = binary spatial weights matrix based on the rook's move on CTM; $–1 < \lambda < 1$, spatial correlation of the residuals; ε = spatially correlated errors, $U \sim N(0,1)$ is spatially independent errors. The final model is selected by stepwise regression based on AIC.

FIT is correlation between the observed and predicted values squared (more reliable than R-squared in evaluation of SAR model).

Likelihood ratio tests the hypothesis that the SAR model is an improvement over the OLS model. The p-value associated with the test statistic is given in parentheses.

Table 13. Comparison between OLS model and SAR model for the natural logarithm of the rescaled probability of observing spruce mortality conditional on spruce forest presence in a given climate zone, Pr (D|S,Ci), in the Colorado as a polynomial function.

Variable	OLS Model		SAR Model	
	Coefficient	Standard Error	Coefficient	Standard Error
Intercept	–24.259	5.8110	–26.8017	6.2298
T	10.812	3.1027	12.1099	3.3172
P	2.273	0.6517	2.4782	0.7041
T^2	–1.945	0.4249	–2.1708	0.4542
P^2				
TP				
T^3				
P^3				
T^2P				
TP^2				
λ			0.0458	(0.8371)
R^2	0.6918		0.7902	
FIT			0.6894	
AICC	208.4		215.1	
Likelihood Ratio			0.0353	(0.8509)
Moran's I for Residuals	0.02272	(0.6769)	0.004454	(0.7807)

OLS full model:$\ln(P_r) = \beta_0 + \beta_1 T + \beta_2 P + \beta_3 T^2 + \beta_4 P^2 + \beta_5 TP + \beta_6 T^3 + \beta_7 P^3 + \beta_8 T^2 P + \beta_9 TP^2 + U$, where $U \sim N(0, \sigma^2)$;
SAR full model:$\ln(P_r) = \beta_0 + \beta_1 T + \beta_2 P + \beta_3 T^2 + \beta_4 P^2 + \beta_5 TP + \beta_6 T^3 + \beta_7 P^3 + \beta_8 T^2 P + \beta_9 TP^2 + \varepsilon$, where $\varepsilon = \lambda W \epsilon + \eta$ and $\eta \sim N(0, \sigma^2)$;
P_r = rescaled probability; T = temperature zone; P = precipitation zone; W = binary spatial weights matrix based on the rook's move on CTM; $–1 < \lambda < 1$, spatial correlation of the residuals; ε = spatially correlated errors, $U \sim N(0,1)$ is spatially independent errors. The final model is selected by stepwise regression based on AICC.
FIT is correlation between the observed and predicted values squared (more reliable than R-squared in evaluation of SAR model).
Likelihood ratio tests the hypothesis that the SAR model is an improvement over the OLS model. The p-value associated with the test statistic is given in parentheses.

Table 14. Comparison between OLS model and SAR model for differential influences of spruce mortality in a given climate zone, Δi, in the Colorado as a polynomial function of the temperature and precipitation zones.

Variable	OLS Model		SAR Model	
	Coefficient	Standard Error	Coefficient	Standard Error
Intercept	–0.7010	0.3042	–0.7520	0.2295
T	0.3360	0.2383	0.3834	0.1823
P	0.4854	0.2173	0.4703	0.1652
T^2	–0.1048	0.0708	–0.1177	0.0540
P^2	–0.1901	0.0704	–0.1828	0.0539
TP				
T^3	0.0124	0.0064	0.0136	0.0049
P^3	0.0146	0.0065	0.0139	0.0050
T^2P	–0.0139	0.0033	–0.0143	0.0025
TP^2	0.0192	0.0036	0.0192	0.0027
λ			–0.2447	(0.2565)
R^2	0.787		0.8542	
FIT			0.7964	
AICC	–32.08		–32.92	
Likelihood Ratio			0.8404	(0.3593)
Moran's I for Residuals	–0.1039	0.5955	–0.03317	(0.9946)

OLS full model:$\Delta_i = \beta_0 + \beta_1 T + \beta_2 P + \beta_3 T^2 + \beta_4 P^2 + \beta_5 TP + \beta_6 T^3 + \beta_7 P^3 + \beta_8 T^2 P + \beta_9 TP^2 + U$, where $U \sim N(0, \sigma^2)$;
SAR full model:$\Delta_i = \beta_0 + \beta_1 T + \beta_2 P + \beta_3 T^2 + \beta_4 P^2 + \beta_5 TP + \beta_6 T^3 + \beta_7 P^3 + \beta_8 T^2 P + \beta_9 TP^2 + \varepsilon$, where $\varepsilon = \lambda W \epsilon + \eta$ and $\eta \sim N(0, \sigma^2)$;
Δ_i = differential influences; T = temperature zone; P = precipitation zone; W = binary spatial weights matrix based on the rook's move on CTM; $-1 < \lambda < 1$, spatial correlation of the residuals; ε = spatially correlated errors, $U \sim N(0,1)$ is spatially independent errors. The final model is selected by stepwise regression based on AICC.
FIT is correlation between the observed and predicted values squared (more reliable than R-squared in evaluation of SAR model).
Likelihood ratio tests the hypothesis that the SAR model is an improvement over the OLS model. The p-value associated with the test statistic is given in parentheses.

Table 15. Comparison between OLS model and SAR model for the natural logarithm of the rescaled probability of observing spruce forest in given climate zone, Pr (S|Ci), in Alaska as a polynomial function of the temperature and precipitation zones.

Variable	OLS Model		SAR Model	
	Coefficient	Standard Error	Coefficient	Standard Error
Intercept	–1.6896	1.1569	–2.1042	0.4766
T	0.8501	0.6079	1.0164	0.2427
P	–0.7145	1.0583	–0.2518	0.4415
T^2	–0.1997	0.1125	–0.2131	0.0482
P^2	0.1367	0.3525	0.0131	0.1474
TP	0.5601	0.2310	0.4217	0.0909
T^3				
P^3	–0.0732	0.0387	–0.0621	0.0164
T^2P	–0.0829	0.0319	–0.0722	0.0138
TP^2	0.0442	0.0319	0.0577	0.0136
λ			–0.8438	(0.0000)
R^2	0.9743		0.998	
FIT			0.9903	
AICC	32.58		17.07	
Likelihood Ratio			15.51	(1e–04)
Moran's I for Residuals	–0.4881	(0.003168)	–0.2591	(0.1542)

OLS full model:$\ln(P_r) = \beta_0 + \beta_1 T + \beta_2 P + \beta_3 T^2 + \beta_4 P^2 + \beta_5 TP + \beta_6 T^3 + \beta_7 P^3 + \beta_8 T^2 P + \beta_9 TP^2 + U$, where $U \sim N(0, \sigma^2)$;
SAR full model:$\ln(P_r) = \beta_0 + \beta_1 T + \beta_2 P + \beta_3 T^2 + \beta_4 P^2 + \beta_5 TP + \beta_6 T^3 + \beta_7 P^3 + \beta_8 T^2 P + \beta_9 TP^2 + \varepsilon$, where $\varepsilon = \lambda W \epsilon + \eta$ and $\eta \sim N(0, \sigma^2)$;
P_r = rescaled probability; T = temperature zone; P = precipitation zone; W = binary spatial weights matrix based on the rook's move on CTM; $–1 < \lambda < 1$, spatial correlation of the residuals; ε = spatially correlated errors, $U \sim N(0,1)$ is spatially independent errors. The final model is selected by stepwise regression based on AICC.
FIT is correlation between the observed and predicted values squared (more reliable than R-squared in evaluation of SAR model).
Likelihood ratio tests the hypothesis that the SAR model is an improvement over the OLS model. The p-value associated with the test statistic is given in parentheses.

Table 16. Comparison between OLS model and SAR model for the natural logarithm of the rescaled probability of observing spruce mortality in given climate zone, Pr (D|Ci), in Alaska as a polynomial function of the temperature and precipitation zones.

Variable	OLS Model		SAR Model	
	Coefficient	Standard Error	Coefficient	Standard Error
Intercept	–23.5667	12.7354	–20.2475	7.3833
T	12.5223	15.3099	10.8577	9.1350
P	–11.7747	5.2987	–13.3558	2.9474
T^2	0.7498	5.6214	1.2596	3.3667
P^2	2.6036	1.2169	2.9208	0.7173
TP				
T^3	–0.7762	0.6328	–0.8247	0.3847
P^3				
T^2P	1.0337	0.4419	1.0669	0.2813
TP^2	–0.7656	0.3993	–0.8098	0.2515
λ			–0.619	(0.0024)
R^2	0.7998		0.9694	
FIT			0.8625	
AICC	163		157.5	
Likelihood Ratio			5.491	(0.0191)
Moran's I for Residuals	–0.3094	0.08523	–0.1558	(0.4703)

OLS full model:$\ln(P_r) = \beta_0 + \beta_1 T + \beta_2 P + \beta_3 T^2 + \beta_4 P^2 + \beta_5 TP + \beta_6 T^3 + \beta_7 P^3 + \beta_8 T^2 P + \beta_9 TP^2 + U$, where $U \sim N(0, \sigma^2)$;

SAR full model:$\ln(P_r) = \beta_0 + \beta_1 T + \beta_2 P + \beta_3 T^2 + \beta_4 P^2 + \beta_5 TP + \beta_6 T^3 + \beta_7 P^3 + \beta_8 T^2 P + \beta_9 TP^2 + \varepsilon$, where $\varepsilon = \lambda W \epsilon + \eta$ and $\eta \sim N(0, \sigma^2)$;

P_r = rescaled probability; T = temperature zone; P = precipitation zone; W = binary spatial weights matrix based on the rook's move on CTM; $–1 < \lambda < 1$, spatial correlation of the residuals; ε = spatially correlated errors, $U \sim N(0,1)$ is spatially independent errors. The final model is selected by stepwise regression based on AICC.

FIT is correlation between the observed and predicted values squared (more reliable than R-squared in evaluation of SAR model).

Likelihood ratio tests the hypothesis that the SAR model is an improvement over the OLS model. The p-value associated with the test statistic is given in parentheses.

Table 17. Comparison between OLS model and SAR model for the natural logarithm of the rescaled probability of observing spruce mortality conditional on spruce forest presence in given climate zone, Pr(D|S,Ci), in Alaska as a polynomial function of the temperature.

Variable	OLS Model		SAR Model	
	Coefficient	Standard Error	Coefficient	Standard Error
Intercept	−12.6587	11.2137	−11.7937	6.8530
T	−2.1701	13.4806	−1.9941	8.4675
P	−10.4264	4.6656	−10.5711	2.7417
T^2	5.7411	4.9498	5.4971	3.1199
P^2	2.1729	1.0715	2.0850	0.6651
TP				
T^3	−1.3555	0.5572	−1.2880	0.3562
P^3				
T^2P	1.2064	0.3891	1.1201	0.2598
TP^2	−0.8219	0.3516	−0.7422	0.2324
λ			−0.5766	(0.0061)
R^2	0.8492		0.976	
FIT			0.8869	
AICC	156.9		152.9	
Likelihood Ratio			3.943	(0.0471)
Moran's I for Residuals	−0.2475	(0.1901)	−0.1722	(0.408)

OLS full model:$\ln(P_r) = \beta_0 + \beta_1 T + \beta_2 P + \beta_3 T^2 + \beta_4 P^2 + \beta_5 TP + \beta_6 T^3 + \beta_7 P^3 + \beta_8 T^2 P + \beta_9 TP^2 + U$, where $U \sim N(0, \sigma^2)$;

SAR full model:$\ln(P_r) = \beta_0 + \beta_1 T + \beta_2 P + \beta_3 T^2 + \beta_4 P^2 + \beta_5 TP + \beta_6 T^3 + \beta_7 P^3 + \beta_8 T^2 P + \beta_9 TP^2 + \varepsilon$, where $\varepsilon = \lambda W \epsilon + \eta$ and $\eta \sim N(0, \sigma^2)$;

P_r = rescaled probability; T = temperature zone; P = precipitation zone; W = binary spatial weights matrix based on the rook's move on CTM; $-1 < \lambda < 1$, spatial correlation of the residuals; ε = spatially correlated errors, $U \sim N(0,1)$ is spatially independent errors. The final model is selected by stepwise regression based on AIC.

FIT is correlation between the observed and predicted values squared (more reliable than R-squared in evaluation of SAR model).

Likelihood ratio tests the hypothesis that the SAR model is an improvement over the OLS model. The p-value associated with the test statistic is given in parentheses.

Table 18. Comparison between OLS model and SAR model for differential influences of spruce mortality in a given climate zone, Δi, in Alaska as a polynomial function of the temperature and precipitation zones.

Variable	OLS Model		SAR Model	
	Coefficient	Standard Error	Coefficient	Standard Error
Intercept	−1.139	0.2884	−1.2422	0.1667
T	1.3206	0.2374	1.3977	0.1542
P	0.2276	0.1954	0.2442	0.1198
T^2	−0.2818	0.0601	−0.3008	0.0407
P^2	−0.0113	0.0447	−0.0119	0.0288
TP				
T^3				
P^3				
T^2P	0.0414	0.0161	0.0448	0.0110
TP^2	−0.0419	0.0146	−0.0444	0.0099
λ			−0.5420	(0.0113)
R^2	0.8702		0.9656	
FIT			0.9013	
AICC	1.54		−2.52	
Likelihood Ratio			4.059	(0.0439)
Moran's I for Residuals	−0.2728	0.1363	−0.1103	(0.6685)

OLS full model: $\Delta_i = \beta_0 + \beta_1 T + \beta_2 P + \beta_3 T^2 + \beta_4 P^2 + \beta_5 TP + \beta_6 T^3 + \beta_7 P^3 + \beta_8 T^2 P + \beta_9 TP^2 + U$, where $U \sim N(0, \sigma^2)$;

SAR full model: $\Delta_i = \beta_0 + \beta_1 T + \beta_2 P + \beta_3 T^2 + \beta_4 P^2 + \beta_5 TP + \beta_6 T^3 + \beta_7 P^3 + \beta_8 T^2 P + \beta_9 TP^2 + \varepsilon$, where $\varepsilon = \lambda W \epsilon + \eta$ and $\eta \sim N(0, \sigma^2)$;

Δ_i = differential influences; T = temperature zone; P = precipitation zone; W = binary spatial weights matrix based on the rook's move on CTM; $-1 < \lambda < 1$, spatial correlation of the residuals; ε = spatially correlated errors, $U \sim N(0,1)$ is spatially independent errors. The final model is selected by stepwise regression based on AICC.

FIT is correlation between the observed and predicted values squared (more reliable than R-squared in evaluation of SAR model).

Likelihood ratio tests the hypothesis that the SAR model is an improvement over the OLS model. The p-value associated with the test statistic is given in parentheses.

Table 19. Area estimates associated with differential climate effects on the probability of active subalpine-fir mortality in the spruce-fir forests of Colorado.

Type	Differential Effects	CTM			OLS Model		
		Area (Hectares)	Percent by type	Percent of Total	Area (Hectares)	Percent by type	Percent of Total
Host disadvantage	High ($\Delta_i < -0.7$)	0	0.00	0.00	0	0.00	0.00
	Medium ($-0.7 < \Delta_i < -0.4$)	1,154,660	40.31	7.12	12,796,242	59.79	7.10
	Low ($-0.4 < \Delta_i < -0.15$)	1,709,770	59.69	10.54	8,607,011	40.21	4.78
	Total	2,864,430	100.00	17.66	21,403,253	100.00	11.87
No advantage	($-0.15 < \Delta_i < 0.15$)	12,800,497	100.00	78.91	158,014,625	100.00	87.66
Host advantage	Low ($0.4 > \Delta_i > 0.15$)	557,560	100.00	3.44	831,979	99.97	0.46
	Medium ($0.7 > \Delta_i > 0.4$)	17	0.00	0.00	212	0.03	0.00
	High ($\Delta_i < 0.7$)	0	0.00	0.00	0	0.00	0.00
	Total	557,576	100.00	3.44	832,191	100.00	0.46
	Grand Total	16,222,503	-	100.00	180,250,069	-	100.00

Table 20. Area estimates associated with differential climate effects on the probability of active subalpine-fir mortality in the spruce-fir forests of Alaska.

Type	Differential Effects	CTM			SAR Model		
		Area (Hectares)	Percent by type	Percent of Total	Area (Hectares)	Percent by type	Percent of Total
Host disadvantage	High ($\Delta_i < -0.7$)	3,731,800	18.61	2.53	16,321,600	81.39	11.06
	Medium ($-0.7 < \Delta_i < -0.4$)	16,321,600	81.39	11.06	0	0.00	0.00
	Low ($-0.4 < \Delta_i < -0.15$)	0	0.00	0.00	3,731,800	18.61	2.53
	Total	20,053,400	100.00	13.59	20,053,400	100.00	13.59
No advantage	($-0.15 < \Delta_i < 0.15$)	37,408,700	100.00	25.36	40,265,800	100.00	27.30
Host advantage	Low ($0.4 > \Delta_i > 0.15$)	16,075,200	17.85	10.90	19,334,800	22.17	13.11
	Medium ($0.7 > \Delta_i > 0.4$)	34,350,400	38.15	23.29	24,391,100	27.97	16.53
	High ($\Delta_i < 0.7$)	39,624,700	44.00	26.86	43,467,300	49.85	29.47
	Total	90,050,300	100.00	61.05	87,193,200	100.00	59.11
	Grand Total	147,512,400	-	100.00	147,512,400	-	100.00
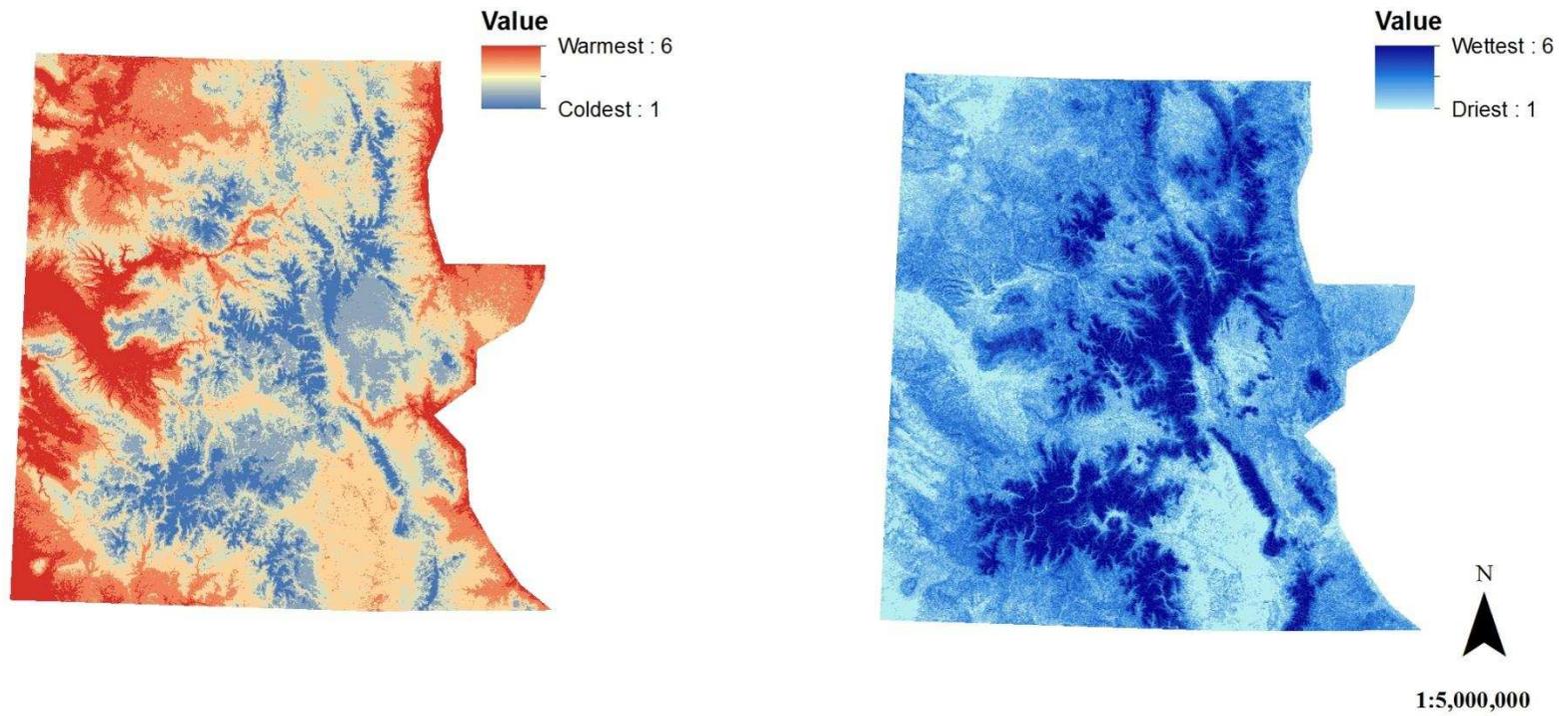
Figure 1. Maps represent delineated area for 6 discrete values of temperature zones (left) and 6 discrete values of precipitation zones (right) of the Colorado. The study area was delineated by the area indicates the presence of forest cover in Colorado.
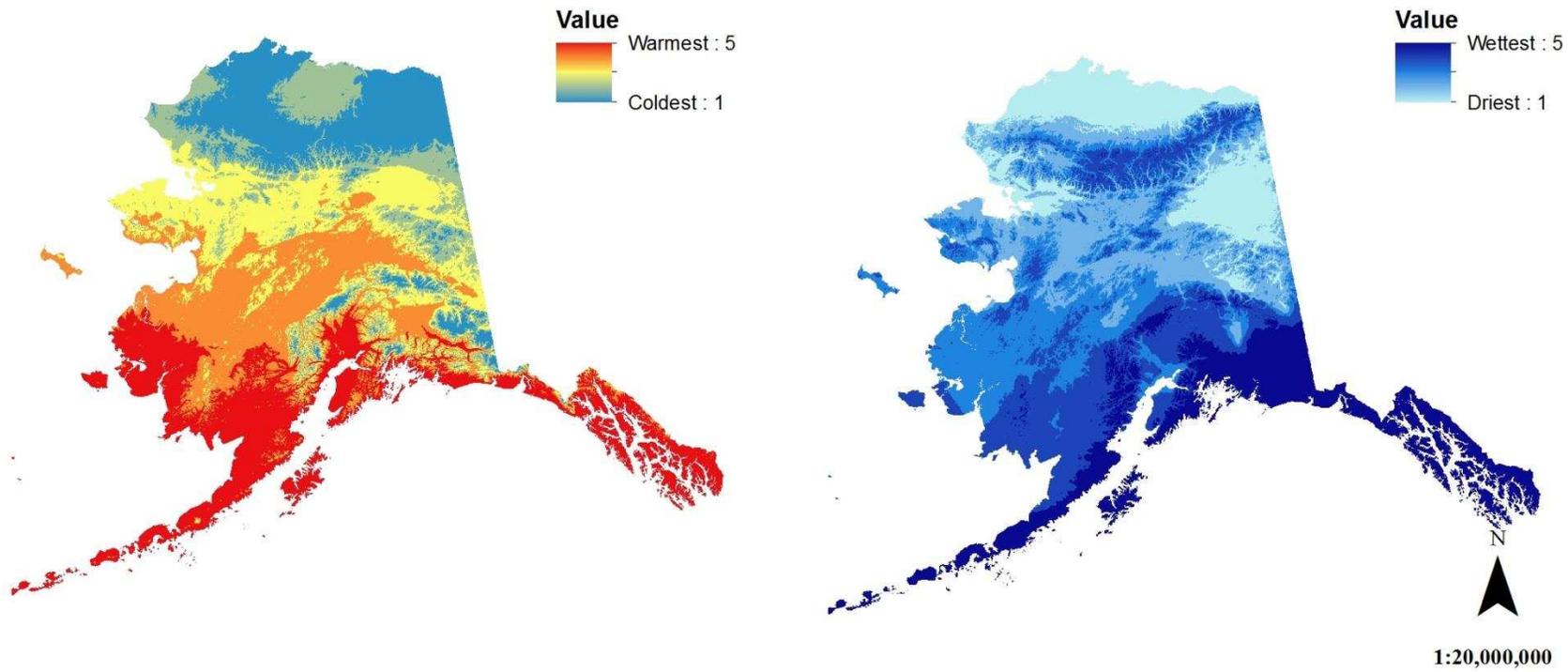
Figure 2. Maps represent delineated area for 5 discrete values of temperature zones (left) and 5 discrete values of precipitation zones (right) of Alaska.
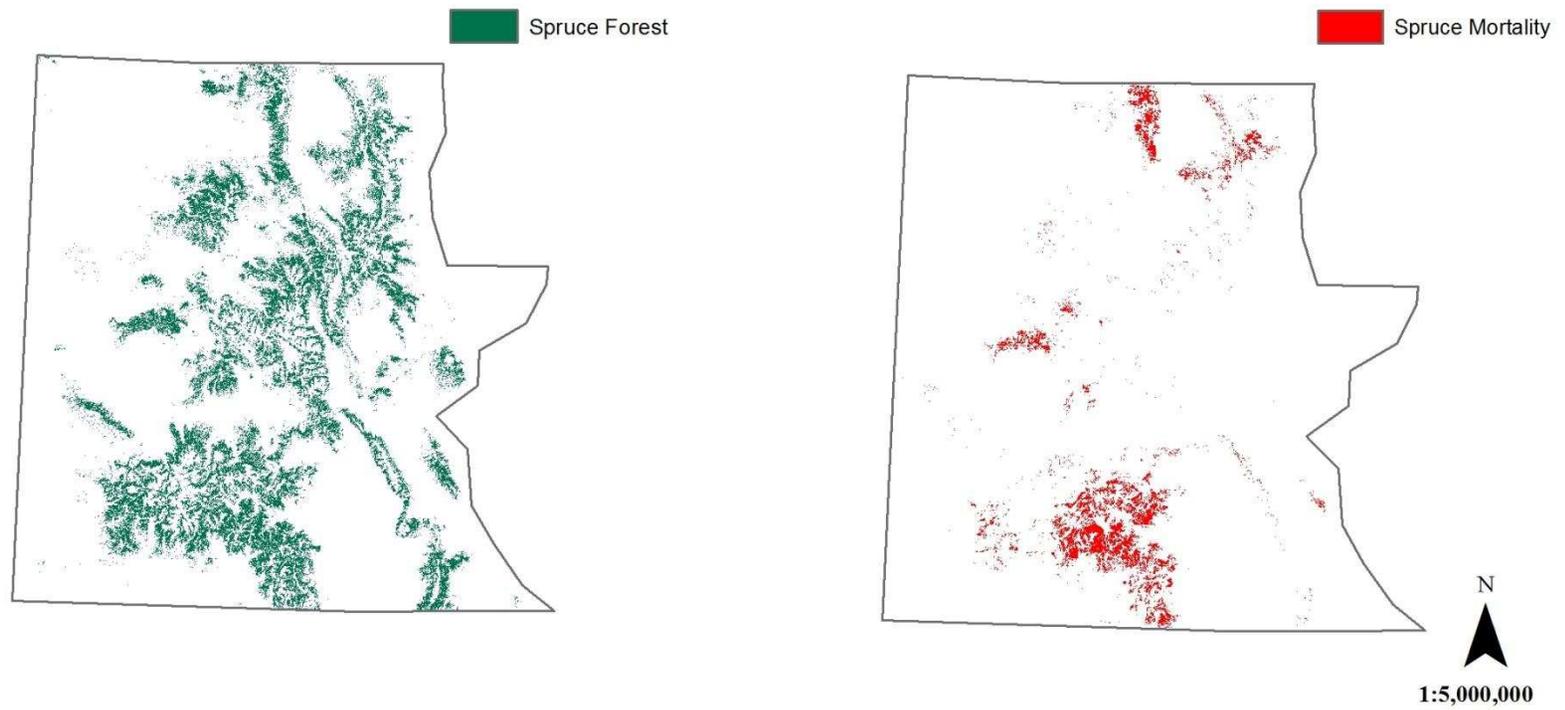
Figure 3. Maps indicate the presence of spruce forest (left) and presence of spruce mortality (right) in the Colorado. The study area was delineated by the layer represent forest land cover in Colorado.
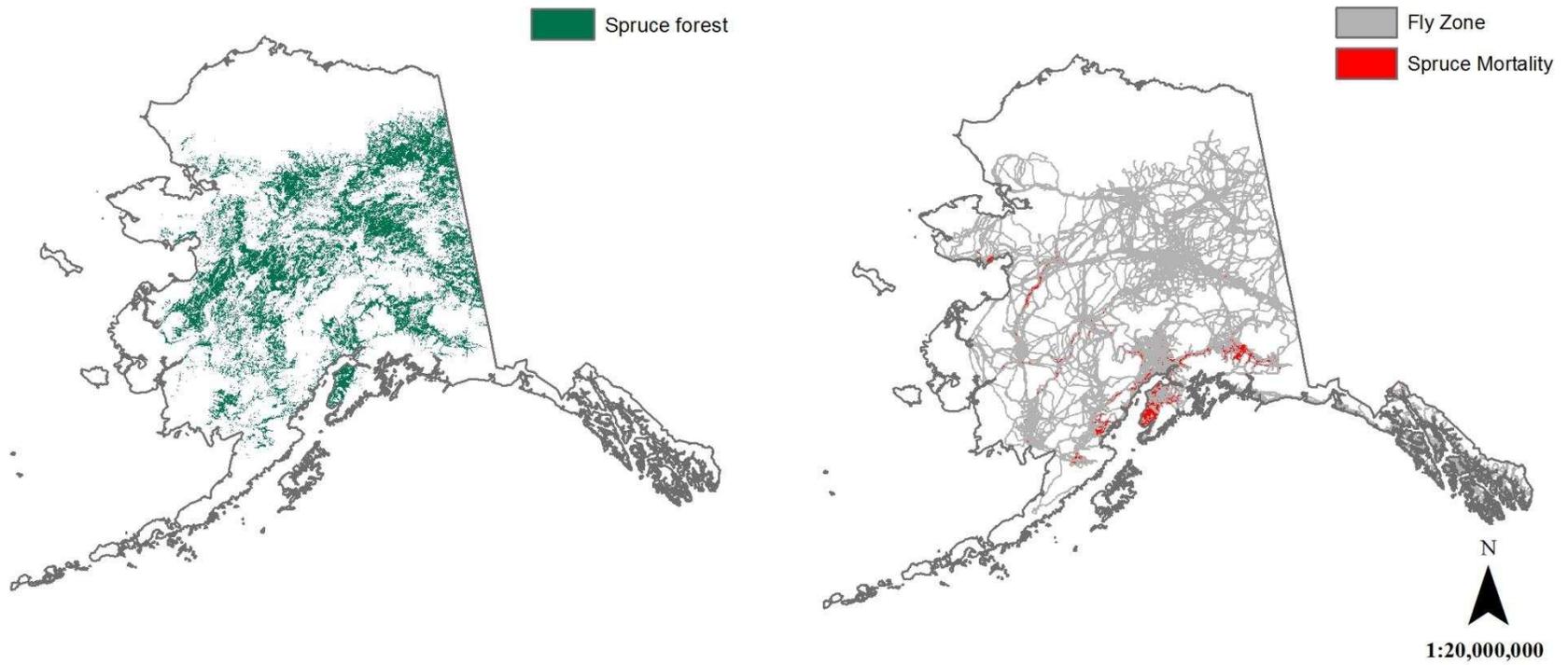
Figure 4. Maps indicate the presence of all species of spruce (left) and presence of spruce mortality on the survey flight line (right) in Alaska.
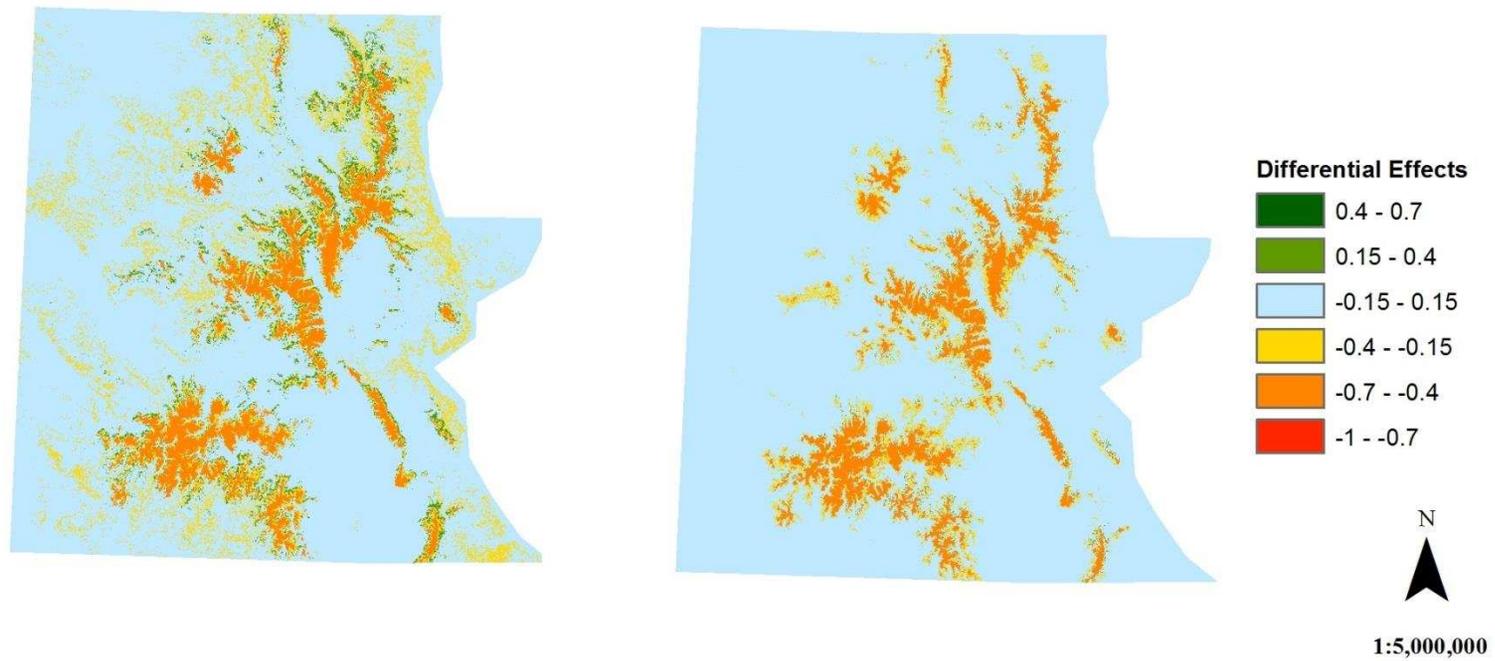
Figure 5. Map showing the differential effects of probability of observing spruce mortality conditional on observing spruce forest from CTM (left) and OLS model (right) for Colorado. The study area was delineated by the layer represent forest land cover in Colorado.
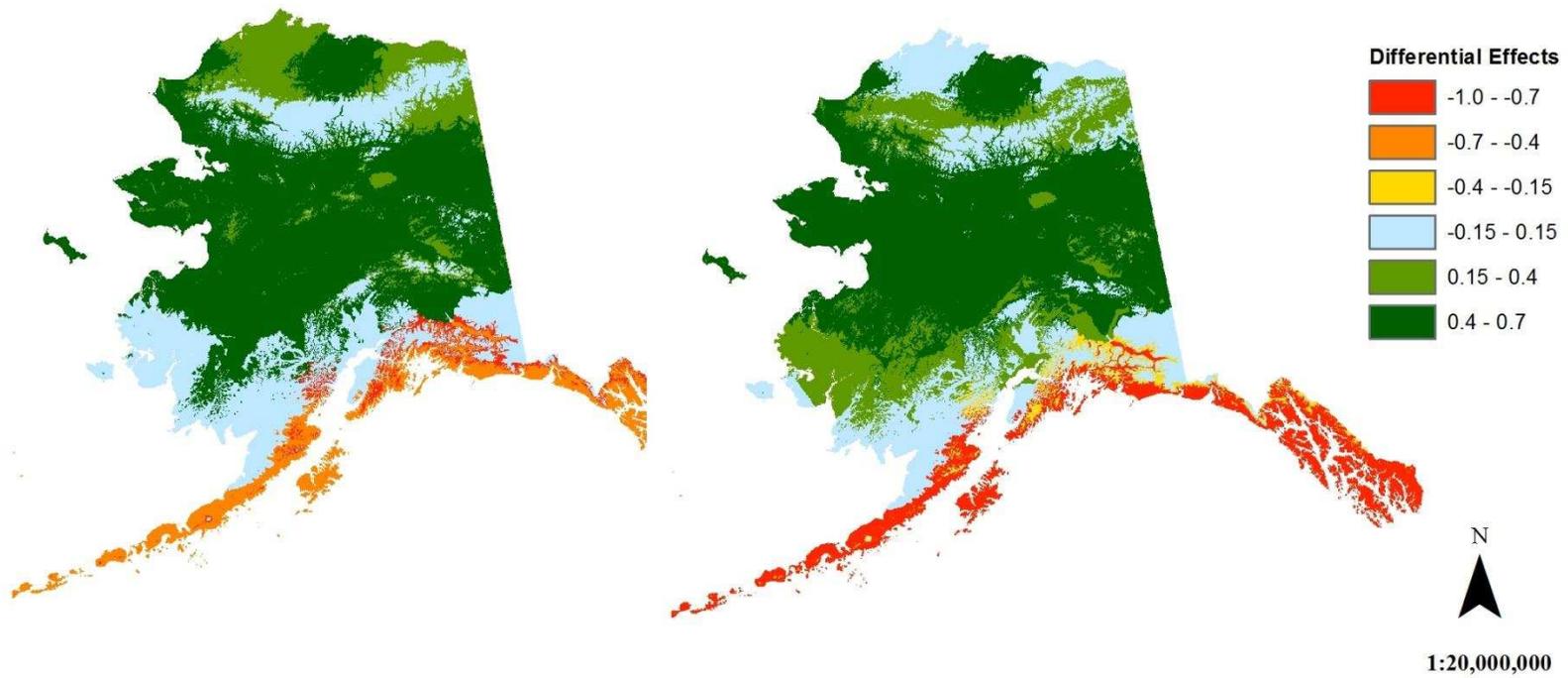
Figure 6. Map showing the differential effects of probability of observing spruce mortality conditional on observing spruce forest from CTM (left) and SAR model (right) for Alaska.
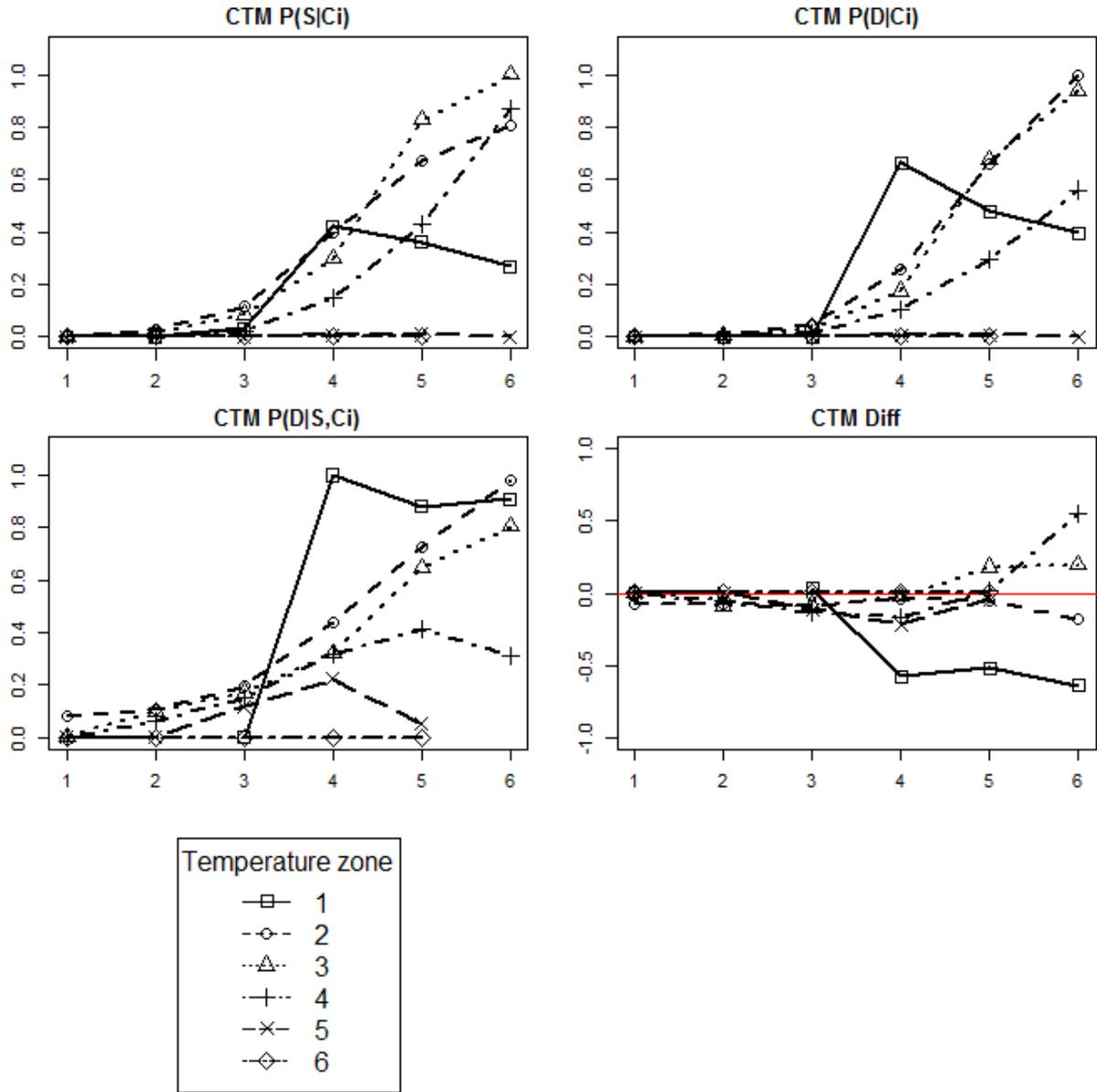
Figure 7. Probability of observing spruce forest in a given climate zone (top left), probability of observing spruce mortality in a given climate zone (top right), probability of observing spruce mortality conditional on spruce forest presence in a given climate zone (bottom left), and differential effects of probability of observing spruce mortality conditional on observing spruce forest (bottom right) from CTM of Colorado.
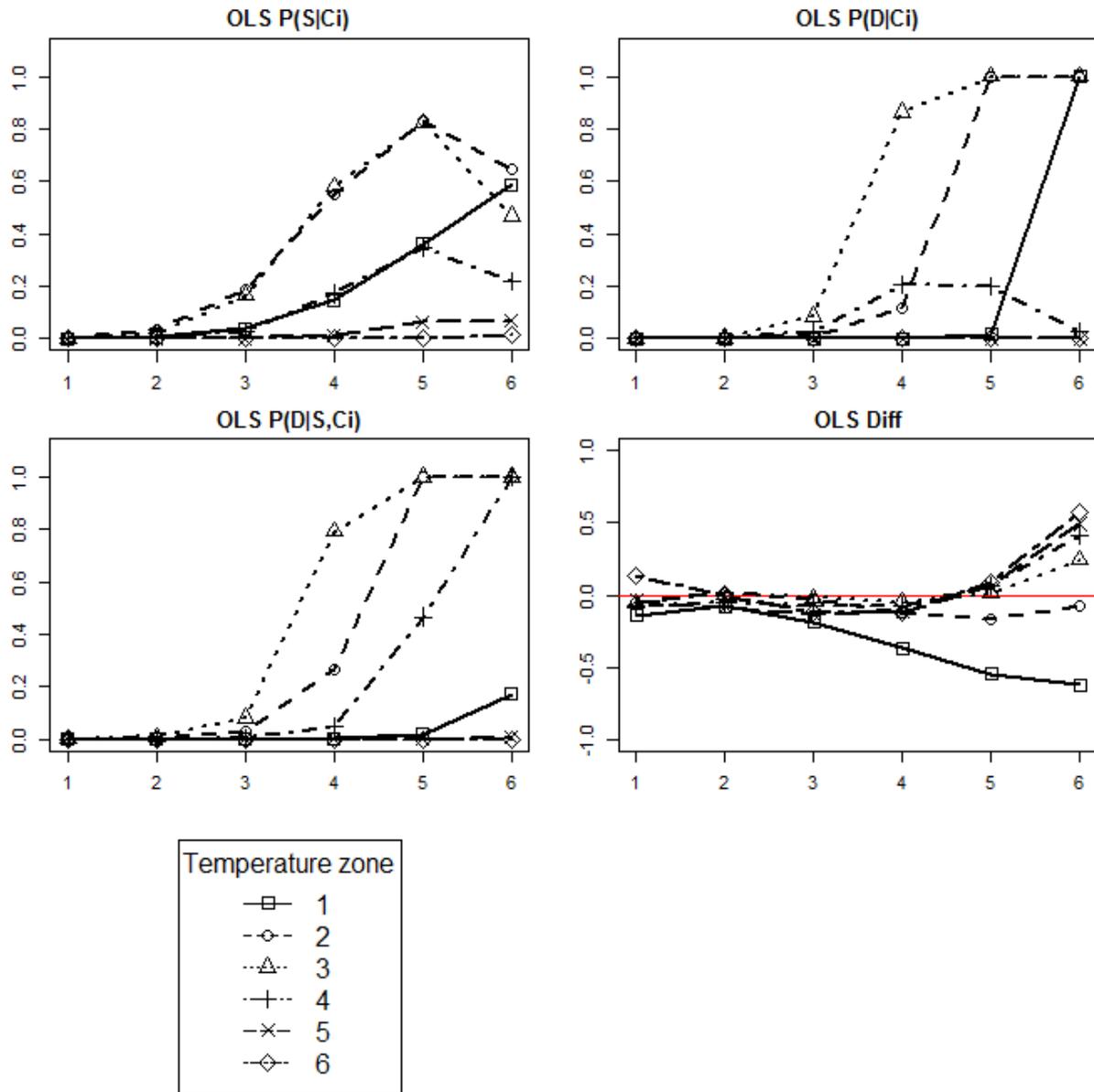
Figure 8. Probability of observing spruce forest in a given climate zone (top left), probability of observing spruce mortality in a given climate zone (top right), probability of observing spruce mortality conditional on spruce forest presence in a given climate zone (bottom left), and differential effects of probability of observing spruce mortality conditional on observing spruce forest (bottom right) from OLS model of Colorado.
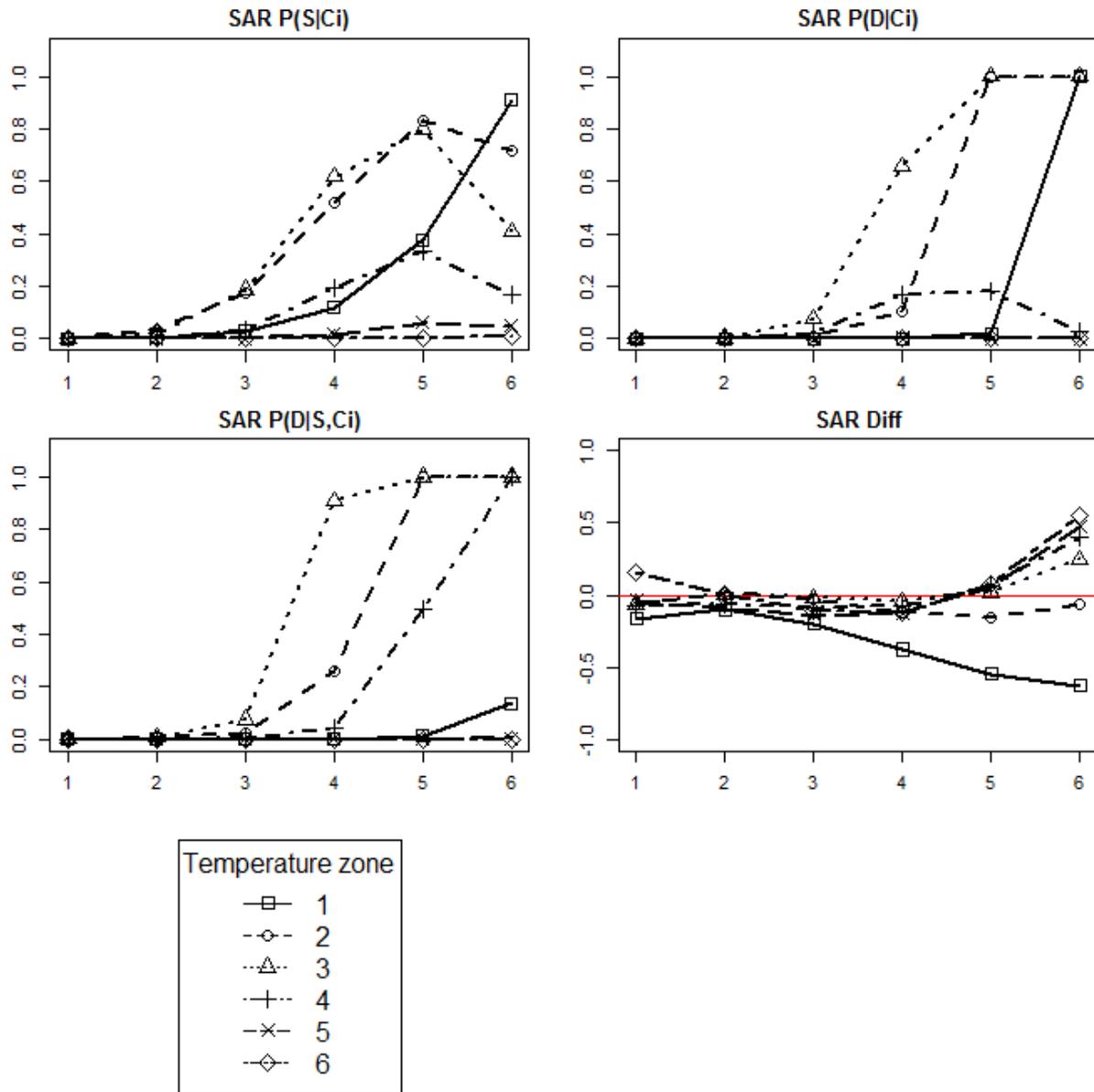
Figure 9. Probability of observing spruce forest in a given climate zone (top left), probability of observing spruce mortality in a given climate zone (top right), probability of observing spruce mortality conditional on spruce forest presence in a given climate zone (bottom left), and differential effects of probability of observing spruce mortality conditional on observing spruce forest (bottom right) from SAR model of Colorado.
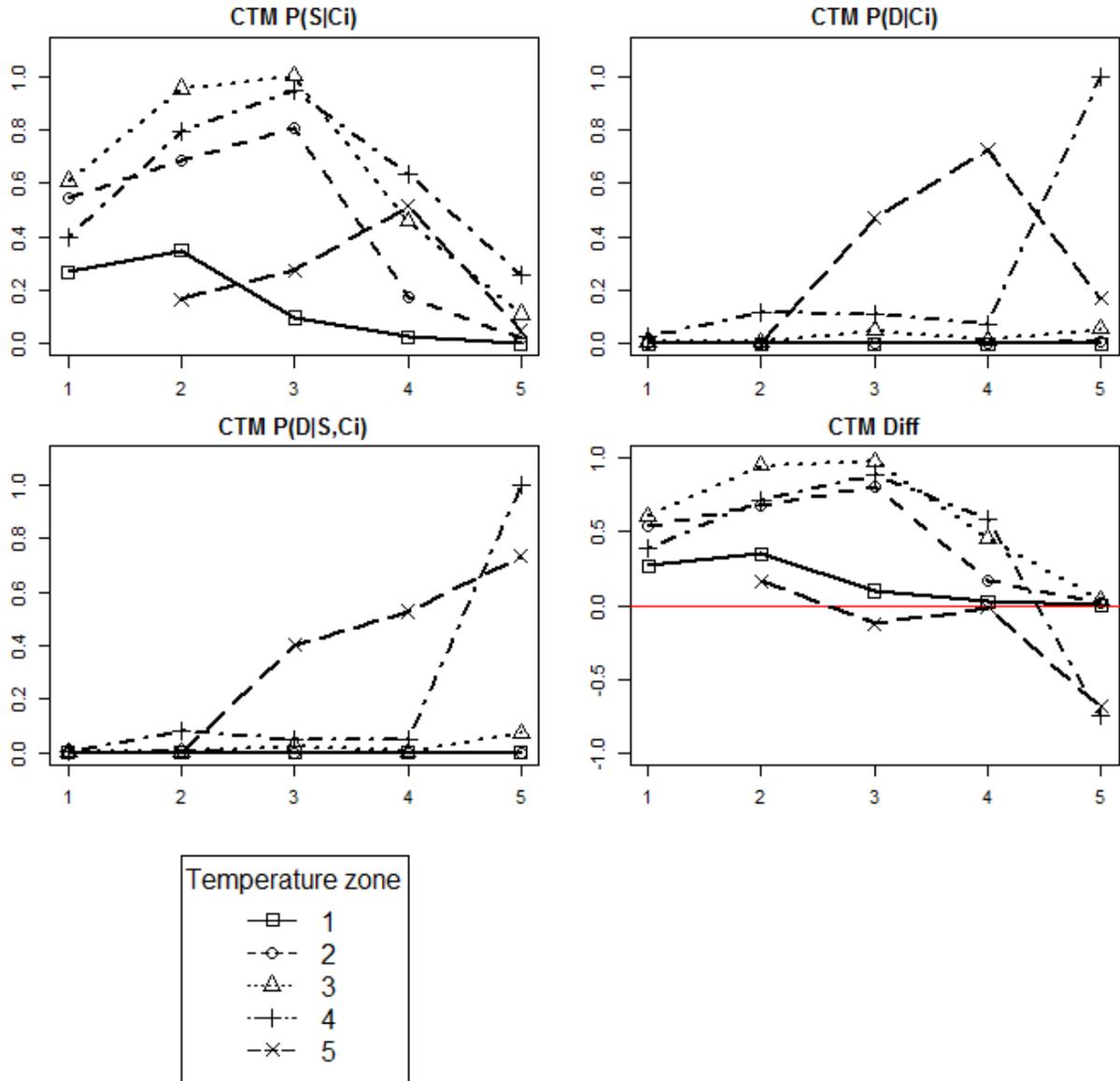
Figure 10. Probability of observing spruce forest in a given climate zone (top left), probability of observing spruce mortality in a given climate zone (top right), probability of observing spruce mortality conditional on spruce forest presence in a given climate zone (bottom left), and differential effects of probability of observing spruce mortality conditional on observing spruce forest (bottom right) from CTM of Alaska.
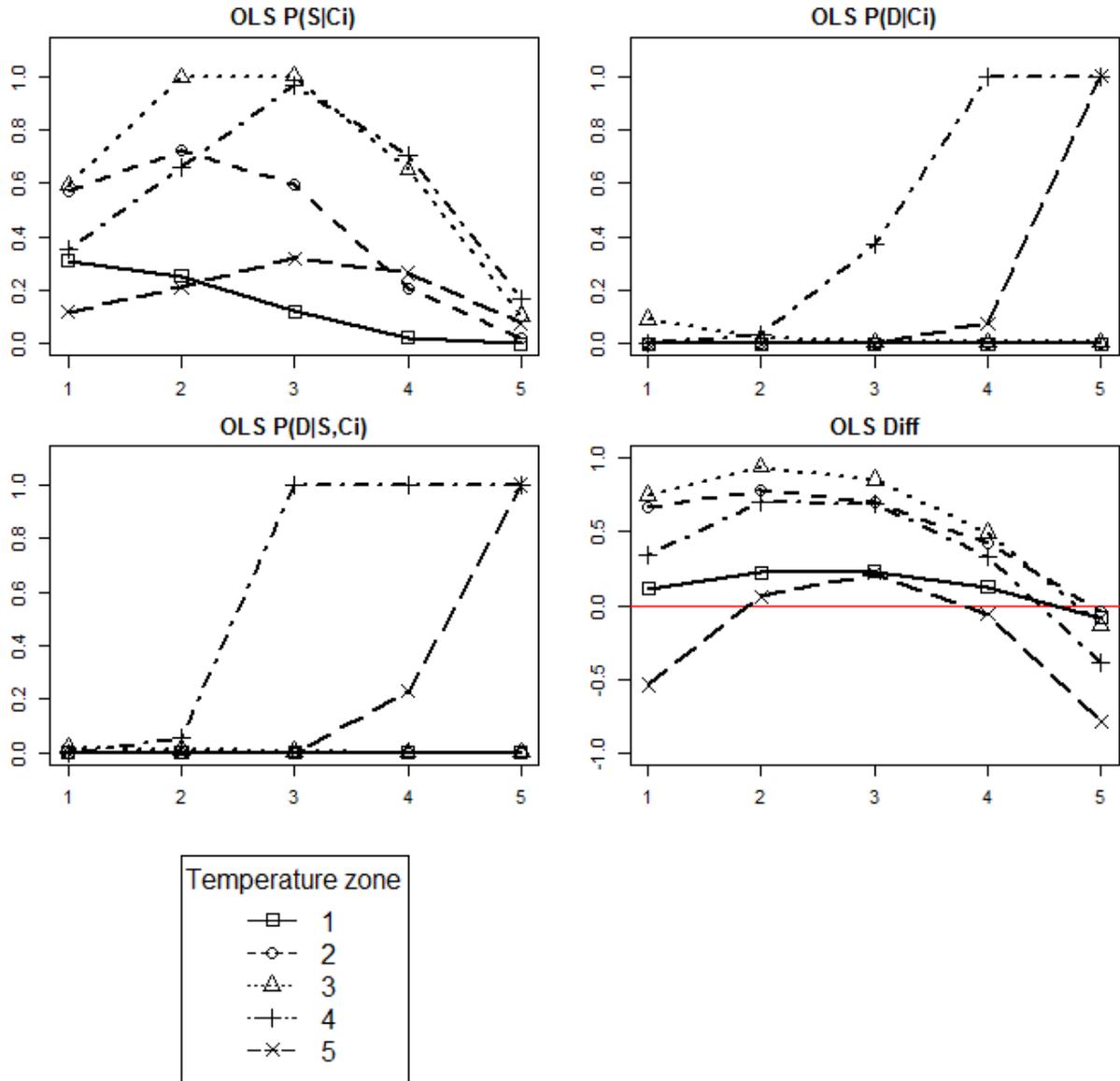
Figure 11. Probability of observing spruce forest in a given climate zone (top left), probability of observing spruce mortality in a given climate zone (top right), probability of observing spruce mortality conditional on spruce forest presence in a given climate zone (bottom left), and differential effects of probability of observing spruce mortality conditional on observing spruce forest (bottom right) from OLS model of Alaska.
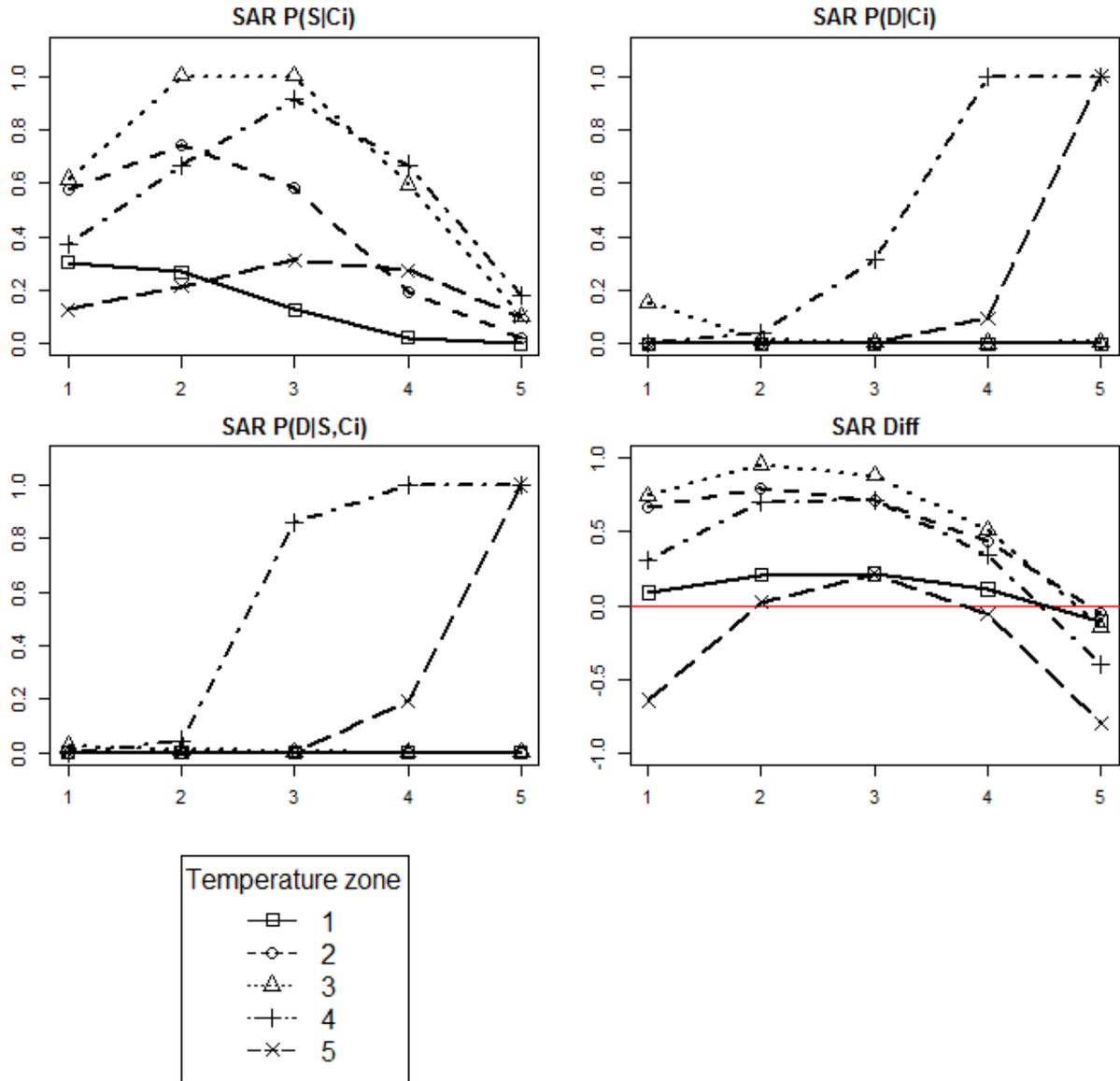
Figure 12. Probability of observing spruce forest in a given climate zone (top left), probability of observing spruce mortality in a given climate zone (top right), probability of observing spruce mortality conditional on spruce forest presence in a given climate zone (bottom left), and differential effects of probability of observing spruce mortality conditional on observing spruce forest (bottom right) from SAR model of Alaska.
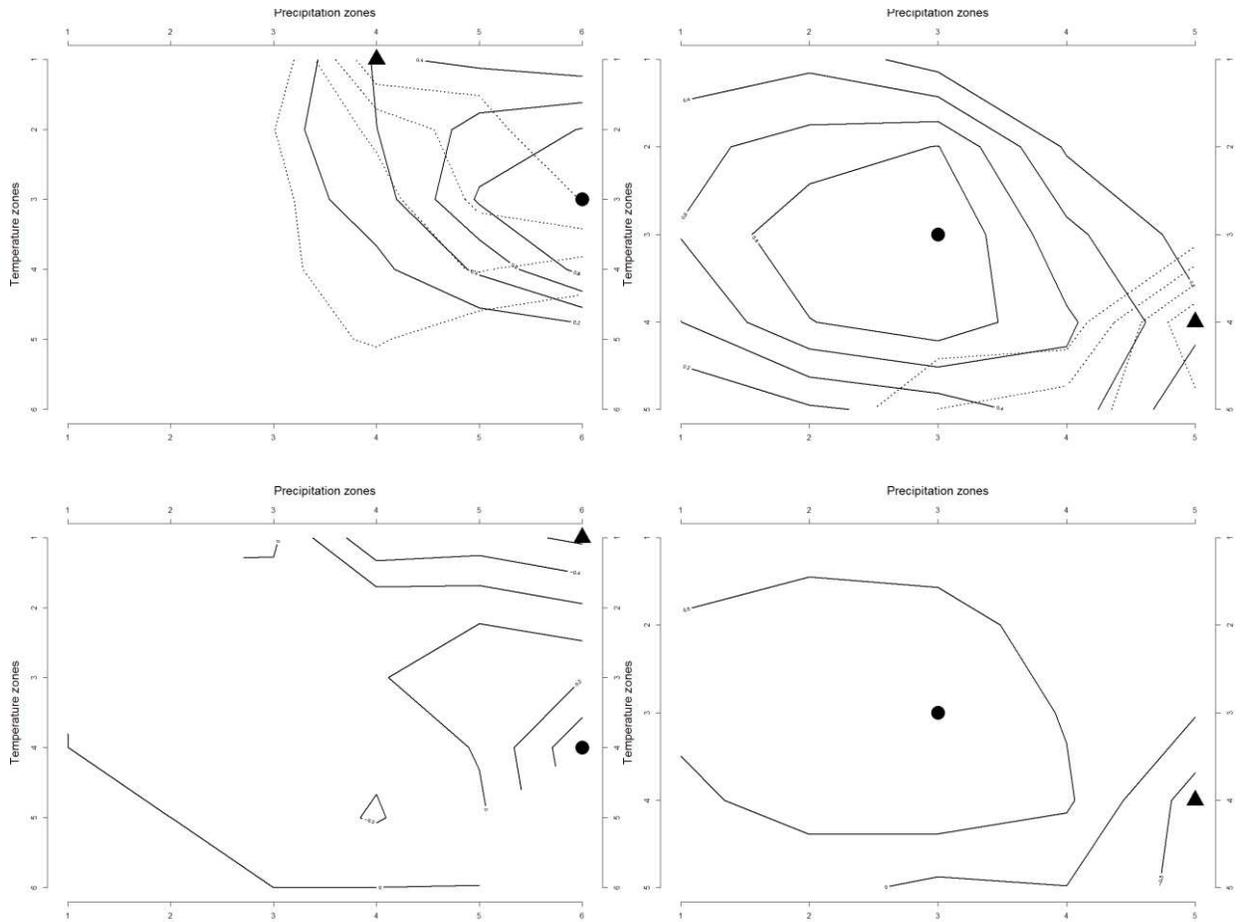
Figure 13. Above, spatial association between the probability of observing spruce (solid contour lines) and the probability of observing spruce mortality given the presence of spruce forests (dotted contour lines) for Colorado (left) and Alaska (right). The symbols represent the maximum probabilities (black circle – spruce forests, black triangle – spruce mortality). Below, solid contour lines show risk map for spruce mortality for Colorado (left) and Alaska (right). The symbols represent the maximum differential effects (black circle – maximum positive value, black triangle – minimum negative value).

LITERATURE CITED

Acharya, T., Ray, A.K., 2005. Image Processing: Principles and Applications. John Wiley & Sons.

Allen, C.D., Macalady, A.K., Chenchouni, H., Bachelet, D., McDowell, N., Vennetier, M., Kitzberger, T., Rigling, A., Breshears, D.D., Hogg, E.H. (Ted), Gonzalez, P., Fensham, R., Zhang, Z., Castro, J., Demidova, N., Lim, J.-H., Allard, G., Running, S.W., Semerci, A., Cobb, N., 2010. A global overview of drought and heat-induced tree mortality reveals emerging climate change risks for forests. For. Ecol. Manag., 259, 660–684.

Anderegg, W.R.L., Berry, J.A., Field, C.B., 2012. Linking definitions, mechanisms, and modeling of drought-induced tree death. Trends Plant Sci. 17, 693–700.

Aquirre-Bravo, C., Reich, R.M., 2006. Spatial statistical modeling and classification of climate for the state of Colorado and adjacent lands of neighboring states. Rocky Mt. Res. Stn. USDA For. Serv. Fort Collins Colo, 123 p.

Araújo, M.B., Peterson, A.T., 2012. Uses and misuses of bioclimatic envelope modeling. Ecology 93, 1527–1539.

Austin, M.P., Smith, T.M., 1990. A new model for the continuum concept. Progress in Theoretical Vegetation Science. Springer, 35–47.

Ayres, P.G., 1984. The interaction between environmental stress injury and biotic disease physiology. Annu. Rev. Phytopathol. 22, 53–75.

Bale, J.S., Masters, G.J., Hodkinson, I.D., Awmack, C., Bezemer, T.M., Brown, V.K., Butterfield, J., Buse, A., Coulson, J.C., Farrar, J., Good, J.E.G., Harrington, R., Hartley, S., Jones, T.H., Lindroth, R.L., Press, M.C., Symrnioudis, I., Watt, A.D., Whittaker, J.B., 2002. Herbivory in global climate change research: direct effects of rising temperature on insect herbivores. Glob. Change Biol. 8, 1–16.

Bentz, B.J., Régnière, J., Fettig, C.J., Hansen, E.M., Hayes, J.L., Hicke, J.A., Kelsey, R.G., Negrón, J.F., Seybold, S.J., 2010. Climate change and bark beetles of the Western United States and Canada: Direct and indirect effects. BioScience 60, 602–613.

Bentz, B., Logan, J., MacMahon, J., Allen, C.D., Ayres, M., Berg, E., Carroll, A., Hansen, M., Hicke, J., Joyce, L., Macfarlane, W., Munson, S., Negron, J., Paine, T., Powell, J., Raffa, K., Regniere, J., Reid, M., Romme, B., Seybold, S., Six, D., Tomback, D., Vandygriff, J., Veblen, T., White, M., Witcosky, J., Wood, D., 2009. Bark beetle outbreaks in western North America: Causes and consequences. Bark Beetle Symposium, 42p.

Berg, E.E., David Henry, J., Fastie, C.L., De Volder, A.D., Matsuoka, S.M., 2006. Spruce beetle outbreaks on the Kenai Peninsula, Alaska, and Kluane National Park and Reserve, Yukon Territory: Relationship to summer temperatures and regional differences in disturbance regimes. For. Ecol. Manag., 227, 219–232.

Blois, J.L., Williams, J.W., Fitzpatrick, M.C., Jackson, S.T., Ferrier, S., 2013. Space can substitute for time in predicting climate-change effects on biodiversity. Proc. Natl. Acad. Sci. 110, 9374–9379.

Breshears, D.D., Cobb, N.S., Rich, P.M., Price, K.P., Allen, C.D., Balice, R.G., Romme, W.H., Kastens, J.H., Floyd, M.L., Belnap, J., Anderson, J.J., Myers, O.B., Meyer, C.W., 2005. Regional vegetation die-off in response to global-change-type drought. Proc. Natl. Acad. Sci. U. S. A. 102, 15144–15148.

Chavardès, R.D., Daniels, L.D., Waeber, P.O., Innes, J.L., Nitschke, C.R., 2012. Did the 1976–77 switch in the Pacific Decadal Oscillation make white spruce in the southwest Yukon more susceptible to spruce bark beetle? For. Chron. 88, 513–518.

ESRI, R., 2011. ArcGIS desktop: release 10. Environ. Syst. Res. Inst. CA.

Farber, O., Kadmon, R., 2003. Assessment of alternative approaches for bioclimatic modeling with special emphasis on the Mahalanobis distance. Ecol. Model. 160, 115–130.

Gaylord, M.L., Kolb, T.E., Wallin, K.F., Wagner, M.R., 2007. Seasonal dynamics of tree growth, physiology, and resin defenses in a northern Arizona ponderosa pine forest. Can. J. For. Res. 37, 1173–1183.

Hanson, P.J., Weltzin, J.F., 2000. Drought disturbance from climate change: response of United States forests. Sci. Total Environ., 262, 205–220.

Hard, J.S., 1985. Spruce Beetles Attack Slowly Growing Spruce. For. Sci. 31, 839–850.

Hart, S.J., Veblen, T.T., Eisenhart, K.S., Jarvis, D., Kulakowski, D., 2013. Drought induces spruce beetle (*Dendroctonus rufipennis*) outbreaks across northwestern Colorado. Ecology 95, 930–939.

Herold, N., 2011. Resolution vs minimum mapping unit: Size does matter. Digit. Coast GeoZone.

Holsten, E.H., Werner, R.A., 1990. Comparison of white, Sitka, and Lutz spruce as hosts of the spruce beetle in Alaska. Can. J. For. Res. 20, 292–297.

Huberty, A.F., Denno, R.F., 2004. Plant water stress and its consequences for herbivorous insects: a new synthesis. Ecology 85, 1383–1398.

Jenkins, M.J., Hebertson, E.G., Munson, A.S., 2014. Spruce beetle biology, ecology and management in the Rocky Mountains: an addendum to spruce beetle in the Rockies. Forests 5, 21–71.

Johnson, E.W., Ross, J., 2008. Quantifying error in aerial survey data. Aust. For. 71, 216–222.

Kelsey, R.G., Gallego, D., Sánchez-García, F.J., Pajares, J.A., 2014. Ethanol accumulation during severe drought may signal tree vulnerability to detection and attack by bark beetles. Can. J. For. Res. 44, 554–561.

Larsson, S., 1989. Stressful times for the plant stress: Insect performance hypothesis. Oikos 56, 277–283.

Lundquist, J.E., 2005. Landscape pathology-forest pathology in the era of landscape ecology. 155–165.

Masoud, M., 2012. Influence of climatic zones on the distribution and abundance of damage agents and forest types in Colorado, United States and Jalisco, Mexico. 81 p.

Mattson, W.J., Haack, R.A., 1987. The role of drought in outbreaks of plant-eating insects. BioScience 110–118.

McDowell, N., Pockman, W.T., Allen, C.D., Breshears, D.D., Cobb, N., Kolb, T., Plaut, J., Sperry, J., West, A., Williams, D.G., Yepez, E.A., 2008. Mechanisms of plant survival and mortality during drought: why do some plants survive while others succumb to drought? New Phytol. 178, 719–739.

Pearson, R.G., Dawson, T.P., 2003. Predicting the impacts of climate change on the distribution of species: are bioclimate envelope models useful? Glob. Ecol. Biogeogr. 12, 361–371.

Pickett, S.T., 1989. Space-for-time substitution as an alternative to long-term studies. Long-Term Studies in Ecology. Springer, 110–135.

Pongpattananurak, N., Reich, R.M., Khosla, R., Aguirre-Bravo, C., 2012. Modeling the spatial distribution of soil texture in the State of Jalisco, Mexico. Soil Sci. Soc. Am. J. 76, 199-209.

R Core Team, 2014. R: A language and environment for statistical computing. R Foundation for Statistical Computing, Vienna, Austria.

Reich, R.M., Aguirre-Bravo, C., Bravo, V.A., 2008. New approach for modeling climatic data with applications in modeling tree species distributions in the states of Jalisco and Colima, Mexico. J. Arid Environ. 72, 1343–1357.

Reich, R.M., Aguirre-Bravo, C., Bravo, V.A., Briseño, M.M., 2011. Empirical evaluation of confidence and prediction intervals for spatial models of forest structure in Jalisco, Mexico. J. For. Res. 22, 159–166.

Reich, R.M., Bonham, C.D., Aguirre-Bravo, C., Chazaro-Basañeza, M., 2010. Patterns of tree species richness in Jalisco, Mexico: relation to topography, climate and forest structure. Plant Ecol. 210, 67–84.

Reich, R.M., Davis, R., 2008. Quantitative Spatial Analysis. Colorado State University.

Reich, R.M., Lundquist, J.E., Acciavatti, R.E., 2014. Influence of climatic conditions and elevation on the spatial distribution and abundance of *Trypodendron* ambrosia beetles (Coleoptera: Curculionidae: Scolytinae) in Alaska. For. Sci. 60, 308–316.

Reich, R.M., Lundquist, J.E., Bravo, V.A., 2013. Characterizing spatial distributions of insect pests across Alaskan forested landscape: A case study using Aspen Leaf Miner (*Phyllocnistis populiella* Chambers). J. Sustain. For. 32, 527–548.

Reich, R.M., Lundquist, J.E., Hughes, K., 2016. Host-environment mismatches associated with subalpine fir decline in Colorado. J. For. Res, 1-13.

Schmid, J., Frye, R., 1977. Spruce beetle in the Rockies. Bark Beetles Fuels Fire Bibliogr. 44 p.

Seager, R., Ting, M., Held, I., Kushnir, Y., Lu, J., Vecchi, G., Huang, H.-P., Harnik, N., Leetmaa, A., Lau, N.-C., Li, C., Velez, J., Naik, N., 2007. Model projections of an imminent transition to a more arid climate in Southwestern North America. Science 316, 1181–1184.

Seastedt, T.R., Hobbs, R.J., Suding, K.N., 2008. Management of novel ecosystems: Are novel approaches required? Front. Ecol. Environ. 6, 547–553.

Sherriff, R.L., Berg, E.E., Miller, A.E., 2011. Climate variability and spruce beetle (*Dendroctonus rufipennis*) outbreaks in south-central and southwest Alaska. Ecology 92, 1459–1470.

Upton, G.J., Fingleton, B., 1985. Spatial data analysis by example. Vol. 1: Point pattern and quantitative data. Chichester Wiley 1985, 1.

Wade, T.G., Wickham, J.D., Nash, M.S., Neale, A.C., Riitters, K.H., Jones, K.B., 2003. A comparison of vector and raster GIS methods for calculating landscape metrics used in environmental assessments. Photogramm. Eng. Remote Sens. 69, 1399–1405.

Wargo, P.M., 1985. Interaction of stress and secondary organisms in decline of forest trees, in: Air pollutants effects on forest ecosystems, St. Paul, Mn.(USA), 8-9 May 1985. Acid Rain Foundation.

Werner, R.A., Holsten, E.H., Matsuoka, S.M., Burnside, R.E., 2006. Spruce beetles and forest ecosystems in south-central Alaska: A review of 30 years of research. For. Ecol. Manag. 227, 195–206.

Williams, A.P., Allen, C.D., Macalady, A.K., Griffin, D., Woodhouse, C.A., Meko, D.M., Swetnam, T.W., Rauscher, S.A., Seager, R., Grissino-Mayer, H.D., 2013. Temperature as a potent driver of regional forest drought stress and tree mortality. Nat. Clim. Change 3, 292–297.

ZERO- AND ONE-INFLATED BETA REGRESSION MODEL FOR ESTIMATING

ENVIRONMENTAL ASSOCIATION AND INTENSITY OF ENGELMANN SPRUCE (*Picea*

engelmannii Parry ex Engelm.) MORTALITY IN COLORADO

Introduction

Understanding the effects of climate and environmental association with the distribution and density of forest insects and diseases across the spatial context is a major goal for forest entomologists and land managers (Lundquist, 2005). Especially in the regime of changing climate, understanding the interaction of the forest and its etiology at various spatio-temporal scales via modeling can provide valuable information (Lundquist and Reich, 2014). Modeling the distribution and intensity of outbreak involves combining ecological and statistical theories that played a large part in the development of numerous applications for ecosystem management and decision-making support. Statistical modeling has been applied in many aspects of natural resources management, such as conservation of endangered species (Engler et al., 2004), managing invasive species (Cook et al., 2007), and mapping the risk of infectious diseases (Jones et al., 2008). In studies of forest insects and diseases, statistical modeling has been applied to describe the association between the habitat of forest insects and diseases in the spatial context (Araújo and Peterson, 2012; Hart et al., 2015; Hebertson and Jenkins, 2008).

Outbreak of spruce bark beetles (*Dendroctonus rufipennis* Kirby), native to western North America (Massey and Wygant, 1954; Raffa et al., 2008), takes place in temperate coniferous forest ecosystems. *D. rufipennis* can infest nearly all *Picea* species. In the Colorado Rocky Mountains, the Engelmann spruce (*Picea engelmanniii* Parry ex Engelm.) is the most common *Picea* species affected by the spruce bark beetle (Holsten and Werner, 1990; Schmid and Frye, 1977), with a larger affected area than wildfires (Veblen et al., 1991). Outbreak modifies the composition and structure of the spruce stand

by killing larger trees in spruce-dominated stands, leaving smaller spruces and trees of other species (Schmid and Frye, 1977; Veblen et al., 1991). Outbreak results in large-scale removal of vegetation in the subalpine forest ecosystem without removing the standing dead trees (Schmid and Frye, 1977). This leads to the accumulation of fuel across the landscape, altering the behavior of wildfires to be higher in intensity, severity, and occurrence (DeRose and Long, 2009; Jenkins et al., 2012; Schmid and Frye, 1977). Other outbreak effects relate to changing the amount of streamflow and nitrogen runoff (Bethlahmy, 1975; Griffin et al., 2011), changing forest biodiversity, and changing landscape heterogeneity (Kaiser et al., 2013; Kurz et al., 2008).

It is difficult to identify the complex association between causal agents and environmental factors because of the high variability at both the spatial and temporal scale. In this study, we hypothesize that the occurrence and intensity of Engelmann spruce mortality is additively associated with both climate factors and plot-level characteristics of vegetation, such that a suboptimal state of habitat for *P. engelmannii* due to local individuals encountering environmental conditions either impacts host susceptibility or affects population dynamics of casual agents. These conditions favor a higher chance for mortality occurrence and increase the intensity of the infested host. Persistent suboptimal conditions of habitat could lead the local host population to a state of marginal population, in which either survival or regeneration do not favor host population's tenacity over the long term (Kawecki, 2008). For example, drought-prone sites (those deficient of persistent water) or even excessive-moisture sites can have physiological effects on local spruce species and can cause the population to be predisposed to bark beetle infestation and other diseases (Hard and Holsten, 1985; Hart et al., 2013; Sherriff et al., 2011).

Features of stand structure and composition are essential factors associated with host mortality at both spatial and temporal scales. Stands with older-age spruce may gradually become susceptible to bark beetles. The slow diameter growth rate of an old or highly competitive stand is one indicator for susceptibility to spruce bark beetles. Structure-induced susceptibility is also found in large-volume stands, stands with a high basal area, stands with a high proportion of spruce composition, and stands with a high crown competition (DeRose et al., 2013; Doak, 2004; Hard, 1985; McCambridge and Stevens, 1982;

Raffa et al., 2005; Reynolds and Holsten, 1994). Furthermore, stands with dense, large trees have higher phloem content, which is eventually a major food source for bark beetle brood development, favoring the growth of population (Berryman, 1982). Aggressive fire suppression could consequently lead to high competition for scarce water resources within a stand (Breece et al., 2008). Diversity in a stand, the spatial characteristics of heterogeneity, and connectivity of extent may restrain spread and reduce the magnitude of mortality from spreading outbreak (DeRose and Long, 2012; Fettig et al., 2008; Kausrud et al., 2012).

Pattern and distribution of ecological process at the landscape scale have been interesting to scientists for a long time (Pielou, 1977; Turner, 1989). Since the proposal of a method to model the spatially explicit occupancy rate of a species (Hoeting et al., 2000; MacKenzie et al., 2002), the probabilistic occupancy model has become regarded with great favor in ecological studies. The occupancy model, which focus on correlation between responses and covariates, focuses on describing the probability of the existence of interested organisms given a set of habitats. This kind of model is used for assessing the influences of the hypothesized environmental covariates on the presence and absence of an interested organism in the survey unit. Recently, many fields in ecology have increasingly used the occupancy model for questioning ecosystem changes and the emergence of vulnerabilities to address theoretical and practical issues (Clark, 2005; Keith et al., 2008). Many approaches have been developed to deal with the association of known covariates (Meier et al., 2010; Zimmermann and Kienast, 1999) and with unknown latent processes (Royle et al., 2007). The modeling of occupancy response to environmental factors is related to the concept of ecological niche (MacArthur et al., 1966). There are numerous statistical methods used to model species' distributional and abundant responses. Generalized linear models (or generalized additive models) are usually developed and applied to describe the association between data of spatial distribution and environmental covariates (Guisan and Thuiller, 2005).

The original likelihood method of model fitting has a computational limit in the ability to accommodate multistage and mixed structures that model could be composed of more than single sub-model. This kind of model usually involve in inclusion of variance of sampling or mechanistic process,

93

and temporally or spatially correlated structure (MacKenzie, 2006), or making predictions for multiple observed variables (Hobbs and Hilborn, 2006). On the other hand, the Bayesian approach is the only computational method available for a hierarchical structure of mixed models. The Bayesian-likelihood framework allows for random variables of mixed structures to be possibly incorporated into the model (Gelman and Hill, 2006). Structured parameters dependent on other levels of problems can be simultaneously simulated by the Bayesian model using the Markov chain Monte Carlo (MCMC) method, so we can address the several connected problems within one multilevel model (Hooten and Hobbs, 2015). A multilevel model incorporating generalized linear mixed model (GLMM) can deal with the problem of needing the linear predictor function of fixed and random effects from covariates to be associated with a link function of the response data. These relationships conditionally depend on the predictors and response data arising from an appropriately designated probabilistic distribution function (Breslow and Clayton, 1993).

The effective model must be able to strongly address the spatio-temporal dependent structure and to account for the numerical skewness due to excessive absent responses (Chelgren et al., 2011; Zuur et al., 2009). Disregarding these characteristics might lead to incorrect statistical inference. Data collected from the spatial extent could be dependent on obscure processes related to the proximities between sampling units. Integrating the uncertainty from spatial dependence could lead to more accurate estimation of model parameters instead of just the average effects from the function associated with environmental covariates (Hobbs and Hilborn, 2006; Wikle, 2002). Spatial dependence could be modeled by the geostatistical point-process model using the multivariate Gaussian process for spatial errors (Banerjee et al., 2008; Diggle, 1983). In the spatial point-process or kriging model, the response variables at every sample location are associated with explanatory variables at their own locations via the predictor function, and the errors term is correlated among each sampling location point. Sometimes, the errors term may include an additional non-spatially uncorrelated error, or nugget effect (Davis and Goetz, 1990; Latimer et al., 2009). However, spatial dependence should be under the assumption of the absence of

local microevolution that the changing in the response to habitat could cause shifting of species distribution (Record et al., 2013).

Skewness from the high proportion of absence, or zero, in survey data may violate the assumed probability distribution function and could severely bias the model estimates (Shono, 2008). The removal of absent data prior to analysis may solve this problem, but it could bias the analysis. There are numerous modeling approaches to deal with zero-inflated data (Ridout et al., 1998). Zero-inflated models are types of mixture models applied to describe the association of zero and non-zero responses, with the explanatory variables separate from the estimation of numerical responses such as the frequency of detections and other continuous data. A common approach is to model the zero/non-zero data using a binomial distribution with parameters predicted by a link function such as logit or probit. This kind of model treats zero data as a true absence. After modeling absence, the positive values of data or parameters describing the data are modeled using a standard probability distribution function for continuous data or by using a Poisson distribution for count data (Chelgren et al., 2011).

However, there are not many applications of zero-inflated approaches in ecology to model proportion or density data where values range from zero to one. Nishii and Tanaka (2012) developed an approach to model the proportion of forest area cover in the spatial grid by decomposing a model into two likelihood parts composed of multinomial logistic regression to separate extreme data of zero to one responses from the proportional data. The partial forest cover ratio data were then modeled using the logit link normal regression model. Ospina and Ferrari (Ospina and Ferrari, 2012, 2008) proposed a class of inflated models to describe proportional data by regressing on the parameters of beta distribution using a standard distribution function instead of directly modeling the proportional data. This model assumes that the response data have a mixed continuous-discrete distribution, in which extreme data are modeled by binomial distribution and beta distribution is used to indirectly describe continuous proportional data via parameters of probability distribution function.

In this study, we developed a spatial Bayesian multistage mixture model for *P. engelmannii* mortality response caused by *D. rufipennis*. We used a model based on three structures of likelihood to

describe the occurrence and intensity of mortality, as well as account for spatial dependence by implementing a geostatistical point-pattern approach. The presence and absence of Engelmann spruce mortality were described by Bernoulli distribution, and the extreme response values of entire stand mortality were then modeled with the same distribution. The rest of the continuous mortality proportion was described by beta distribution. The spatial dependence portion was integrated into each step of the model using the multivariate Gaussian process with an exponential correlation function.

We used the developed model to address four questions in the study:

4. How do varying climatic conditions, stand structure, and composition associate with the presence of Engelmann spruce mortality, conditional on sampled spruce forest?

5. How do varying climatic conditions, stand structure, and composition associate with the full stand mortality (100% mortality) of Engelmann spruce, conditional on sampled spruce forest?

6. How do varying climatic conditions, stand structure, and composition associate with the proportion of partial mortality of Engelmann spruce, conditional on sampled spruce forest?

7. How does the association between Engelmann spruce mortality and habitat affect the spatial distribution of spruce mortality and its intensity in Colorado using predictions from the model?

Our goal in this study was to combine the information found in the features of abiotic climate data, biotic vegetation structure and composition collected in the field, and spatially dependent uncertainty in order to provide a description of association with presence and intensity responses, as well as to provide spatial predictions at the landscape scale.

Material and Methods

Field data collection

During July and August 2013 and 2014, field data were collected from 55 sites within the western part of Colorado. The study area was selected and delineated based on raster layers representing the vegetation cover obtained from the Colorado Division of Wildlife as part of the Gap Analysis Program (http://ndis1.nrel.colostate.edu/cogap/cogaphome.html) to indicate the habitat of *P. engelmannii* in

Colorado. Survey plot sampling was conducted in eight national forests: Roosevelt, Routt, White River, Uncompahgre, Grand Mesa, San Juan, Rio Grande, and Pike (Figure 14). The locations of survey sites were randomly assigned along the forest road conditional on the presence of habitat area, and each study site must be at least 50 meters from the forest road. Each study site was surveyed using variable-size plot sampling conditional on the presence of forest-type vegetation, so the plot locations without existence of the tree species were left out of the samples. At each study site, we implemented multiple-plot adaptive sampling. Three sampling plots were assigned at the site where the centered plot had forest cover. The other two plots, subplots, were randomly chosen to be aligned 50 meters from the centered plot in either the direction of north-south or east-west (Figure 15). The same sampling method of forest tree species and stand composition was conducted for other plots with at least one available sampled tree.

From the total of 153 survey plots, we sampled both living and dead trees of all species using a relascope for a variable-radius sampling method, which, in a previous study, did not have any significant accuracy differences compared to the fixed-plot sampling methods for forest inventory (Piqué et al., 2011). Each sampled tree considered inside the plot was identified for species and for mortality caused by *Dendroctonus rufipennis*, which can be assumed by the presence of feeding galleries with fan-shaped and gregarious feeding pattern on the inner bark of the dead, measured by diameter at breast height (DBH). The DBH data were converted to basal area for each species in each plot. Then we used the basal area to calculate the features of stand characteristics and composition. The main response variable of mortality proportion was calculated by the ratio between basal area of the dead and total basal area of *P. engelmannii*. The other plot-level characteristics included relative dominance (RD) compared to the other species and average basal area per tree (BT). Relative dominance was calculated by dividing basal area of *P. engelmannii* by the sum of basal area of every other species in the plot. Relative dominance represents the species composition and dominance in the plot. We calculated basal area per tree by dividing the sum of basal area by the number of sampled *P. engelmannii* in the plot. Basal area per tree represents the average size and age class of the sampled species. Another stand characteristic collected from each plot

was the number of stories, representing stand structure complexity (S). The number of stories was

visually measured by separating stand into dominance, co-dominance, and sub-dominance.

Each covariate collected in the survey plots was transformed into categorical data to account for

the possible non-linear association with response. This made the model selection easier by leaving out of

the model the complex components of multinomial functions. Each covariate was splitted by equalization

of frequency and then round the value into integer. Relative dominance of *P. engelmannii* was broken up

into four classes: RD1 for 0–25%, RD2 for 25–50%, RD3 for 50–75%, and RD4 for 75–100%. Average

basal area per tree was classified into three categories: BT1 for 0–1 square feet/tree, BT2 for 1–2 square

feet /tree, and BT3 for >2 square feet /tree. The stand structure was categorized into three classes: S1 for

stand with one story, S2 for stand with two stories, and S3 for stand with at least three stories. The

distribution of categorical covariates in sample plots is provided in Figure 17.

Climate Data

Besides the covariates for local stand characteristics and composition, we additionally assigned

the climate zone data for each plot location to describe the relationship between the occurrence and

intensity of mortality with the climatic factors. A particular climate zone was classified by a specific pair

of temperature zone and precipitation zone. Climate data for each plot were obtained from a previous

study (Aquirre-Bravo and Reich, 2006) by spatially intersecting the locations of study plots with the

climate zone map (Figure 16). The benefit of using zones to describe climate characteristics is that it

provides an opportunity to examine the roles of climatic factors on outbreak dynamics across the

landscape (Aquirre-Bravo and Reich, 2006; Reich et al., 2014). Additionally, we can reduce the spatio-

temporal variability and alleviate the sampling and process error of the prediction from the climate model.

Climate zones have been used in several previous studies. Reich and colleagues (2010) defined climate

zones for a natural resources monitoring program in Jalisco, Mexico. Climate zone was also used to

model soil texture composition (Pongpattananurak et al., 2012), to model climate association with tree

species richness (Reich et al., 2008), to model forest stand structure (Reich et al., 2011), to model the

abundance of causal agents in various forest types (Masoud, 2012), and to determine the influence of climate on forests insects in Alaska (Reich et al., 2013).

Hierarchical Model Framework

From here forward, we make frequent use of linear algebra notation to avoid the redundant usage of collective terms for covariates. We use italic letters (e.g., *a* or *A*) to represent the random variable and a square bracket notation (e.g., [*a*|*b*]) to represent probability distributions; in this case, [*a*|*b*] represents the probability distribution of random variable *a* conditional on random variable *b* *without specification of the type of probability distribution function*. For a particular probability distribution function, we use the notation to specify the type of distribution function for the random variable—e.g., Normal(*a*, *b*) to represent the Gaussian probability function of a random variable with specified parameters *a* and *b*. For notation of linear algebra, we use bold, uppercase letters for matrices (e.g., **A),** and we use bold, lowercase letters for vectors (e.g., **x**).

In this study, the hierarchical Bayesian framework was implemented to account for the GLMM. There are many studies that implement the hierarchical Bayesian model, but there are only a few studies in forest health and pathology that apply the Bayesian method (Giovanini et al., 2013; Haas et al., 2011; Stadelmann et al., 2013). Conceptually, the hierarchical model is based on a hypothetical probability distribution describing likelihood. From the conditional probability perspective, we can see the joint distribution of random variables, [*a*, *b*, *c*], as a hierarchical structure of conditional probability, [*a*, *b*, *c*] = [*a*, *b* | *c*][*c*] = [*a* | *b*, *c*][*b* | *c*][*c*]. The idea behind these three random variables is that there is a hierarchical structure of processes from the response data, *a*, to the set of parameters, *c*, through an unknown latent process, *b*, that conveys the association from the model parameters to the responses.

The hierarchical structure of GLMM can be specified by likelihood model framework. From the example of joint distribution [*a*, *b*, *c*], we can rewrite the equation into the likelihood framework by substituting *a* with vector **y**, representing the response variables from sample. Random variable *b* is substituted with the unknown latent process of vector **z**, and random variable *c* is replaced by vector ***θ***,

representing model parameters. Therefore, we can write the likelihood function of the model from the conditional probability function:

$$L(\boldsymbol{\theta}|\boldsymbol{y}) \propto [\boldsymbol{y}, \boldsymbol{z}|\boldsymbol{\theta}] = [\boldsymbol{y}|\boldsymbol{z}, \boldsymbol{\theta}][\boldsymbol{z}|\boldsymbol{\theta}] \tag{1}$$

From the likelihood modeling's framework, we can fit the parameters, $\boldsymbol{\theta}$, given the data, **y,** by maximizing the product of likelihood function for every sample point. The challenge of the likelihood model is that when the hierarchical structure of model is too complicated (e.g., by including processes of variation from spatio-temporal error processes), it's nearly impossible to find the parameters that optimize the likelihood function. In Bayesian modeling, the prior distribution of the parameters, $[\boldsymbol{\theta}]$, can be updated by prior belief, which could be from meta-analysis information, preliminary data analysis, or could be specified with uninformative probability distribution. Priors are added to the likelihood function, so we get the following joint probability function:

$$[\boldsymbol{y}, \boldsymbol{z}, \boldsymbol{\theta}] = [\boldsymbol{y}|\boldsymbol{z}, \boldsymbol{\theta}][\boldsymbol{z}|\boldsymbol{\theta}][\boldsymbol{\theta}] \tag{2}$$

From the Bayesian viewpoint, parameters are treated as random variables arising from a probability distribution instead of being treated as a fixed value. Therefore, the posterior distribution, which is the marginal probability distribution of model parameters conditional on the data, can be analytically transformed from the joint distribution between likelihood function and priors using Bayes' theorem:

$$[\boldsymbol{\theta}, \boldsymbol{z}|\boldsymbol{y}] = \frac{[\boldsymbol{y}, \boldsymbol{z}|\boldsymbol{\theta}][\boldsymbol{\theta}]}{\int [\boldsymbol{y}|\boldsymbol{\theta}][\boldsymbol{\theta}]d\boldsymbol{\theta}} \tag{3}$$

$$[\boldsymbol{\theta}, \boldsymbol{z}|\boldsymbol{y}] = \frac{[\boldsymbol{y}, \boldsymbol{z}|\boldsymbol{\theta}][\boldsymbol{\theta}]}{[\boldsymbol{y}]} \tag{4}$$

From the equation, the conditional parameters, $\boldsymbol{\theta}$, can be described by the prior distribution and can be used in the hierarchical model structure to describe the multistage processes of the responses, $\boldsymbol{y}$. Because it is nearly impossible for us to know the probability of responses, $p(\boldsymbol{y})$, we can utilize the Bayesian equation for posterior distribution by the decomposition of equation (4):

$$[\boldsymbol{\theta}, \boldsymbol{z}|\boldsymbol{y}] \propto [\boldsymbol{y}, \boldsymbol{z}|\boldsymbol{\theta}][\boldsymbol{\theta}] \tag{5}$$

However, it is very challenging to specify the components of Bayesian modeling of complicated hierarchical structure, and it is difficult to evaluate the posterior distribution by the analytical method. The MCMC posterior sampling method was developed to deal with the complexity of the Bayesian hierarchical model (see the details of this approach in Gilks, 2005).

Model specification

In zero- and one-inflated mixed models, we consider the hierarchical logistic model where the logit (or the probit) link function describes the binary response of presence/absence of data of interested features. In this application, we assumed the occurring observation in the plot to represent the true presence and absence of mortality (the detection is perfect), and the niche-related features of the sites have no measurement errors. A simple occupancy model for the presence/absence of mortality with heterogeneous probabilities can be written as a zero-inflated binomial data model (with probability p_i) that depends on the Bernoulli process (z_i, the presence of mortality), varying among sample plots ($i = 1, \dots, n$). We get the estimated parameters, p_i, for the probability of the occurrence of mortality at plot i, and we can specify the probability of occurrence of mortality of *P. engelmannii* at a sample plot with a Bernoulli distribution as follows:

$$\mathrm{p}(\boldsymbol{z}) = \begin{cases} p_i & ; z_i = 1 \\ 1 - p_i & ; z_i = 0 \end{cases} \tag{6}$$

$$z_i = \begin{cases} 1 & ; y_i > 0 \\ 0 & ; y_i = 0 \end{cases} \tag{7}$$

$$\boldsymbol{z} \sim \mathrm{Bernoulli}(\boldsymbol{p})$$

given that y_i is the proportional mortality in terms of basal area of *P. engelmannii* at plot i. The next step is to apply another occupancy model for the occurrence of full mortality ($y_i = 1$), conditional on the presence of mortality in the plot with heterogeneous probability values. Since both 0 and 1 are not in the domain of beta distribution, the extreme values must be modeled separately from the beta regression model. This model can be written as a one-inflated binomial data model (with probability ϕ_i) that depends on the Bernoulli process (m_i, full mortality or partial mortality binary variable), varying among

sites given that mortality occurs. This process model, combined with the model for the occurrence of mortality inflated to the extreme data of zero and one, leaves out the proportional data of y_i that $0 < y_i < 1$. The estimated parameters, ϕ_i, for the probability of full mortality at plot i can specified by a Bernoulli distribution as follows:

$$\mathrm{p}(\boldsymbol{m}) = \begin{cases} \phi_i & ; m_i = 1 \\ (1 - \phi_i) & ; m_i = 0 \end{cases} \tag{8}$$

$$m_i = \begin{cases} 1 & ; y_i = 1 \\ 0 & ; 0 < y_i < 1 \end{cases} \tag{9}$$

$$\boldsymbol{m} \sim \mathrm{Bernoulli}(\boldsymbol{\phi})$$

Then we apply another model to account for the proportion of mortality in the plots with a heterogeneous mean proportion of mortality. This model can be written as a beta regression model (with responding variable y_i), in which the predicted value varies among sites given that the latent variable for mean proportion of mortality (μ_i) is between 0 and 1. This sub-model is based on the assumption that there's an error structure from conducting sampling with the latent error parameters, σ_s^2. The estimated response, y_i, for the proportion of mortality at plot i can be specified by a beta distribution as follows:

$$\mathrm{p}(\boldsymbol{y} | 0 < \boldsymbol{y} < 1) = \frac{y_i^{\alpha_i - 1}(1 - y_i)^{\beta_i - 1}}{\mathrm{B}(\alpha_i, \beta_i)} \tag{10}$$

$$\mathrm{B}(\alpha_i, \beta_i) = \frac{\Gamma(\alpha_i)\Gamma(\beta_i)}{\Gamma(\alpha_i + \beta_i)} \tag{11}$$

$$\boldsymbol{y} \sim \mathrm{Beta}(\boldsymbol{\alpha}, \boldsymbol{\beta})$$

given Γ is the gamma function and $\boldsymbol{\alpha}$ and $\boldsymbol{\beta}$ are the vectors of parameters for the beta distribution function at each data point. We can account for the response, y_i, to the latent of estimated mean of the response, μ_i, and sampling error, σ_s^2, by the analytical method of moment matching between regression estimates and can obtain the parameters of beta distribution function as a function of the mean of mortality proportion and the sampling variance:

$$\boldsymbol{\alpha} = \left(\frac{1 - \boldsymbol{\mu}}{\sigma_s^2} - \frac{1}{\boldsymbol{\mu}} \right) \boldsymbol{\mu}^2 \tag{12}$$

102

$$\boldsymbol{\beta} = \boldsymbol{\alpha}(\frac{1}{\boldsymbol{\mu}} - 1) \tag{13}$$

given $\boldsymbol{\mu}$ is the vector of responses of the linear regression model and σ_s^2 is the sample variance of the random variable describing the proportion of mortality for *P. engelmannii*. Then we get the full conditional probability for the zero- and one-inflated beta regression model as follows:

$$p(\boldsymbol{y}) = \begin{cases} 1 - p_i & ; y_i = 0 \\ p_i \phi_i & ; y_i = 1 \\ p_i(1 - \phi_i)\left(\dfrac{y_i^{\alpha_i-1}(1 - y_i)^{\beta_i-1}}{B(\alpha_i, \beta_i)}\right) & ; 0 < y_i < 1 \end{cases} \tag{14}$$

In this study, the GLMM was implemented to describe the association between the responses and local habitat covariates. The logit link function was used to predict both probabilities of presence/absence for presence/absence data and the latent mean of the proportional data. So the probability and the mean of proportion can be written as an inverse logit function of the predictors (Finley et al., 2007), given $\boldsymbol{X}$ and $\boldsymbol{\gamma}$ are the habitat covariates and the linear coefficients at location i, respectively. We get the simple GLMM for each response:

$$\boldsymbol{p} = \frac{\exp(\boldsymbol{X\gamma})}{1 + \exp(\boldsymbol{X\gamma})} \tag{15}$$

$$\text{logit}(\boldsymbol{p}) = \boldsymbol{X\gamma} \tag{16}$$

We also used this type of function with the same covariates in the model of $\boldsymbol{\phi}$ and $\boldsymbol{u}$. To account for the spatial dependence of responses, a spatially explicit regression model with multivariate normal (MVN) distribution of spatial errors with exponential decay covariance function can be written as follows:

$$\text{logit}(\boldsymbol{p}) = \boldsymbol{X\gamma} + \boldsymbol{w} + \epsilon \tag{17}$$

$$\epsilon \sim \text{Normal}(0, \sigma_\epsilon^2)$$

$$\boldsymbol{w} \sim \text{MVN}(\boldsymbol{\mu_w}, \Sigma)$$

$$\Sigma = \sigma_w^2 \boldsymbol{C} \tag{18}$$

$$\boldsymbol{C} = \exp(-\lambda \boldsymbol{D}) \tag{19}$$

We used the same spatial structure for both $\boldsymbol{\phi}$ and $\boldsymbol{\mu}$. Vector $\boldsymbol{w}$ added to the regression model is the latent Gaussian process spatial errors. Spatial error term is given by an MVN (Banerjee et al., 2008), with $\boldsymbol{\mu_w}$ being the mean of MVN (0 in our case) and Σ being the spatial covariance matrix. Spatial covariance matrix incorporates spatial dependence between pairs of observations, which is represented by σ_w^2, the variance effect parameter, and $\boldsymbol{C}$, the exponential correlation matrix as a function of the distance between pairs of points, $\boldsymbol{D}$. λ is the exponential decay parameter associated with this function. While ϵ in the model represents the error term, this does not depend on the spatial proximity, or the nugget effect (Diggle, 1983). The distance matrix, the spatial correlation matrix, and the spatial covariance matrix can be written as follows:

$$\boldsymbol{D} = \begin{bmatrix} d_{ii} & \cdots & d_{in} \\ \vdots & \ddots & \vdots \\ d_{ni} & \cdots & d_{nn} \end{bmatrix}, \quad \boldsymbol{C} = \begin{bmatrix} 1 & \cdots & c_{in} \\ \vdots & \ddots & \vdots \\ c_{ni} & \cdots & 1 \end{bmatrix}, \quad \Sigma = \begin{bmatrix} \sigma_w^2 & \cdots & \sigma_w^2 c_{in} \\ \vdots & \ddots & \vdots \\ \sigma_w^2 c_{ni} & \cdots & \sigma_w^2 \end{bmatrix} \tag{20}$$

The hierarchical model used in this study was developed under the Bayesian framework (Gelman and Hill, 2006). The Bayesian model commences by composing the likelihood function for each model. The concept of hierarchical structure modeling is shown by directed acyclic graphs in Figure 18. The likelihood function for the model for probability of occurrence and proportion of mortality can be summarized as follows:

$$L\left(\boldsymbol{\gamma}, \lambda, \sigma_w^2, \sigma_\epsilon^2 \big| \boldsymbol{y}_{\text{binary}}\right) \propto \prod^n \text{Bernoulli}\left(\boldsymbol{y}_{\text{binary}} \big| g(\boldsymbol{\gamma}, \boldsymbol{w}, \sigma_\epsilon^2)\right) \text{MVN}(\boldsymbol{w} \big| \boldsymbol{0}, c(\lambda, \sigma_w^2)) \tag{21}$$

$$L(\boldsymbol{\gamma}, \lambda, \sigma_w^2, \sigma_s^2, \sigma_\epsilon^2 \big| \boldsymbol{y}_{\text{cont.}}) \propto \prod^n \text{Beta}\left(\boldsymbol{y}_{\text{cont.}} \big| f_\alpha(g(\boldsymbol{\gamma}, \boldsymbol{w}, \sigma_\epsilon^2)), f_\beta(\sigma_s^2)\right) \text{MVN}(\boldsymbol{w} \big| \boldsymbol{0}, c(\lambda, \sigma_w^2)) \tag{22}$$

Given $g()$ is an inverse logit function including the latent spatial error term, $f()$ is the moment-matching function for the parameters of beta distribution function, $\boldsymbol{\alpha}$ and $\boldsymbol{\beta}$, and $c()$ is the spatially exponential covariance function with parameters λ and σ_w^2. Then we completed the hierarchical Bayesian model by assigning prior distributions to the model parameters. Intercept and coefficient model parameters $\boldsymbol{\gamma}$ were assigned by the flat normal distribution with zero mean (Normal(0, var $= 1.0 \times$

10^5)). The spatial variance effect and non-spatial variance term, σ_w^2 and σ_ϵ^2, received priors of the narrow

density near zero because sparse priors of the variance parameters can lead to convergence failure in

MCMC. The over-parameterized model fitting required informative prior distributions on the variance

parameters, with relatively high weight placed on values near zero (Gelman and Hill, 2006). Selection of

priors for variance parameters is still an active research topic in Bayesian statistics. Parameters for the

spatial covariance are difficult to estimate in hierarchical models (Zhang and Wang, 2010). We therefore

specified priors for spatial parameters in a preliminary analysis by fitting the GLM model, but without

latent spatial effects, and then implementing kriging analysis with the GeoR package (Ribeiro Jr and

Diggle, 2001) to the empirical residuals of the results. The parameters from the kriging covariance model

were used as the central value of uniform prior for spatial decay, λ, and gamma prior for variance effect,

σ_w^2.

All the model fitting was performed by JAGS (Plummer, 2004) software coding from R

programming interface (R Core Team, 2014). We fitted the model using the MCMC method with

Metropolis and the Gibbs sampling algorithm to update the parameters by JAGS through the rjags

package for R (Plummer, 2013). The sampling was run on three independent MCMC chains of 60,000

iterations (100,000 iterations with thinning for every five iterations for three chains) with 10,000 burn-ins

for each chain. Initial parameters for each chain were randomly initialized within a feasible range.

Gelman-Rubin diagnostics were applied to assess the convergence.

Model validation and selection

We fitted the competing models with different combinations of covariates. To compare

alternative models, we used the Deviance Information Criterion (DIC) (Spiegelhalter et al., 2002). DIC is

the sum of the loss function (a measure of the model fit) represented by Bayesian deviance, $\widehat{D}$, and the

effective number of parameters, p_D (a penalty for the model complexity). In contrast to Akaike

Information Criterion (AIC) and Bayesian Information Criterion (BIC), DIC is the true Bayesian

information criterion, whose calculations encompass all MCMC iterations. The lower DIC values suggest best-fit models. DIC can be estimated as the following equation:

$$\text{DIC} = \widehat{D} + 2p_D \tag{23}$$

$$\widehat{D} = -2\log[\boldsymbol{y}|E(\boldsymbol{\theta}|\boldsymbol{y})] \tag{24}$$

$$p_D = \overline{D} - \widehat{D} \tag{25}$$

$$\overline{D} = \int -2\log[\boldsymbol{y}|\boldsymbol{\theta}][\boldsymbol{\theta}|\boldsymbol{y}]\,d\boldsymbol{\theta} \tag{26}$$

Furthermore, we used the posterior predictive check for other comparison criterion; the mean squared prediction error (MSPE) is implemented to assess the accuracy of the prediction relative to the true value:

$$\text{MSPE} = \sum_{}^{n} \frac{(y_i - \widehat{y}_i)}{n} \tag{27}$$

given $\widehat{\boldsymbol{y}}$ is the model prediction. A smaller value of MSPE implies more effectiveness of a model's predictability. Besides MSPE, the other scoring function we used for validation was log predictive density (LPD), estimated by averaging over the iteration of the sum of likelihood conditional on model parameters at each iteration of *k* within MCMC chains:

$$\text{LPD} = \log[\widehat{\boldsymbol{y}}|\boldsymbol{y}] \approx \log\left(\frac{\sum^{K}[\widehat{\boldsymbol{y}}|\boldsymbol{y},\boldsymbol{\theta}^k]}{K}\right) \tag{28}$$

Prediction domain

The prediction of the hierarchical Bayesian model, $\widehat{y}$, can be applied from the parameters conditional on the observational data. The prediction probabilities of the mortality occurrence and the proportion of mortality is given by the following:

$$p(\widehat{\boldsymbol{y}}|\boldsymbol{y}) = \int p(\widehat{\boldsymbol{y}}|\boldsymbol{\theta})p(\boldsymbol{\theta}|\boldsymbol{y})d\boldsymbol{\theta} \tag{29}$$

We can see from the equation that the prediction values were iteratively calculated across the parameter spectrum of MCMC. However, we ignored the prediction of spatial structure for the prediction because it is difficult to determine the directional randomness of the spatial errors. To calculate the

prediction for each iteration *k* in MCMC chains, the conditional prediction value was calculated from the local environmental covariates via model parameters of iterations of *k*:

$$\hat{y}_k = \hat{X}\beta_k \tag{30}$$

The prediction at a new site that was excluded from the sample locations requires the values of each covariate to be known. The climate covariates of temperature and precipitation zone already cover the whole study area. The plot-level covariates describing stand characteristics were obtained by applying linear interpolation by the inverse distance weight (IDW) method, considering 12 neighbors' value. The interpolation was applied in all grids of neighboring sites, conditional on the presence of *P. elgelmanni* (see Figure 19 and Table 22) given by vegetation cover data from the Colorado Division of Wildlife as part of the Gap Analysis Program. The kriging interpolation method was implemented by ArcMap (ESRI, 2011). The prediction was implemented in 20,547 of the 1000- × 1000-meter grids across the landscape.

Results

Probability of mortality given the presence of *P. engelmannii*

To measure the impact of environmental factors on the occurrence mortality conditional on the presence of *P. engelmannii*, the hierarchical Bayesian zero-inflated model was implemented to regress on the latent variable of probability of mortality presence, $\boldsymbol{p}$. The candidate model with different combinations of environmental covariates was verified with DIC. Furthermore, LPD and MSPE posterior predictive check were implemented to assess the predictability of the model. All candidate models and their validation criteria are shown in Table 23. The best-fitted model, that yielding the lowest DIC, was selected from the candidate models. The selected model describing the environmental association with the presence of mortality includes the climatic covariates of temperature zone (T) and precipitation zone (P) and two other plot-level covariates: complexity of crown structure (S) and average basal area per tree (BT). The summary of posterior distribution of parameters is given in Table 25. Comparative posterior density is shown in Figure 21. The posterior predictive check of the Bernoulli simulation model using the latent process of the probability of observing mortality indicates that despite the model having an

acceptable predictive power of 80.4% accuracy, sensitivity of the model is low due to only 63.1% of true

positive results (Table 24).

The GLMM of logit link function, including the Gaussian process of spatial error, was applied to

account for the spatial variability of the conditional probability for the occurrence of *P. engelmannii*

mortality, $\boldsymbol{p}$. From the results, there appears to be a spatially dependent structure on the logistic regression

function for the probability of mortality. The preliminary analysis of kriging residuals yields an estimated

value for the exponential decay parameter, λ, of 0.027 (range parameter of 37.037 km) with the posterior

along the distance shown in Figure 20. The estimated variance effect for the covariance function, σ_w^2, is

7.106. The detailed results of the exponential spatial covariance parameters are described in Table 25. For

associating the presence of mortality with the local habitat covariates, there are negative effects from

temperature zones 1 and 2 relative to temperature zone 3, and there are no significant effects from

temperature zones 4 and 5 compared to temperature zone 3. As seen in Figure 21, there is an

overwhelmingly negative effect from temperature zone 1. The effects of precipitation zones 1, 2, and 4

have no significant difference relative to precipitation zone 3, while precipitation zone 4 is the only zone

with a significant positive effect. For the stand characteristic covariates, the highly complex stand

structures, S2 and S3, have significant negative effects on the occurrence of mortality relative to the

single stand structure. The effects of the size class show that there are significant positive effects from

average basal area per tree for size classes BT2 and BT3 relative to the smallest size class, BT1, with the

largest size class, BT3, having a smaller effect than the moderate size class, BT2. The predicted map of

the probability of mortality conditional on the presence of *P. engelmannii* with the selected model is

given in Figure 22. The spatial context of prediction matches well with observation in the field, where the

plots with mortality are observed more in the northern area of the study extent. The summary of the

predicted probability of mortality is shown in Table 28.

Environmental association of the probability of entire plot mortality given the presence of mortality

To measure the impact of the environmental factors on the occurrence of full mortality ($y_i = 1$)

of *P. engelmannii* conditional on the presence of mortality, the hierarchical Bayesian one-inflated model

was implemented to regress on the latent variable of probability of the presence of full mortality, ϕ. The candidate model with different combinations of environmental covariates was verified with DIC. All candidate models and their validation criteria are shown in Table 23. The best-fitted model, that yielding the lowest DIC, was selected from the candidate models. The best-fitted model includes the climatic covariates of temperature zone (T) and precipitation zone (P) and stand-level covariates of number of stories (S) and relative dominance (RD). The summary of posterior distribution of parameters is given in Table 26, and the comparative posterior density is shown in Figure 23. The posterior predictive check of the Bernoulli simulation model using the latent process of probability of observing full mortality across MCMC iterations shows that the model has a high predictive power of 100% accuracy in predicting plots with full mortality (Table 24).

The GLMM of logit link function, including the Gaussian process of spatial error term, was applied to account for the spatial variability of the conditional probability of the occurrence of full mortality of *P. engelmannii* in the sample plot, ϕ. From the preliminary results, there is no effect of large scale spatial structure for the logistic function. The estimated value of exponential decay parameters, λ, from the empirical residuals kriging model is 0.149 (range parameter of 6.725 km), with the posterior and correlogram shown in Figure 20, while the estimated spatial variance effect, σ_w^2, is 0.686. The results of posterior for model parameters are shown in Table 26, while comparative posterior densities are expressed in Figure 23. For the association between occurrence of full mortality and climatic covariates, there is no available mortality site with temperature zone 1, and there are significant effects relative to the baseline of temperature zone 3 compared with the rest of the temperature zones. Temperature zones 2 and 4 have negative effects relative to the baseline, while the effect of temperature zone 5 has the positive effects on the response. Additionally, precipitation zones 2 and 4 have negative effects on the probability of full mortality relative to precipitation zone 3. Precipitation zone 5 has the most significant positive effect compared to the baseline, while precipitation zone 1 has no significant effect relative to precipitation zone 3. For the influence of stand-level characteristics on the presence of full mortality, the higher-complexity stand structures, S2 and S3, have positive effects relative to single-story structures.

109

The effects of the relative dominance of *P. engelmannii* are negative for the higher-dominance classes, RD2, RD3, and RD4, compared with the lowest class, RD1, with highly negative effects of RD2 and RD3. The predicted map of the probability of full mortality conditional on presence of mortality by the selected model is given in Figure 24. The summary of the predicted probability of mortality is shown in Table 28.

Environmental association of the proportion of mortality given partial mortality

A hierarchical Bayesian beta regression model was implemented to describe the influence of environmental factors on the proportion of mortality conditional on the partial mortality of *P. engelmannii*, $\boldsymbol{y}$. Given that there is sampling error on the responses collected from the field, the proportion of mortality is represented by the beta distribution latent state of the mean of proportion for the mortality, $\boldsymbol{\mu}$, and the sampling error, σ_s^2. The model with various combinations of covariates was verified with DIC. All candidate models and their validation criteria are shown in Table 23. The best-fitted model, that yielding the lowest DIC, was selected from the candidate models. The model with the lowest DIC includes the covariates of precipitation zone (P) and stand-level covariates of stand structure complexity (S), relative dominance (RD), and size class (BT). The summary of posterior of parameters is given in Table 27, and comparative posterior density is shown in Figure 25. The posterior predictive check of the model from the latent process of mean proportion of mortality is expressed as the median of residuals in Figure 27.

The GLMM of logit link function for the mean of proportion was modeled to include the Gaussian process of spatial error term to account for the spatial variability of the proportion of mortality conditional on observing partial mortality. From the preliminary results, there is no strong evidence of the effect of large scale spatial structure for the logistic function. The estimated value of exponential decay parameters, λ, from the empirical residuals kriging model is 0.145 (range parameter of 6.916 km), with the posterior and correlogram shown in Figure 20, while the estimated spatial variance effect, σ_w^2, is 1.028. The distribution of parameters is shown in Table 27 and Figure 25. There are significant positive climatic effects of precipitation zone 4, and there are small negative effects of precipitation zones 1 and 2

relative to precipitation zone 3. There is no sample in precipitation zone 5 having partial mortality. For stand characteristic covariates, the higher-complexity stand structures, S2 and S3, have small negative effects relative to the single story, S1, while the relative dominance of *P. engelmannii* has a small positive effect in the higher dominance class, RD4, compared with the lowest dominant class, RD1. However, there is no difference in effects of other dominant classes compared to RD1. The largest size class, BT3, is the only size class that has a negative effect compared to the baseline at size class 1. The predicted map of the proportion of mortality conditional on partial mortality presence by the selected model is given in Figure 26. The summary of the predicted proportion of mortality is shown in Table 28.

Discussion

The influences of climate and habitat factors on occurrence and intensity spruce mortality are not well understood. In this study, we explored the effects of climate and stand-level habitat characteristics on the occurrence and proportion of mortality for *P. engelmannii*. We answered the proposed questions by developing a hierarchical Bayesian zero-and one-inflated beta model to address the multilevel problems where there are multiple responses. We adapted this general class of model concept, proposed by Ospina and Ferrari (2012, 2008), by applying two-stage Bernoulli random variables to indicate the occurrence of the extreme value of the proportion of mortality, representing the sample with absence, $y_i = 0$, and full mortality, $y_i = 1$. The proportional responses were addressed by beta distribution, allowing more flexibility by modeling the association between covariates and the latent states of mean proportion and also incorporating stochasticity from the sampling errors, σ_s^2. Each step of the model was performed by logistic function to deal with probabilities and continuous proportional responses. The multivariate Gaussian latent process was included in the function to express the exponential spatial errors term.

From the model output, spatial distribution of the occurrence and intensity of mortality of *P. engelmannii* were both associated with the local covariates of temperature zone, precipitation zone, class of stand structure level, relative dominance class, and size class described by average basal area per tree. Climate variables play crucial roles in both occurrence and intensity of mortality. The colder temperature

zones (T1 and T2) have highly negative effects on both the probability of mortality occurrence and the probability of full mortality occurrence, while the high temperature zone (T5) is positively associated with the presence of full mortality. Although high precipitation zones are positively associated with the presence and proportion of mortality (P4 is associated with the presence and proportion of partial mortality while P5 is associated with the occurrence of full mortality), the effects are small compared with the negative effects from temperature factors. Therefore, the climate zone that is cold and humid has a negative cumulative effect, while a warm and humid climate has the most positive effect on observations of mortality.

Despite there being no evidence of increasing mortality when precipitation is lower, there is an apparent positive effect in the warmer climate zones that could be related to the water vapor deficit associated with drought events, according to a study of historic spruce mortality in Colorado (Chavardès et al., 2012; Hart et al., 2013). The deviation of temperature and precipitation from optimal can cause direct and indirect detrimental effects on the physiological processes of trees, resulting in increased susceptibility (Ayres, 1984; Huberty and Denno, 2004; Williams et al., 2013). Warmer climate also affects the population dynamics of forest insects by shortening life cycle (Bale et al., 2002; Huberty and Denno, 2004). The Climate Release Hypothesis (CRH) states that climate changes might affect susceptibility of host and pest populations, with the conditions favoring a high probability of mortality for host trees (Huberty and Denno, 2004; Larsson, 1989; Mattson and Haack, 1987). Since climate has a trend of warming in the near future (Seager et al., 2007), the shifting of climate zones across the landscape may cause more spruce forest to become more susceptible to insects and diseases.

The results from this study indicate that stand characteristics are important factors, as well as climate. Stand susceptibility can be determined with the average diameter, basal area, species composition, and physiographic location (Schmid and Frye, 1977). Mortality occurrence is positively associated with single-story stands (S1) with medium to large size classes (BT2 and BT3) of *P. engelmannii*. The higher-complexity stand structures (S2 and S3) have highly positive associations with the probability of full mortality, while medium to high dominance classes (RD2, RD3, and RD4) have

112

negative effects on full mortality. For the proportion of partial mortality, the largest size class (BT3) and the highest dominance class (RD4) have negative effects on the proportion of mortality. These results correspond with the previous model study stating that the dominance and heterogeneity of *P. engelmannii* and large basal area of stand are the most influential factors on spruce beetle outbreak (DeRose et al., 2013; Doak, 2004). Stand characteristics, combined with climate variability, influence the success of spruce beetle populations (Bentz et al., 2010). In contrast, the covariates show highly positive effects on the presence of mortality, but did have negative effects on the probability of full mortality and the proportion of mortality. This may be explained by the marginal population concept that the subdominance of *P. engelmannii* in a mixed-structure stand might be affected by the natural thinning of the subdominance in stands or by the suboptimal physiological conditions, resulting in the absence of establishment and regeneration and high susceptibility due to physiological stress on the existing population (Anderegg et al., 2012; Wargo, 1985). However, we need further study is required focusing on the stand-scale ecology of species, such as regeneration and establishment through the temporal scale encompassing the different stage of subalpine spruce-fir systems.

The inclusion of spatial structure in the model helps describe the spatial process, including the processes not included in the covariates. The parameters, λ, of the exponential spatial process were used to account for the unmeasured local stand characteristics such as the similarity of geographic features, the demographic and dispersion of the insects and diseases from multiple epicenters, the temporal synchrony of insect life cycle, the historic local disturbance, local micrometeorological features, and even the local shift in habitat association caused by microevolution. These features are difficult to measure and can cause spatial correlation between proximate samples, which may lead to bias in estimating parameters. However, the spatial dependent structure must rely on the simplified assumption on the spatial characteristics. It is difficult to assume the stationary and anisotropy of the regional scale of spatial structure due to small scale variability. Moreover, the sampling sites are too sparsely distributed across the forested landscape, making it is difficult to describe the significant spatial structure (Zimmerman, 2006).

The applications of statistical modeling approaches to spatial data could help us figure out the importance of the environmental factors on the spatial extent, distribution, and intensity of forest mortality. The models were also used to extrapolate the association between covariates and responses in the unobserved sites. Nevertheless, the model is only the average of habitat association over the temporal scale conditional on the samples. Due to data being collected over two years, there is only one realization to represent the true impact on the occurrence and intensity of mortality. So the model parameters might not be strong enough to represent the true model, and the described association can be changed as the habitat characteristics change through time, especially when the changes might come from stochastic factors affecting growth and succession of forest stand or from ecological disturbance events. Further, the stand characteristics we used in the model are recent features at the local spatio-temporal scale, but all the dead trees that existed in the plot were counted and measured, so the association described by the model might possess high bias. These factors likely weaken the predictability of the model compared to other sets of data in different spatial extents and times. The data collection in temporal orders, the additional records for the time that mortality occurred, and the record on the changing of stand characteristics and environmental conditions through time are required to help us build a mechanistic model that can describe the processes and association of mortality.

Table 21. Summary statistics for the average annual temperature and precipitation associated with the temperature (T) and precipitation (P) zones in the study area.

Zone	Minimum	Mean	Maximum	CV%
	Average precipitation (mm)			
P1	30.4	33.9	36.7	5.2
P2	36.7	39.5	42.7	4.3
P3	42.7	46.0	50.7	4.8
P4	50.7	55.5	60.6	5.2
P5	60.6	65.6	83.7	5.2
	Average temperature (°C)			
T1	–5.7	–1.7	–0.3	55.1
T2	–0.3	1.3	2.4	54.7
T3	2.4	3.5	4.4	16.6
T4	4.4	5.3	6.3	10.0
T5	6.3	7.4	8.4	8.0

Table 22. Frequency of climate and habitat covariates of the prediction domain that were used to predict the mortality and intensity of *P. engelmannii* on the study area. Stand characteristics variables were quantified from inverse distance weight (IDW) method from the 12 nearest neighbors. The covariates include temperature zones (T), precipitation zones (P), number of stories (S), relative dominance (RD), and average basal area per tree (BT).

Covariate\Class	1	2	3	4	5
T	3797	9062	6252	1396	40
P	382	1871	4664	7628	5976
S	7596	12091	860	-	-
RD	1311	11979	7117	122	-
BT	3163	14976	2408	-	-

Table 23. List of candidate model with information criteria and posterior predictive check. Three stages of model consist of zero-inflated model for dealing with the presence of spruce mortality, one-inflated model for dealing with the presence of full mortality conditional on the presence of mortality, and beta regression model for dealing with the proportion of partial mortality. The covariates include temperature zones (T), precipitation zones (P), number of stories (S), relative dominance (RD), and average basal area per tree (BT).

Model Parameters	DIC	ΔDIC	LPD	MSPE
Zero-Inflated Logistic Regression Model				
T + P + S + BT	90.020	0.000	–41.205	0.115
T + P + S + RD + BT	91.040	1.020	–40.683	0.111
T + S + BT	92.970	2.950	–43.512	0.118
T + S + RD + BT	93.410	3.390	–42.622	0.115
P + S + BT	93.740	3.720	–46.294	0.124
T + P + S	94.370	4.350	–43.944	0.122
T + P + S + RD	94.510	4.490	–42.912	0.115
One-Inflated Logistic Regression Model				
T + P + S + RD	<0.001	0.000	>-0.001	<0.001
T + P + S + RD + BT	<0.001	<0.001	>-0.001	<0.001
T + P + RD + BT	12.710	12.710	–5.536	0.065
P + S + RD	16.660	16.660	–7.328	0.080
T + P + S + BT	17.770	17.770	–7.704	0.090
T + P + RD	18.340	18.340	–8.112	0.091
T + S + RD + BT	21.000	21.000	–8.860	0.095
Beta Regression Model				
P + S + RD + BT	–9.169	0.000	12.082	0.039
T + P + S + RD + BT	–9.006	0.163	13.790	0.035
T + P + RD + BT	–8.679	0.490	12.259	0.039
P + RD + BT	–8.501	0.668	10.775	0.044
T + P + ST + RD	–8.246	0.923	12.134	0.039
P + S + RD	–6.408	2.761	9.789	0.048
T + P + RD	–5.162	4.007	8.495	0.050

Table 24. Posterior predictive check of the presence/absence responses for zero-inflated model (ZIM) and one-inflated model (OIM).

Predictive check	ZIM	OIM
True positive	0.631	1.000
False zero	0.369	0.000
True zero	0.867	1.000
False positive	0.133	0.000
True prediction	0.804	1.000
False prediction	0.196	0.000

Table 25. Quantile, mean, and standard deviation of model parameters of the best fitted zero-inflated regression model. The letter T represent temperature zones, P represent precipitation zones, S represent number of stories, and BT represent average basal area per tree. λ represent coefficient of spatial structure while σ_w^2 represent variance effect on spatial dependence.

	2.50%	25%	50%	75%	97.50%	Mean	SD
Intercept	-0.5867	0.290429	0.755457	1.22278	2.127683	0.757257	0.690462
T1	-19.8086	-18.5164	-17.847	-17.1795	-15.8948	-17.8494	0.997102
T2	-3.22495	-2.43716	-2.03272	-1.63042	-0.88259	-2.03676	0.598114
T4	-1.92202	-1.00866	-0.53404	-0.05795	0.849928	-0.53412	0.705771
T5	-2.66897	-1.50788	-0.90749	-0.30573	0.824886	-0.90978	0.89165
P1	-2.47281	-1.32117	-0.72767	-0.14068	0.959555	-0.73423	0.874583
P2	-1.16524	-0.11467	0.42575	0.96516	1.97242	0.421486	0.800289
P4	1.094344	1.886409	2.307247	2.727188	3.554886	2.309701	0.626042
P5	-1.43384	-0.32991	0.223995	0.765433	1.794287	0.212742	0.820657
S2	-4.96294	-4.16602	-3.74994	-3.33595	-2.55048	-3.75238	0.614563
S3	-6.47113	-5.57145	-5.10368	-4.65127	-3.79908	-5.11399	0.682038
BT2	0.887743	1.615916	2.006812	2.399999	3.159492	2.01059	0.58187
BT3	-0.07357	0.75829	1.185512	1.610857	2.430151	1.181886	0.637167
λ	0.013663	0.014901	0.016946	0.021228	0.03661	0.019162	0.005983

Table 26. Quantile, mean, and standard deviation of model parameters of the best fitted one-inflated regression model. The letter T represent temperature zones, P represent precipitation zones, S represent number of stories, and RD represent relative dominance. λ represent coefficient of spatial structure while σ_w^2 represent variance effect on spatial dependence.

	2.50%	25%	50%	75%	97.50%	Mean	SD
Intercept	45.391	46.679	47.351	48.032	49.322	47.353	1.002
T2	–94.544	–93.269	–92.594	–91.926	–90.628	–92.595	0.996
T4	–25.419	–24.134	–23.462	–22.791	–21.484	–23.461	1
T5	65.23	66.521	67.193	67.862	69.176	67.194	1
P2	–1.976	–0.675	–0.002	0.672	1.948	–0.005	0.999
P3	–49.138	–47.834	–47.165	–46.48	–45.213	–47.163	1.002
P5	–73.007	–71.727	–71.063	–70.38	–69.099	–71.057	0.998
P6	72.17	73.445	74.124	74.804	76.077	74.124	1.001
S2	136.83	138.112	138.794	139.464	140.749	138.791	1
S3	91.67	92.963	93.633	94.316	95.611	93.638	1.003
RD2	–141.15	–139.87	–139.19	–138.53	–137.24	–139.20	1
RD3	–143.08	–141.78	–141.12	–140.44	–139.16	–141.11	0.998
RD4	–49.239	–47.939	–47.26	–46.588	–45.287	–47.263	1.003
λ	0.01	0.014	0.019	0.024	0.028	0.019	0.006
σ_w^2	0.57	0.668	0.724	0.783	0.905	0.727	0.085

Table 27. Quantile, mean, and standard deviation of model parameters of the best fitted beta regression model. The letter P represent precipitation zones, S represent number of stories, RD represent relative dominance, and BT represent average basal area per tree. λ represent coefficient of spatial structure, σ_w^2 represent variance effect on spatial dependence, and σ_s^2 represent non-spatial sampling errors.

	2.50%	25%	50%	75%	97.50%	Mean	SD
Intercept	−1.311	−0.451	−0.010	0.430	1.303	−0.011	0.663
P2	−2.177	−1.234	−0.731	−0.230	0.751	−0.728	0.747
P3	−2.183	−1.371	−0.949	−0.532	0.274	−0.953	0.626
P5	0.063	0.728	1.056	1.370	1.967	1.044	0.484
S2	−1.377	−0.826	−0.535	−0.238	0.348	−0.530	0.439
S3	−2.001	−1.082	−0.608	−0.129	0.810	−0.604	0.715
RD2	−0.943	−0.302	0.032	0.375	1.044	0.037	0.504
RD3	−1.238	−0.475	−0.077	0.319	1.092	−0.077	0.591
RD4	−2.110	−1.443	−1.084	−0.724	−0.023	−1.080	0.532
BT2	−1.064	−0.519	−0.238	0.037	0.574	−0.242	0.417
BT3	−2.520	−1.686	−1.258	−0.832	−0.002	−1.260	0.638
λ	0.003	0.005	0.007	0.008	0.009	0.006	0.002
σ_s^2	0.098	0.149	0.189	0.241	0.388	0.203	0.076
σ_w^2	1.030	1.071	1.094	1.116	1.159	1.094	0.033

Table 28. Posterior prediction results from zero-inflated model (ZIM), one-inflated model (OIM), and beta regression model (BRM). The results were shown by the 95% credible interval of quantiles for posterior distribution. Given 2.50% and 97.50% are lower bound and upper bound of credible interval respectively while 50.00% is median (central value) of the interval. Percent columns show relative frequency of the prediction for each prediction class.

| Predicted interval	2.50%		50%		97.50%	
	Area (Sq.km.)	percent	Area (Sq.km.)	percent	Area (Sq.km.)	percent
ZIM						
0-20%	15307	74.5	9878	48.08	5621	27.36
20-40%	982	4.78	3903	19	2887	14.05
40-60%	1351	6.58	1299	6.32	611	2.97
60-80%	1576	7.67	1171	5.7	4134	20.12
80-100%	1331	6.48	4296	20.91	7294	35.5
OIM						
0-20%	14349	69.84	13862	67.46	13631	66.34
20-40%	0	0.00	4	0.02	0	0.00
40-60%	0	0.00	388	1.89	0	0.00
60-80%	0	0.00	0	0.00	0	0.00
80-100%	6198	30.16	6293	30.63	6916	33.66
BRM						
0-20%	12878	62.68	2837	13.81	0	0.00
20-40%	6717	32.69	7044	34.28	131	0.64
40-60%	952	4.63	7664	37.30	2585	12.58
60-80%	0	0.00	3002	14.61	11021	53.64
80-100%	0	0.00	0	0.00	6810	33.14
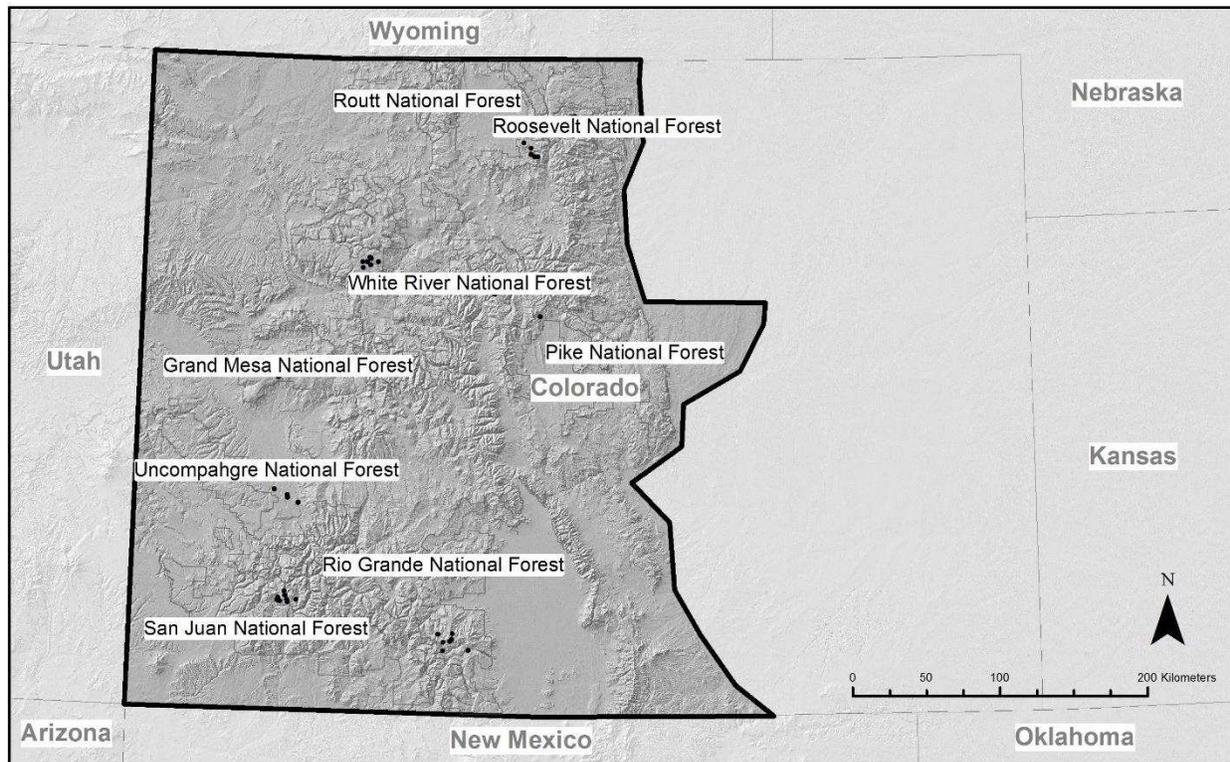
Figure 14. Study area in western Colorado and locations of 55 study sites (black dots). The study area was

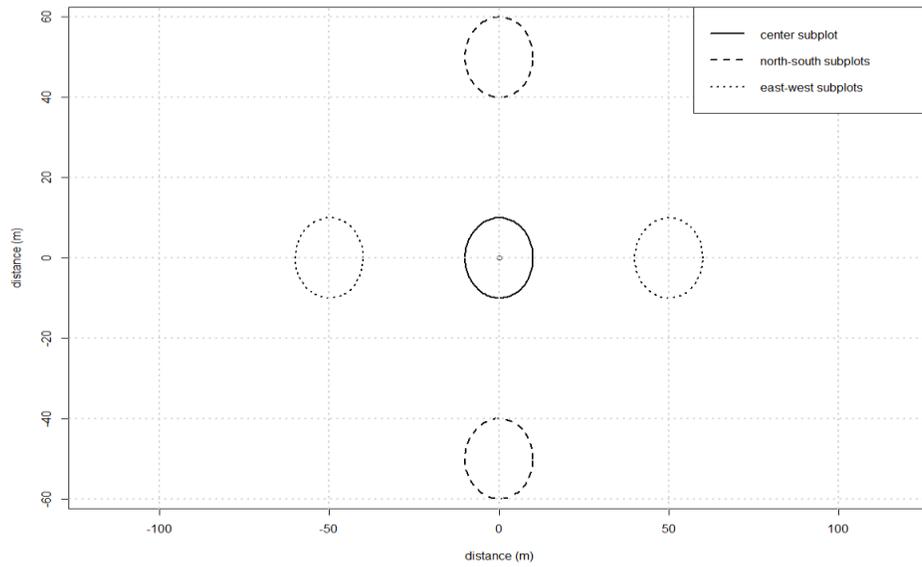delineated by the layer represent forest land cover in Colorado.

Figure 15. Conceptual diagram of survey subplot orientation. Subplots were either randomly placed along

the north-south direction (dashed circles) or east-west direction (dotted circles). Each subplot be at least
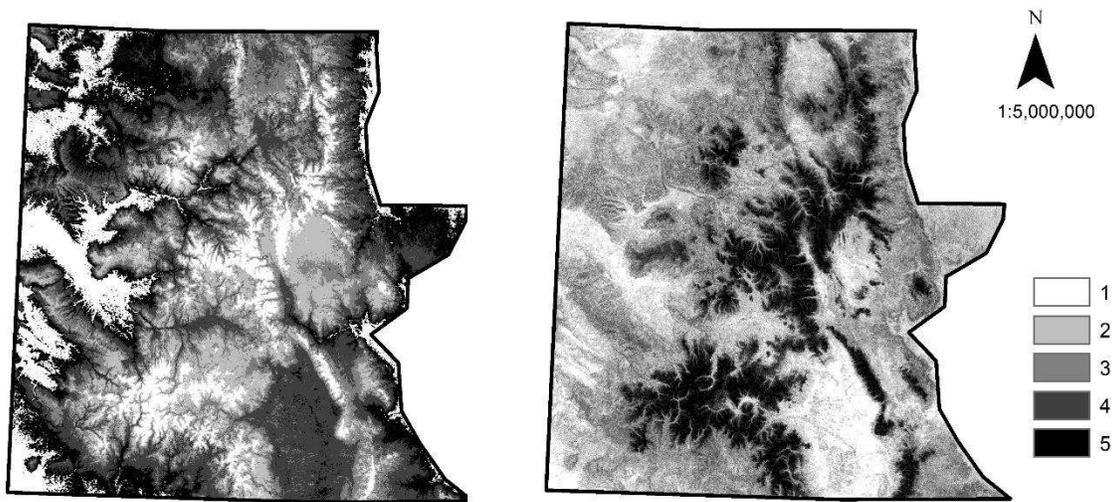
50 meters separate from each other.

Figure 16. Maps represent temperature zones (left) and precipitation zones (right). The study area was delineated by the layer represent forest land cover in Colorado.
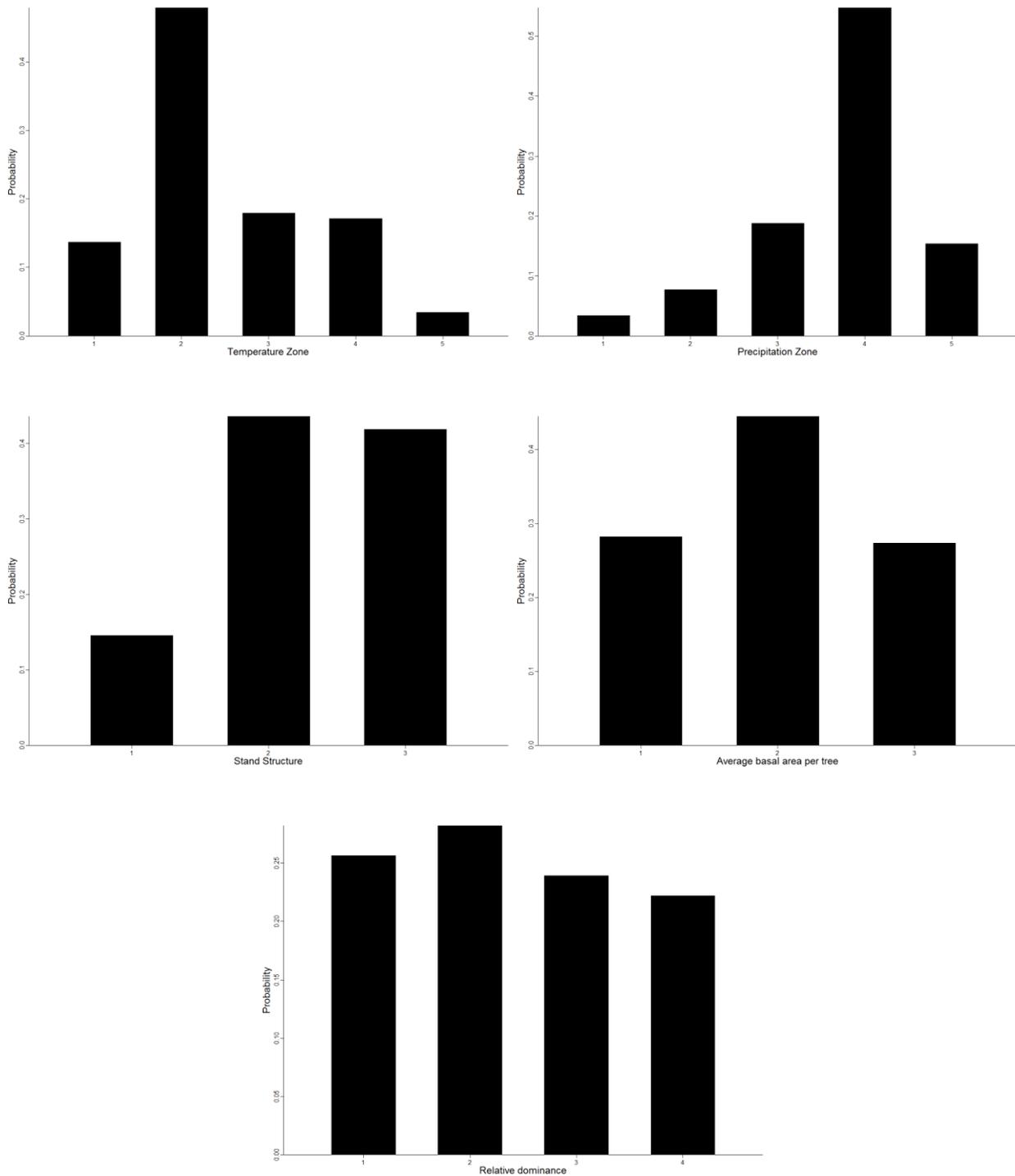
Figure 17. Histogram of field data covariates composed of temperature zone, precipitation zone, stand structure, relative dominance, and basal area per tree. Each covariate was categorized into classes to deal with non-linear relationship between covariates and responses.
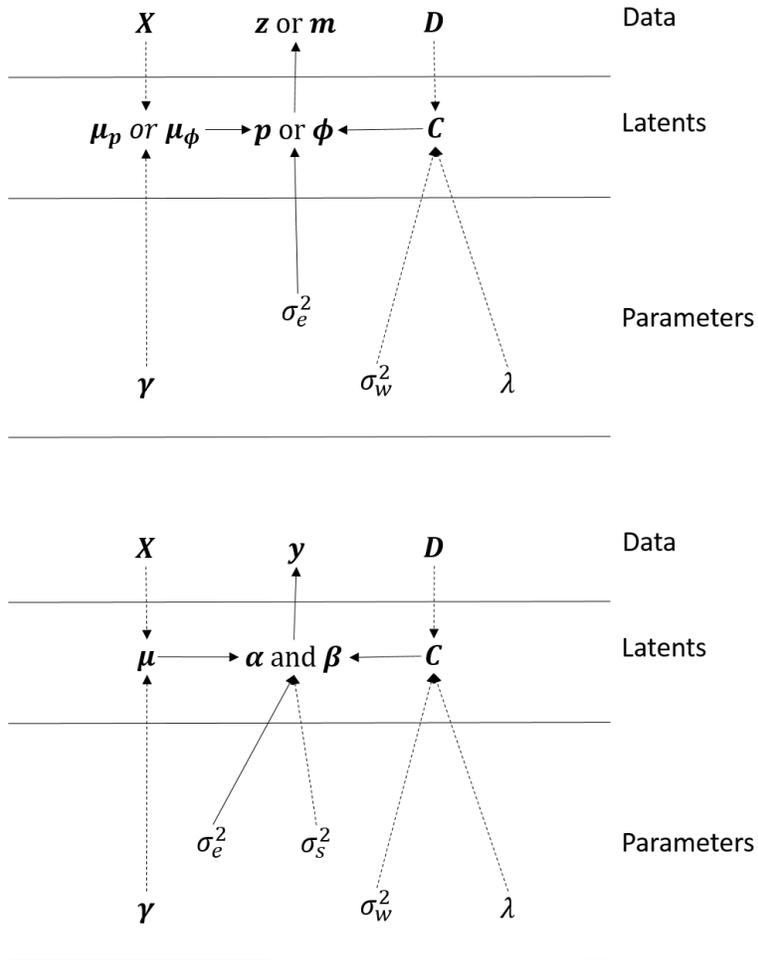
Figure 18. Conceptual diagram of the hierarchical Bayesian model (Directed Acyclic Graph) of zero- and one-inflated beta model. Above is the model for p and ϕ, the binomial regression. Below is the beta model for continuous proportion, y. Solid lines represent stochastic relationship while dashed lines represent deterministic relationship.
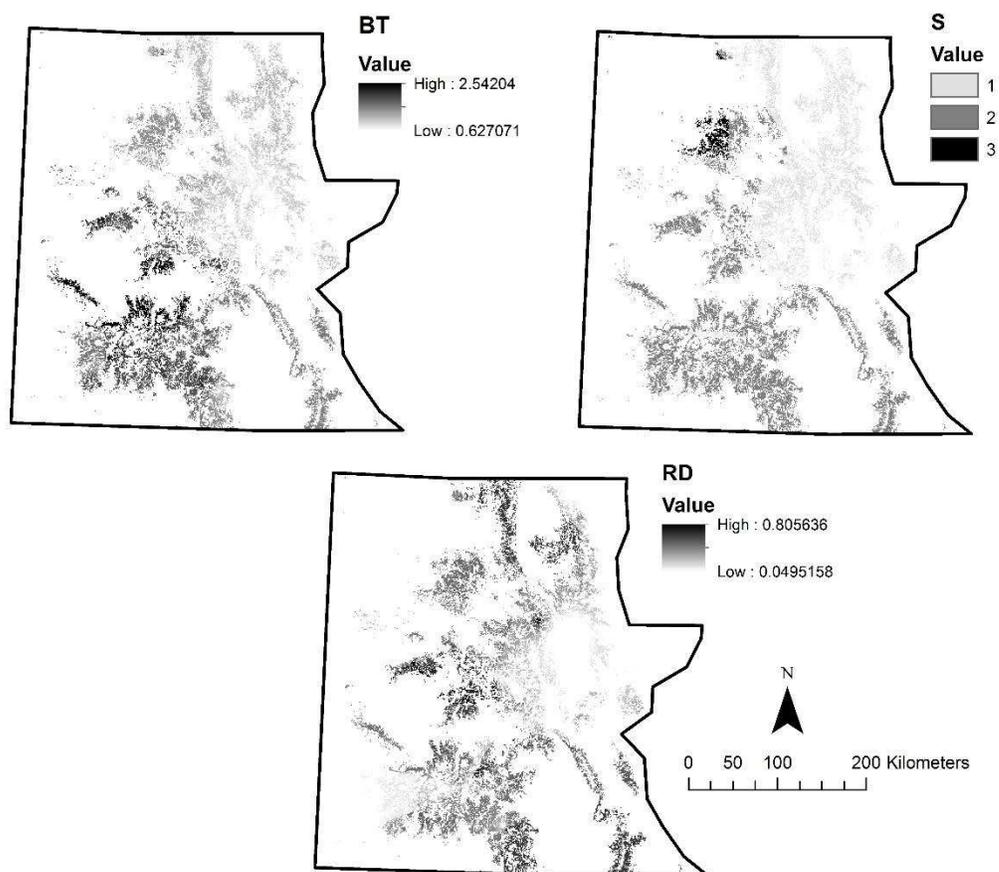
Figure 19. Map of interpolated covariates from linear inverse distance weight (IDW) with 12 nearest neighbors. Top left is basal area per tree (BT). Top right is stand structure (S). Bottom is relative dominance (RD). The study area was delineated by the layer represent forest land cover in Colorado.
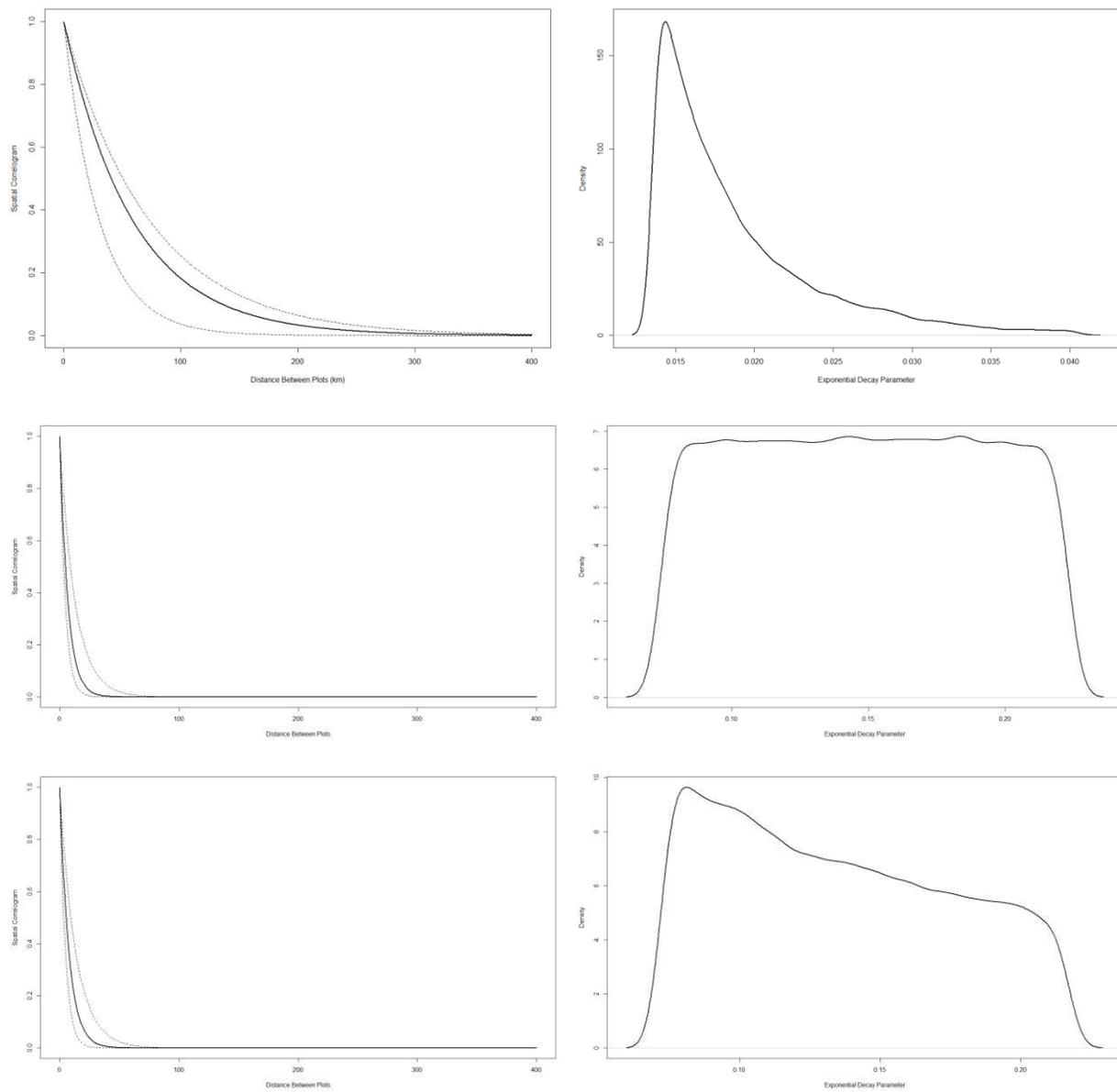
Figure 20. Posterior of correlogram (left) and posterior of exponential decay parameters, λ, for the zero-inflated model (top), one-inflated model (middle), and beta regression model (bottom). The spatial dependent structure only appears in the zero-inflated model (range parameter = 37 kilometers).
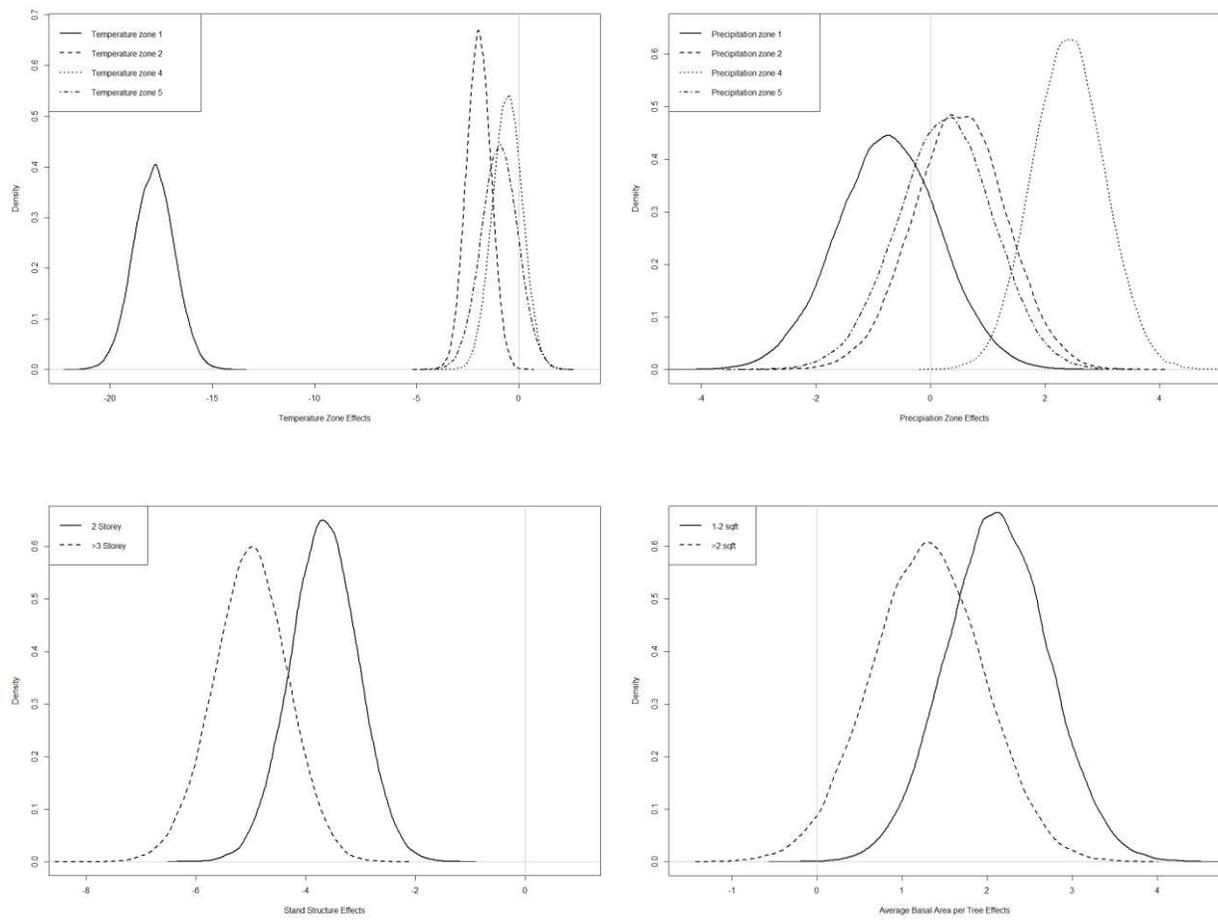
Figure 21. Posterior distribution of parameters of the best-fitted zero-inflated model. The covariates of temperature zone (T), precipitation zones (P), number of stories (S), and average basal area per tree (BT) were included in the best-fitted model.
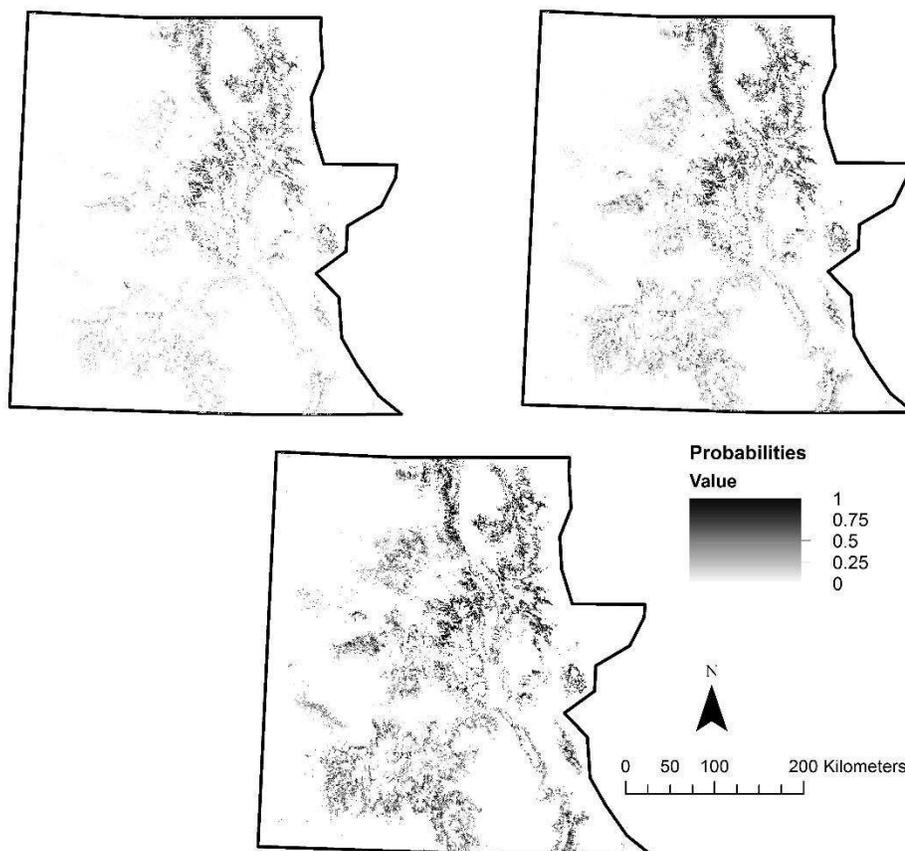
Figure 22. Prediction map from the best-fitted zero-inflated model. Top left is the prediction at 0.025 quantile. Top right is the prediction at median. Bottom is the prediction at 0.975 quantile. The study area was delineated by the layer represent forest land cover in Colorado.
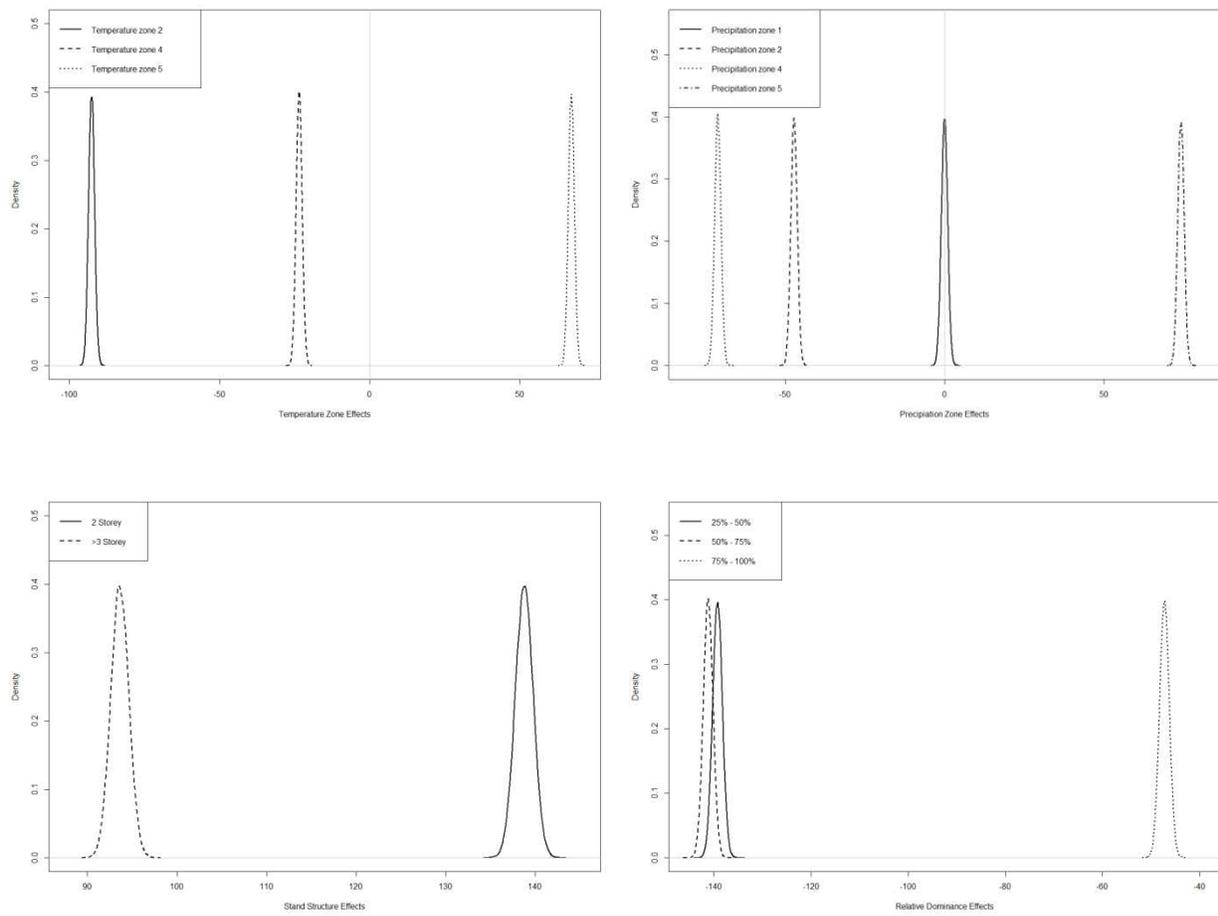
Figure 23. Posterior distribution of parameters of the best-fitted one-inflated model. The covariates of temperature zone (T), precipitation zones (P), number of stories (S), and relative dominance (RD) were included in the best-fitted model.
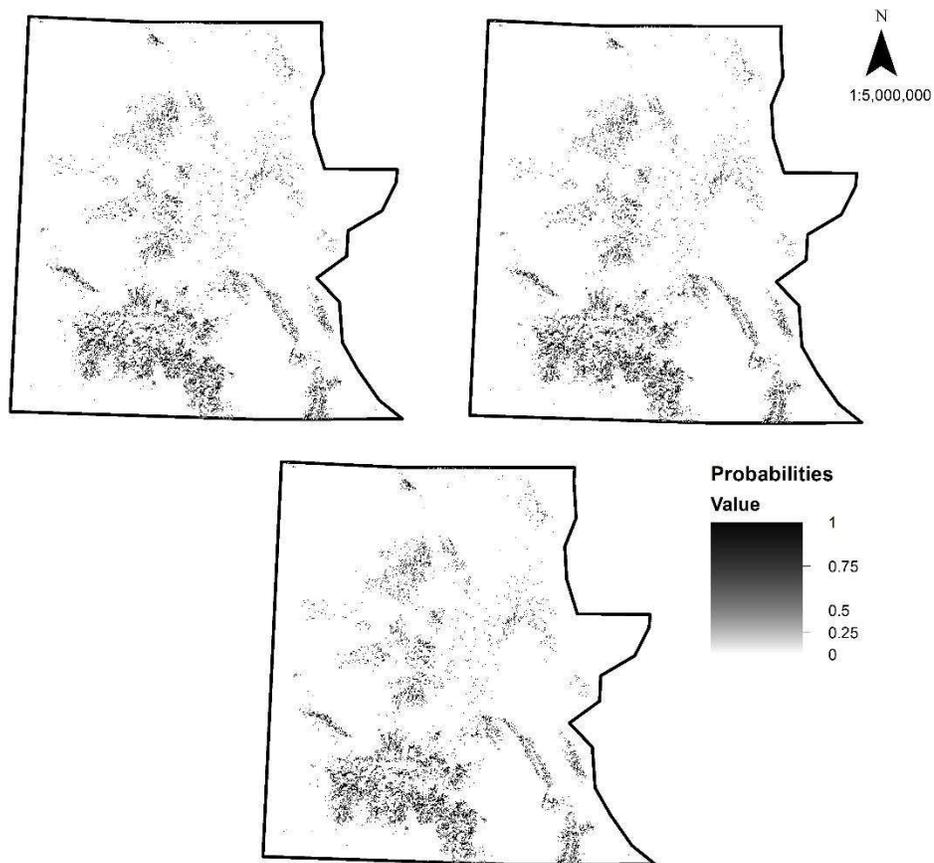
Figure 24. Prediction map from the best-fitted one-inflated model. Top left is the prediction at 0.025 quantile. Top right is the prediction at median. Bottom is the prediction at 0.975 quantile. The study area was delineated by the layer represent forest land cover in Colorado.
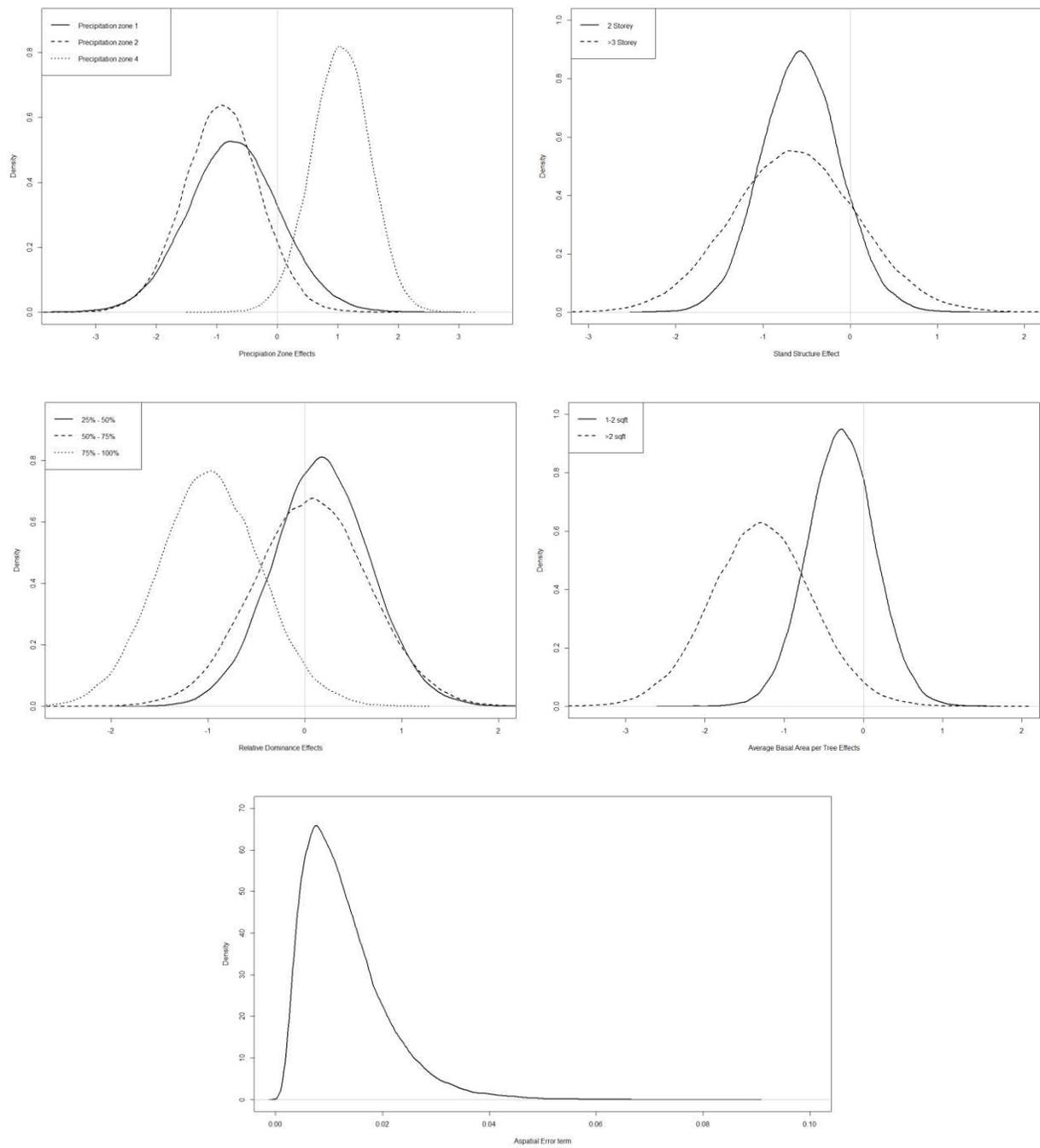
Figure 25. Posterior distribution of parameters of the best-fitted beta regression model. The covariates of precipitation zones (P), number of stories (S), relative dominance (RD), and average basal area per tree (BT) were included in the best-fitted model.
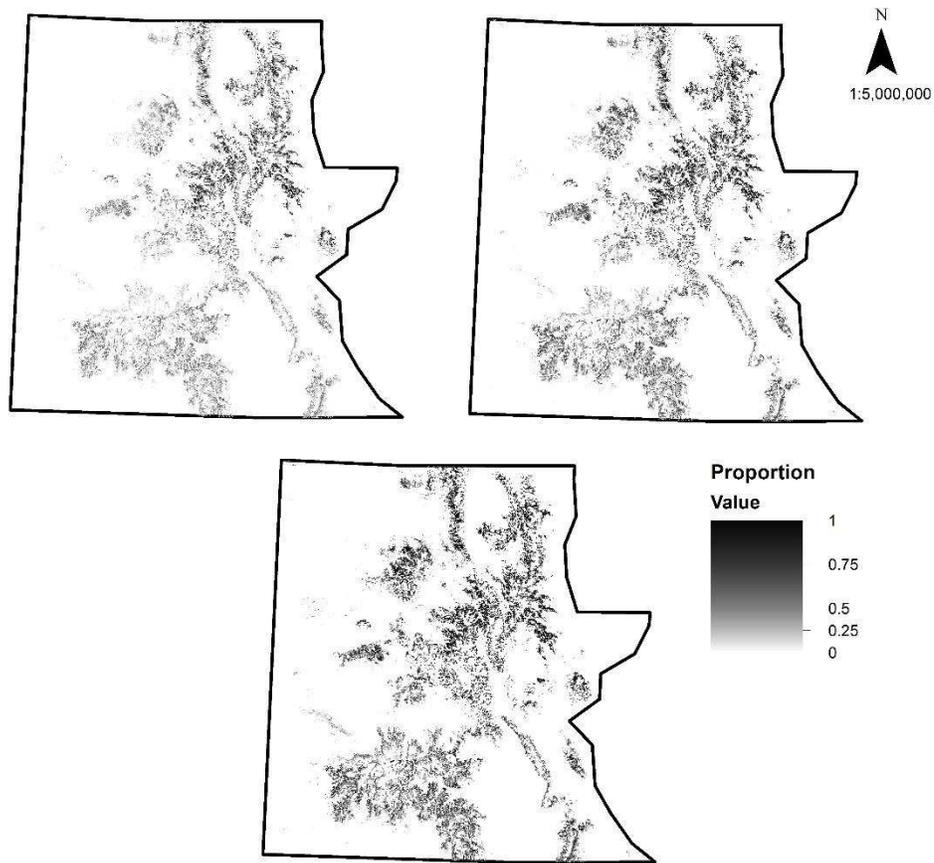
Figure 26. Prediction map from the best-fitted beta regression model. Top left is the prediction at 0.025 quantile. Top right is the prediction at median. Bottom is the prediction at 0.975 quantile. The study area was delineated by the layer represent forest land cover in Colorado.
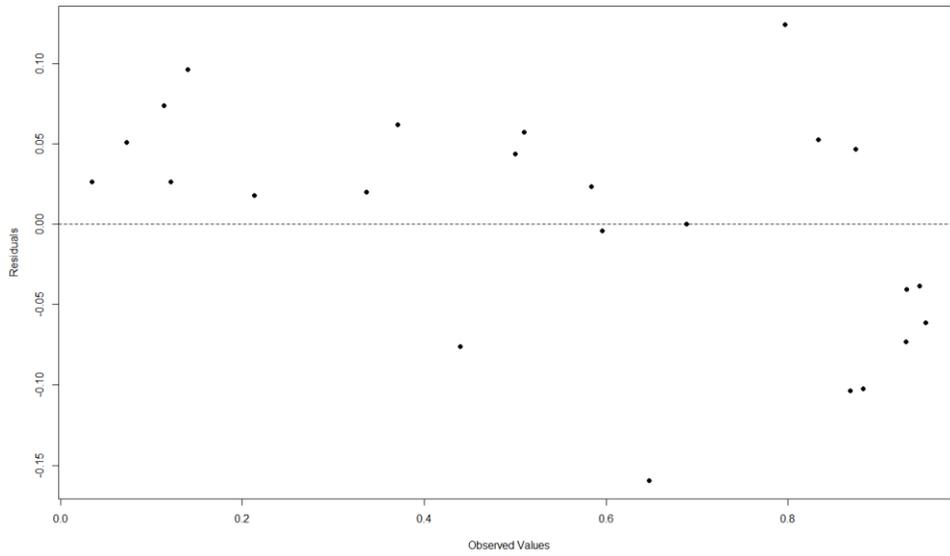
Figure 27. Median of the empirical residuals of the best-fitted beta regression model.

LITERATURE CITED

Anderegg, W.R.L., Berry, J.A., Field, C.B., 2012. Linking definitions, mechanisms, and modeling of drought-induced tree death. Trends Plant Sci. 17, 693–700.

Aquirre-Bravo, C., Reich, R.M., 2006. Spatial statistical modeling and classification of climate for the state of Colorado and adjacent lands of neighboring states. Rocky Mt. Res. Stn. USDA For. Serv. Fort Collins CO, 123 p.

Araújo, M.B., Peterson, A.T., 2012. Uses and misuses of bioclimatic envelope modeling. Ecology 93, 1527–1539.

Ayres, P.G., 1984. The interaction between environmental stress injury and biotic disease physiology. Annu. Rev. Phytopathol. 22, 53–75.

Bale, J.S., Masters, G.J., Hodkinson, I.D., Awmack, C., Bezemer, T.M., Brown, V.K., Butterfield, J., Buse, A., Coulson, J.C., Farrar, J., Good, J.E.G., Harrington, R., Hartley, S., Jones, T.H., Lindroth, R.L., Press, M.C., Symrnioudis, I., Watt, A.D., Whittaker, J.B., 2002. Herbivory in global climate change research: direct effects of rising temperature on insect herbivores. Glob. Change Biol. 8, 1–16.

Banerjee, S., Gelfand, A.E., Finley, A.O., Sang, H., 2008. Gaussian predictive process models for large spatial data sets. J. R. Stat. Soc. Ser. B Stat. Methodol. 70, 825–848.

Bentz, B.J., Régnière, J., Fettig, C.J., Hansen, E.M., Hayes, J.L., Hicke, J.A., Kelsey, R.G., Negrón, J.F., Seybold, S.J., 2010. Climate change and bark beetles of the Western United States and Canada: Direct and indirect effects. BioScience 60, 602–613.

Berryman, A.A., 1982. Population dynamics of bark beetles. Bark Beetles North Am. Conifers 264–314.

Bethlahmy, N., 1975. A Colorado episode: beetle epidemic, ghost forests, more streamflow. Northwest Sci. 49, 95–105.

Breece, C.R., Kolb, T.E., Dickson, B.G., McMillin, J.D., Clancy, K.M., 2008. Prescribed fire effects on bark beetle activity and tree mortality in southwestern ponderosa pine forests. For. Ecol. Manag. 255, 119–128.

Breslow, N.E., Clayton, D.G., 1993. Approximate inference in generalized linear mixed models. J. Am. Stat. Assoc. 88, 9–25.

Chavardès, R.D., Daniels, L.D., Waeber, P.O., Innes, J.L., Nitschke, C.R., 2012. Did the 1976–77 switch in the Pacific Decadal Oscillation make white spruce in the southwest Yukon more susceptible to spruce bark beetle? For. Chron. 88, 513–518.

Chelgren, N.D., Adams, M.J., Bailey, L.L., Bury, R.B., 2011. Using multilevel spatial models to understand salamander site occupancy patterns after wildfire. Ecology 92, 408–421.

Clark, J.S., 2005. Why environmental scientists are becoming Bayesians. Ecol. Lett. 8, 2–14.

Cook, A., Marion, G., Butler, A., Gibson, G., 2007. Bayesian inference for the spatio-temporal invasion of alien species. Bull. Math. Biol. 69, 2005–2025.

Davis, F.W., Goetz, S., 1990. Modeling vegetation pattern using digital terrain data. Landsc. Ecol. 4, 69–80.

DeRose, R.J., Bentz, B.J., Long, J.N., Shaw, J.D., 2013. Effect of increasing temperatures on the distribution of spruce beetle in Engelmann spruce forests of the Interior West, USA. For. Ecol. Manag. 308, 198–206.

DeRose, R.J., Long, J.N., 2012. Factors Influencing the Spatial and Temporal Dynamics of Engelmann Spruce Mortality during a Spruce Beetle Outbreak on the Markagunt Plateau, Utah. For. Sci. 58, 1–14.

DeRose, R.J., Long, J.N., 2009. Wildfire and spruce beetle outbreak: Simulation of interacting disturbances in the Central Rocky Mountains. Ecoscience 16, 28–38.

Diggle, P.J., 1983. Statistical analysis of spatial point patterns. 148 p.

Doak, P., 2004. The impact of tree and stand characteristics on spruce beetle (Coleoptera: Scolytidae) induced mortality of white spruce in the Copper River Basin, Alaska. Can. J. For. Res. 34, 810–816.

Engler, R., Guisan, A., Rechsteiner, L., 2004. An improved approach for predicting the distribution of rare and endangered species from occurrence and pseudo-absence data. J. Appl. Ecol. 41, 263–274.

ESRI, R., 2011. ArcGIS desktop: release 10. Environ. Syst. Res. Inst. CA.

Fettig, C.J., Borys, R.R., McKelvey, S.R., Dabney, C.P., 2008. Blacks Mountain Experimental Forest: bark beetle responses to differences in forest structure and the application of prescribed fire in interior ponderosa pine. First Findings from Blacks Mountain Interdisciplinary Research. Can. J. For. Res. 38, 924–935.

Finley, A.O., Banerjee, S., McRoberts, R.E., 2007. A Bayesian approach to multi-source forest area estimation. Environ. Ecol. Stat. 15, 241–258.

Gelman, A., Hill, J., 2006. Data analysis using regression and multilevel/hierarchical models. Cambridge University Press. 648 p.

Gilks, W.R., 2005. Markov Chain Monte Carlo, Encyclopedia of Biostatistics. John Wiley & Sons, Ltd.

Giovanini, J., Kroll, A.J., Jones, J.E., Altman, B., Arnett, E.B., 2013. Effects of management intervention on post-disturbance community composition: An experimental analysis using Bayesian hierarchical models. PLOS ONE 8, 10 p.

Griffin, J.M., Turner, M.G., Simard, M., 2011. Nitrogen cycling following mountain pine beetle disturbance in lodgepole pine forests of Greater Yellowstone. For. Ecol. Manag. 261, 1077–1089.

Guisan, A., Thuiller, W., 2005. Predicting species distribution: offering more than simple habitat models. Ecol. Lett. 8, 993–1009.

Haas, S.E., Hooten, M.B., Rizzo, D.M., Meentemeyer, R.K., 2011. Forest species diversity reduces disease risk in a generalist plant pathogen invasion. Ecol. Lett. 14, 1108–1116.

Hard, J.S., 1985. Spruce Beetles Attack Slowly Growing Spruce. For. Sci. 31, 839–850.

Hard, J.S., Holsten, E.H., 1985. Managing white and Lutz spruce stands in south-central Alaska for increased resistance to spruce beetle. 28 p.

Hart, S.J., Veblen, T.T., Eisenhart, K.S., Jarvis, D., Kulakowski, D., 2013. Drought induces spruce beetle (Dendroctonus rufipennis) outbreaks across northwestern Colorado. Ecology 95, 930–939.

Hart, S.J., Veblen, T.T., Mietkiewicz, N., Kulakowski, D., 2015. Negative feedbacks on bark beetle outbreaks: Widespread and severe spruce beetle infestation restricts subsequent infestation. PLoS ONE 10, 16 p.

Hebertson, E.G., Jenkins, M.J., 2008. Climate factors associated with historic spruce beetle (Coleoptera: Curculionidae) outbreaks in Utah and Colorado. Environ. Entomol. 37, 281–292.

Hobbs, N.T., Hilborn, R., 2006. Alternatives to statistical hypothesis testing in Ecology: A guide to self teaching. Ecol. Appl. 16, 5–19.

Hoeting, J.A., Leecaster, M., Bowden, D., 2000. An improved model for spatially correlated binary responses. J. Agric. Biol. Environ. Stat. 5, 102–114.

Holsten, E.H., Werner, R.A., 1990. Comparison of white, Sitka, and Lutz spruce as hosts of the spruce beetle in Alaska. Can. J. For. Res. 20, 292–297.

Hooten, M.B., Hobbs, N.T., 2015. A guide to Bayesian model selection for ecologists. Ecol. Monogr. 85, 3–28.

Huberty, A.F., Denno, R.F., 2004. Plant water stress and its consequences for herbivorous insects: a new synthesis. Ecology 85, 1383–1398.

Jenkins, M.J., Page, W.G., Hebertson, E.G., Alexander, M.E., 2012. Fuels and fire behavior dynamics in bark beetle-attacked forests in Western North America and implications for fire management. For. Ecol. Manag. 275, 23–34.

Jones, K.E., Patel, N.G., Levy, M.A., Storeygard, A., Balk, D., Gittleman, J.L., Daszak, P., 2008. Global trends in emerging infectious diseases. Nature 451, 990–993.

Kaiser, K.E., McGlynn, B.L., Emanuel, R.E., 2013. Ecohydrology of an outbreak: mountain pine beetle impacts trees in drier landscape positions first. Ecohydrology 6, 444–454.

Kausrud, K., Økland, B., Skarpaas, O., Grégoire, J.-C., Erbilgin, N., Stenseth, N.C., 2012. Population dynamics in changing environments: the case of an eruptive forest pest species. Biol. Rev. 87, 34–51.

Kawecki, T.J., 2008. Adaptation to marginal habitats. Annu. Rev. Ecol. Evol. Syst. 39, 321–342.

Keith, D.A., Akçakaya, H.R., Thuiller, W., Midgley, G.F., Pearson, R.G., Phillips, S.J., Regan, H.M., Araújo, M.B., Rebelo, T.G., 2008. Predicting extinction risks under climate change: coupling stochastic population models with dynamic bioclimatic habitat models. Biol. Lett. 4, 560–563.

Kurz, W.A., Dymond, C.C., Stinson, G., Rampley, G.J., Neilson, E.T., Carroll, A.L., Ebata, T., Safranyik, L., 2008. Mountain pine beetle and forest carbon feedback to climate change. Nature 452, 987–990.

Larsson, S., 1989. Stressful times for the plant stress: Insect performance hypothesis. Oikos 56, 277–283.

Latimer, A.M., Banerjee, S., Sang Jr, H., Mosher, E.S., Silander Jr, J.A., 2009. Hierarchical models facilitate spatial analysis of large data sets: a case study on invasive plant species in the northeastern United States. Ecol. Lett. 12, 144–154.

Lundquist, J.E., 2005. Landscape pathology-forest pathology in the era of landscape ecology. 155–165.

Lundquist, J.E., Reich, R.M., 2014. Landscape Dynamics of Mountain Pine Beetles. For. Sci. 60, 464–475.

MacArthur, R., Recher, H., Cody, M., 1966. On the Relation between Habitat Selection and Species Diversity. Am. Nat. 100, 319–332.

MacKenzie, D.I., 2006. Occupancy estimation and modeling: Inferring patterns and dynamics of species occurrence. Academic Press. 344 p.

MacKenzie, D.I., Nichols, J.D., Lachman, G.B., Droege, S., Andrew Royle, J., Langtimm, C.A., 2002. Estimating site occupancy rates when detection probabilities are less than one. Ecology 83, 2248–2255.

Masoud, M., 2012. Influence of climatic zones on the distribution and abundance of damage agents and forest types in Colorado, United States and Jalisco, Mexico. URL https://dspace.library.colostate.edu/bitstream/10217/71925/1/Masoud_colostate_0053N_11434.pdf

Massey, C., Wygant, N., 1954. Biology and control of the Engelmann spruce beetle in Colorado. Bark Beetles Fuels Fire Bibliogr. 37 p.

Mattson, W.J., Haack, R.A., 1987. The role of drought in outbreaks of plant-eating insects. BioScience 110–118.

McCambridge, W.F., Stevens, R.E., 1982. Effectiveness of thinning ponderosa pine stands in reducing Mountain Pine Beetle-caused tree losses in the Black Hills, Preliminary Observations. USDA Forest Service, Rocky Mountain Forest and Range Experiment Station. 8 p.

Meier, E.S., Kienast, F., Pearman, P.B., Svenning, J.-C., Thuiller, W., Araújo, M.B., Guisan, A., Zimmermann, N.E., 2010. Biotic and abiotic variables show little redundancy in explaining tree species distributions. Ecography 33, 1038–1048.

Nishii, R., Tanaka, S., 2012. Modeling and inference of forest coverage ratio using zero-one inflated distributions with spatial dependence. Environ. Ecol. Stat. 20, 315–336.

Ospina, R., Ferrari, S.L.P., 2012. A general class of zero-or-one inflated beta regression models. Comput. Stat. Data Anal. 56, 1609–1623.

Ospina, R., Ferrari, S.L.P., 2008. Inflated beta distributions. Stat. Pap. 51, 111–126.

Pielou, E.C., 1977. The latitudinal spans of seaweed species and their patterns of overlap. J. Biogeogr. 299–311.

Piqué, M., Obon, B., Condés, S., Saura, S., 2011. Comparison of relascope and fixed-radius plots for the estimation of forest stand variables in northeast Spain: an inventory simulation approach. Eur. J. For. Res. 130, 851–859.

Plummer, M., 2013. rjags: Bayesian graphical models using MCMC. R Package Version 3.

Plummer, M., 2004. JAGS: Just another Gibbs sampler.

Pongpattananurak, N., Reich, R.M., Khosla, R., Aguirre-Bravo, C., 2012. Modeling the spatial distribution of soil texture in the State of Jalisco, Mexico. Soil Sci. Soc. Am. J. 76, 199.

Raffa, K.F., Aukema, B.H., Bentz, B.J., Carroll, A.L., Hicke, J.A., Turner, M.G., Romme, W.H., 2008. Cross-scale drivers of natural disturbances prone to anthropogenic amplification: The dynamics of bark beetle eruptions. BioScience 58, 501–517.

Raffa, K.F., Aukema, B.H., Erbilgin, N., Klepzig, K.D., Wallin, K.F., 2005. Interactions among conifer Terpenoids and bark beetles across multiple levels of scale: An attempt to understand links between

population patterns and physiological processes, in: Romeo, J.T. (Ed.), Recent Advances in Phytochemistry, Chemical Ecology and Phytochemistry of Forest Ecosystems. Elsevier, pp. 79–118.

R Core Team, 2014. R: A language and environment for statistical computing. R Foundation for Statistical Computing, Vienna, Austria, 2012.

Record, S., Fitzpatrick, M.C., Finley, A.O., Veloz, S., Ellison, A.M., 2013. Should species distribution models account for spatial autocorrelation? A test of model projections across eight millennia of climate change. Glob. Ecol. Biogeogr. 22, 760–771.

Reich, R.M., Aguirre-Bravo, C., Bravo, V.A., 2008. New approach for modeling climatic data with applications in modeling tree species distributions in the states of Jalisco and Colima, Mexico. J. Arid Environ. 72, 1343–1357.

Reich, R.M., Aguirre-Bravo, C., Bravo, V.A., Briseño, M.M., 2011. Empirical evaluation of confidence and prediction intervals for spatial models of forest structure in Jalisco, Mexico. J. For. Res. 22, 159–166.

Reich, R.M., Bonham, C.D., Aguirre-Bravo, C., Chazaro-Basañeza, M., 2010. Patterns of tree species richness in Jalisco, Mexico: relation to topography, climate and forest structure. Plant Ecol. 210, 67–84.

Reich, R.M., Lundquist, J.E., Acciavatti, R.E., 2014. Influence of climatic conditions and elevation on the spatial distribution and abundance of *Trypodendron* ambrosia Beetles (Coleoptera: Curculionidae: Scolytinae) in Alaska. For. Sci. 60, 308–316.

Reich, R.M., Lundquist, J.E., Bravo, V.A., 2013. Characterizing spatial distributions of insect pests across Alaskan forested landscape: A case study using Aspen Leaf Miner (Phyllocnistis populiella Chambers). J. Sustain. For. 32, 527–548.

Reynolds, K.M., Holsten, E.H., 1994. Relative importance of risk factors for spruce beetle outbreaks. Can. J. For. Res. 24, 2089–2095.

Ribeiro Jr, P.J., Diggle, P.J., 2001. geoR: A package for geostatistical analysis. R News 1, 14–18.

Ridout, M., Demétrio, C.G., Hinde, J., 1998. Models for count data with many zeros, in: Proceedings of the XIXth International Biometric Conference, 179–192.

Royle, J.A., Kéry, M., Gautier, R., Schmid, H., 2007. Hierarchical spatial models of abundance and occurrence from imperfect survey data. Ecol. Monogr. 77, 465–481.

Schmid, J., Frye, R., 1977. Spruce beetle in the Rockies. Bark Beetles Fuels Fire Bibliogr. 44 p.

Seager, R., Ting, M., Held, I., Kushnir, Y., Lu, J., Vecchi, G., Huang, H.-P., Harnik, N., Leetmaa, A., Lau, N.-C., Li, C., Velez, J., Naik, N., 2007. Model projections of an imminent transition to a more arid climate in Southwestern North America. Science 316, 1181–1184.

Sherriff, R.L., Berg, E.E., Miller, A.E., 2011. Climate variability and spruce beetle (*Dendroctonus rufipennis*) outbreaks in south-central and southwest Alaska. Ecology 92, 1459–1470.

Shono, H., 2008. Confidence interval estimation of CPUE year trend in delta-type two-step model. Fish. Sci. 74, 712–717.

Spiegelhalter, D.J., Best, N.G., Carlin, B.P., Van Der Linde, A., 2002. Bayesian measures of model complexity and fit. J. R. Stat. Soc. Ser. B Stat. Methodol. 64, 583–639.

Stadelmann, G., Bugmann, H., Wermelinger, B., Meier, F., Bigler, C., 2013. A predictive framework to assess spatio-temporal variability of infestations by the European spruce bark beetle. Ecography 36, 1208–1217.

Turner, M.G., 1989. Landscape ecology: The effect of pattern on process. Annu. Rev. Ecol. Syst. 20, 171–197.

Veblen, T.T., Hadley, K.S., Reid, M.S., 1991. Disturbance and stand development of a Colorado subalpine forest. J. Biogeogr. 707–716.

Wargo, P.M., 1985. Interaction of stress and secondary organisms in decline of forest trees, in: Air Pollutants Effects on Forest Ecosystems, St. Paul, Mn.(USA), 8-9 May 1985. Acid Rain Foundation.

Wikle, C.K., 2002. Spatial modeling of count data: A case study in modelling breeding bird survey data on large spatial domains. Chapman Hall, 199–209.

Williams, A.P., Allen, C.D., Macalady, A.K., Griffin, D., Woodhouse, C.A., Meko, D.M., Swetnam, T.W., Rauscher, S.A., Seager, R., Grissino-Mayer, H.D., 2013. Temperature as a potent driver of regional forest drought stress and tree mortality. Nat. Clim. Change 3, 292–297.

Zhang, H., Wang, Y., 2010. Kriging and cross-validation for massive spatial data. Environmetrics 21, 290–304.

Zimmerman, D.L., 2006. Optimal network design for spatial prediction, covariance parameter estimation, and empirical prediction. Environmetrics 17, 635–652.

Zimmermann, N.E., Kienast, F., 1999. Predictive mapping of alpine grasslands in Switzerland: Species versus community approach. J. Veg. Sci. 10, 469–482.

Zuur, A.F., Ieno, E.N., Walker, N.J., Saveliev, A.A., Smith, G.M., 2009. Mixed effects modelling for nested data. Mixed effects models and extensions in Ecology with R, Statistics for Biology and Health. Springer New York, 101–142.